To the Graduate Council:

I am submitting herewith a dissertation written by David A. Gerard entitled "Ultrastructure, Development and Elemental Composition of the Lorica of Pteromonas protracta (Stein) Lemm." I recommend that it be accepted in partial fulfillment of the requirements for the degree of Doctor of Philosophy, with a major in Botany.

Patricia L. Walne
Patricia L. Walne, Major Professor

We have read this dissertation
and recommend its acceptance:

Otto John Schwarz

James N. Dumont

Fred H. Morris

Accepted for the Council:

L. Evan Pell
Vice Chancellor
Graduate Studies and Research

X

ULTRASTRUCTURE, DEVELOPMENT AND ELEMENTAL COMPOSITION OF THE LORICA OF *PTEROMONAS PROTRACTA* (STEIN) LEMM.

A Dissertation

Presented for the

Doctor of Philosophy

Degree

The University of Tennessee, Knoxville

David A. Gerard

August 1980

ACKNOWLEDGEMENTS

I would like to acknowledge and express my appreciation to the many people who have contributed to the successful completion of this dissertation. I thank my major professor, Dr. P. L. Walne, under whose skillful direction this investigation was carried out. I am particularly appreciative for the example of integrity she has given in both her professional and personal life. I also thank the other members of my graduate committee, Dr. Fred H. Norris, Dr. Otto J. Schwarz, Dr. James N. Dumont and Dr. Elizabeth Gantt for their helpfulness and critical reading of my dissertation.

I am grateful to Mr. Dick Williams for training in scanning and transmission electron microscopy and for technical help. In the Department of Chemical and Metallurgical Engineering, The University of Tennessee, Knoxville, Dr. C. R. Brooks permitted use of the SEM-EDX used in this investigation, and Mr. Bobby McGill provided excellent instrument training and helpful technical discussions. I am also grateful to Dr. Jim Bentley of the Radiation Effects Group, Metallurgical Engineering, ORNL, for operating time on the STEM-EDX used in this investigation.

I am thankful to former graduate student colleagues, Dr. Patricia Pagni, Dr. Russell Porcella and Dr. Larry West for their willingness to give helpful advice and technical assistance. I also wish to acknowledge the helpful comments, technical assistance and friendship of my laboratory colleagues, John Dunlap, Lu Hilenski, Linda Pocratsky and Frank Ralston. I am grateful to the Department of Botany for financial support in the form of a graduate assistantship and a graduate teaching assistantship and

for a research assistantship during the last year of my work supported by a NSF grant to Dr. Walne. I also acknowledge a Sigma Xi Grant-in-Aid of Research received in 1978.

I am grateful to my family and to my wife for their constant faith, love and patience during this time, and particularly to my brother, Dr. Gary Gerard, for his timely encouragement and prodding. Finally, I wish to thank my wife Ruth whose love, friendship and sacrifice made possible the successful completion of this dissertation.

ABSTRACT

The ultrastructure of the phacotacean flagellate, Pteromonas protracta (Volvocales), was investigated, with special reference to lorica structure, composition and development. The bilayered lorica is composed of 2 valves that are closely appressed to the protoplast. The valves are fused, forming a wing which circumscribes the cell. The wing extends from the lorica of 1.5-2.0 um. A third, wedge-shaped lorica segment with 2 flagellar pores is located at the anterior end of the cell and is fused to both valves. The surface of the outer lorica (OL) is covered with a raised hexagonal pattern; a secondary reticulum between the hexagonal ridges, is characterized by numerous puncta. Different culture media affect lorica structure but not basic elemental composition. In mature loricas from modified soil water (MSW) cultures, the OL is dense and amorphous with a scalloped margin which corresponds to the hexagonal surface pattern. The inner lorica (IL) is granulo-fibrillar and closely appressed to the OL. In cells grown in modified Bold's Basal Medium (MBBM), the IL is finely granular, and the OL is broad and diffuse with the hexagonal pattern obscured by a copious mucilaginous layer.

The major elements detected in all loricas analyzed by Scanning Electron Microscopy-Energy Dispersive Spectroscopy (SEM-EDX) and Scanning Transmission Electron Microscopy-Energy Dispersive Spectroscopy (STEM-EDX) are P and Ca, and Si is detected in over 85% of the loricas, regardless of culture medium or age. Sulfur is present in over 50% of the loricas from either medium, while Fe is present in 87% of loricas from MSW cultures but never detected in loricas from MBBM cultures. Other elements such

as Cr, Cl, Al, Mg, K, Mn, Ni and Hg are found in less than 50% of all loricas and are often removed from them by treatment with glusulase, a result suggesting that they are loosely associated with the mucilage component of the loricas. Results of tests with a variety of cytochemical stains indicate that the mucilage is an acidic and negatively charged mucopolysaccaride containing a protein moiety. That Ca is localized in the primary hexagonal pattern and forms the basic structural component of the OL is suggested by analysis of loricas subjected to acetolysis and EDTA and EGTA treatment. Observations of loricas treated with dilute HCl indicate that the Ca might be in the form of calcite.

The Golgi apparatus has been implicated in the production of presumptive lorica precursor material (PLPM) for the first time in any green alga. Two types of PLPM, dense cores and wispy fibrillar material, are visible in the Golgi cisternae and associated vesicles. STEM-EDX analysis of dense cores in the Golgi cisternae and in the OL of the same cell, produce strikingly similar spectra, with Ca, P and Si as the major elements detected. Lorica development begins with the production of a fine "skin" which initially is closely appressed to the plasmalemma and which becomes the IL as development proceeds. As the OL matures, juxtaposition of the dense cores forms the primary hexagonal pattern, while interconnection of the wispy fibrillar material forms the secondary reticulum. The presumptive role of the IL as a template for the orderly development of the OL is discussed.

Ultrastructural studies have shown that the structure and cellular organization in P. protracta are generally similar to other volvocalean flagellates. Features documented for the first time in any member of the

Phacotaceae include 2 types of flagellar hairs, one continuous with the flagellar membrane and the other easily dissociated from it, and the presence of a cruciate flagellar rootlet system with a 4-2-4-2 microtubular arrangement. During mitosis a closed mitotic spindle persists at least into metaphase, and cytokinesis is effected by the production of a phycoplast. Both cytoplasmic and intrachloroplastidic microtubules have been observed in close proximity to the stigma.

TABLE OF CONTENTS

CHAPTER		PAGE
I.	INTRODUCTION	1
II.	MATERIALS AND METHODS	12
	Culture Conditions	12
	Light Microscopy and Cytochemistry	13
	Autoradiography	14
	Transmission Electron Microscopy	14
	Conventional thin sections	15
	Serial sections	15
	Thick sections	15
	Whole mounts	16
	Acetolysis	16
	Glusulase Treatment	16
	Shadow-casting	17
	Scanning Electron Microscopy	17
	Analytical Electron Microscopy	18
III.	RESULTS	20
	Basic Lorica Structure	20
	Effects of Media on Lorica Structure	21
	Lorica Composition	21
	SEM-EDX of untreated loricas	21
	SEM-EDX of glusulase-treated loricas	26
	EDTA-treated loricas	29
	EGTA-treated loricas	29
	Cytochemical stains	29
	Autoradiography	33
	Acetolysis	33
	Hydrochloric acid treatment	33
	Lorica Development	34
	General Cellular Morphology and Ultrastructure	35
	General morphology	35
	General ultrastructure and cellular organization	35
	Nucleus	36
	Endoplasmic reticulum	36
	Golgi apparatus and cytoplasmic vesicles	37
	Membrane flow	37
	Mitochondria	37
	Contractile vacuoles	38
	Flagellar apparatus and cytoplasmic microtubules	38
	Chloroplast, pyrenoid and stigma	40
	Growth curve	40
	Life cycle	41
	Asexual reproduction	41
	Presumptive sexual reproduction	42

CHAPTER PAGE

IV. DISCUSSION. 44
Effects of Culture Conditions on Lorica Structure 44
Lorica Composition. 45
Lorica Development. 48
Involvement of Golgi Apparatus in Lorica Development. . . . 49
Biomineralization 51
Lorica Function 52
General Ultrastructure. 53
Nucleus 53
Contractile vacuole 54
Flagella. 54
Chloroplast, pyrenoid and stigma. 55
Sexual reproduction 56
Phylogeny and Taxonomy. 56

V. SUMMARY AND CONCLUSIONS 59

LITERATURE CITED. 62

APPENDICES. 73

APPENDIX A. CULTURE MEDIA. 74

APPENDIX B. CYTOCHEMICAL STAINS FOR LIGHT MICROSCOPY 76

APPENDIX C. PREPARATIVE PROCEDURES FOR ELECTRON MICROSCOPY . 78

APPENDIX D. SCANNING ELECTRON MICROSCOPY CHEMICALS AND TECHNIQUES 82

APPENDIX E. PLATES AND FIGURE LEGENDS. 83

VITA. 179

LIST OF TABLES

TABLE		PAGE
I.	Partial List of Pertinent Literature on the Family Phacotaceae	3
II.	Partial List of Pertinent Literature on Lorica or Cell Covering Development, Structure and Composition	7
III.	Comparison of Structure and Elemental Composition of Loricas From MSW and MBBM Cultures.	22
IV.	SEM-EDX of Untreated Loricas.	23
V.	SEM-EDX of Loricas From 4 Ages of MBBM Cultures	24
VI.	SEM-EDX of Loricas From 4 Ages of MSW Cultures.	25
VII.	SEM-EDX of Glusulase-Treated Loricas From 4 Ages of MBBM Cultures	27
VIII.	SEM-EDX of Glusulase-Treated Loricas From 4 Ages of MSW Cultures.	28
IX.	SEM-EDX of Loricas Treated for 30 Seconds with 1uM EDTA	30
X.	SEM-EDX of Loricas Treated for 30 Seconds with 1uM EGTA	31
XI.	SEM-EDX of Loricas Treated for 5 Minutes with 1uM EGTA.	32

LIST OF PLATES

PLATE		PAGE
I.	Diagramatic Representation of Vegetative Cell Ultrastructure.	84
II.	TEM: Lorica Surface	86
III.	SEM: Lorica Surface	88
IV.	Wedge-Shaped Lorica Segment.	90
V.	TEM: Lorica Wedge and Flagellar Pore.	92
VI.	Lorica Development	94
VII.	Lorica Structure	97
VIII.	Lorica Assembly.	100
IX.	Golgi Involvement in Lorica Production	103
X.	STEM-EDX of MSW Grown Cell	105
XI.	STEM-EDX of MBBM Grown Cell.	107
XII.	Cytochemical Stains.	109
XIII.	SEM-EDX: Loricas from 14-Day-Old Cultures	112
XIV.	SEM-EDX: Loricas from 2-Month-Old Cultures.	114
XV.	SEM-EDX: Glusulase-Treated Loricas from 14-Day-Old Cultures	116
XVI.	SEM-EDX: Glusulase-Treated Loricas from 2-Month-Old Cultures	118
XVII.	SEM-EDX: Loricas from 14-Day-Old Cultures After 30 sec Treatment with EDTA.	120
XVIII.	SEM-EDX: Loricas from 14-Day-Old Cultures After 30 sec Treatment with EGTA.	122
XIX.	SEM-EDX: Loricas from 14-Day-Old Cultures After 5 min EGTA Treatment	124
XX.	SEM-EDX: Acetolysis Treated Loricas	126

PLATE		PAGE
XXI.	General Morphology.	128
XXII.	SEM: Vegetative Cell	130
XXIII.	Vegetative Cell Ultrastructure.	132
XXIV.	Organelle Relationships	134
XXV.	Ultrastructure of Nucleus	136
XXVI.	Endoplasmic Reticulum and Golgi Apparatus	138
XXVII.	Membrane Flow	140
XXVIII.	Mitochondria and Contractile Vacuoles	142
XXIX.	Flagella Ultrastructure	144
XXX.	Flagella Transverse Sections.	146
XXXI.	Flagellar Apparatus	148
XXXII.	Cytoplasmic Microtubules.	150
XXXIII.	Flagellar Roots	152
XXXIV.	Extra Basal Bodies and Microtubules Associated with the Chloroplast or Stigma	154
XXXV.	Microtubules.	156
XXXVI.	Chloroplast, Pyrenoid and Stigma.	158
XXXVII.	Growth Studies. . .	160
XXXVIII.	Diagramatic Representation of Life Cycle.	162
XXXIX.	Cell Division: Two-Cell Stage.	164
XL.	Cell Division	166
XLI.	Cytokinesis	169
XLII.	Cell Division: Four-Cell Stage	172
XLIII.	Sexual Reproduction	174
XLIV.	Aplanozygote.	177

LIST OF ABBREVIATIONS

Measurements and Other Symbols

C	- centigrade
CPC	- counts per channel
CPD	- critical point dried
ft-c	- foot-candles
g	- gram(s)
hr	- Hour(s)
KeV	- kilo-electron volt
KV	- kilovolt
L/D	- light-to-dark
LM	- light microscopy/microscope
M	- molar concentration
min	- minute(s)
ml	- milliliter(s)
mm	- millimeter(s)
mM	- millimolar
nm	- nanometer
sec	- second(s)
SEM	- scanning electron microscopy/microscope
SEM-EDX	- scanning electron microscopic energy-dispersive X-ray analysis/analyzer
STEM	- scanning transmission electron microscopy/microscope
STEM-EDX	- scanning transmission electron microscopic energy-dispersive X-ray analysis/analyzer
TEM	- transmission electron microscopy/microscope
ug	- microgram
uc	- microliter
um	- micrometer
v/v	- volume-to-volume
w/v	- weight-to-volume

Organelles

BB	- basal body
C	- chloroplast
cm	- chloroplast membrane
cv	- contractile vacuole(s)
d	- dictyosome
fl	- flagella
fp	- flagellar pore
fr	- flagellar ring
IL	- inner lorica
M	- mitochondria
MLS	- multi-layered structure
MT	- microtubule(s)
N	- nucleus
NM	- nuclear membrane
Nu	- nucleolus
OL	- outer lorica
P	- pyrenoid
PLPM	- presumptive lorica precursor material
RER	- rough endoplasmic reticulum
S	- starch
SER	- smooth endoplasmic reticulum
ST	- stigma

CHAPTER I

INTRODUCTION

In the division Chlorophyta, cells of the family Phacotaceae (Volvocales) are unique in their possession of a wall-like structure termed a lorica, which is often separated from the protoplast. The space between the lorica and protoplast is generally filled with fluids similar to the surrounding medium. The shape of the protoplast is often different from the shape of the lorica, which may be entire or bivalved. The flagella may emanate through apertures in the lorica surface, between the lorica valves, or in Pteromonas protracta through pores in an anteriorly located, wedge-shaped lorica segment. Basic cell morphology in the Phacotaceae is similar to Chlamydomonas, with each cell having 2 or 4 flagella, a single cup-shaped chloroplast, 1 or more pyrenoids, contractile vacuoles at the base of the flagella and an intrachloroplastidic stigma. Pteromonas protracta (Stein) Lemm., originally described by Stein (1883), is biflagellated and the only member of the Phacotaceae with a bivalved, smooth-surfaced, strongly compressed lorica with 2 wing-like projections (Smith, 1950). The wings in very young cells are inconspicuous but grow larger as the cells age (Jane, 1944).

The relatively few published studies on members of the Phacotaceae are largely taxonomic in nature, and only two investigations have employed electron microscopy. Porcella and Walne (1980) carried out a comprehensive ultrastructural study of Dysmorphococcus globosus using light microscopy, transmission and scanning electron microscopy and various cytochemical

stains. In the only other ultrastructural study of Pteromonas, Belcher and Swale (1967) described the lorica of P. angulosa as bilayered with a distinct hexagonal surface pattern on its outer surface. For phacotacean organisms with bivalved loricas, there are no data available on lorica development or chemical composition. A list of pertinent literature on the Phacotaceae is presented in Table I.

Loricated organisms are also found in the Chrysophyceae, Euglenineae and marine protozoans. In the Chrysophyceae 3 basic types of loricas have been characterized: 1) those which consist of scales composed of cellulose-like microfibrils, e.g., Epipyxis (Kristiansen, 1972); 2) those composed of long fibrils of various sizes and orientations, e.g., Dinobryon (Karim and Round, 1967; Franke and Herth, 1973); 3) those which consist of interwoven crystals embedded in a previously formed transparent band, e.g., Chrysococcus (Belcher, 1968). In the Euglenineae, Trachelomonas and Colacium are the only loricated genera which have been studied with electron microscopy. In Trachelomonas 2 basic envelope (lorica) types have been observed: fibrillar or weft and granular (Leedale, 1975). Recent evidence indicates, however, that both weft and granular components may be present in the same envelope, depending perhaps on the culture conditions (Dunlap, personal communication). Marine protozoans possess loricas which reportedly contain protein and chitin impregnated with calcarious compounds and quartz crystals (Gold et al., 1970, 1975; Tappan and Leoblich, 1968).

Recent studies by numerous researchers have shown that algal coverings are more diverse in chemical composition than had been suspected earlier. Biochemical analyses of the cell wall of Chlamydomonas reinhardi

TABLE I

PARTIAL LIST OF PERTINENT LITERATURE ON THE FAMILY PHACOTACEAE

Date	Author	Contribution
1883	Stein, F. R.	Wrote the original description of *Pteromonas protracta*.
1889	Dangeard, P. A.	Wrote the original description of *Phacotus*.
1916	Takeda, H.	Wrote the original description of *Dysmorphococcus globosus*.
1925	Skvortzow, B. B.	Described a new genus and species, *Wislouchiella planktonica*.
1927	Pascher, A.	Described and illustrated 2 members of the Phacotaceae in a report on rare algae.
1927	Pascher, A.	Described and illustrated 7 species of *Pteromonas* found in Europe.
1930	Conrad, W.	Described 2 new species of *Pteromonas*.
1938	Bold, H. C.	Reported the occurrence of *Dysmorphococcus variabilis* in the United States.
1941	Singh, J.	Isolated 2 species of *Phacotus* from soil.
1942	Brinley, F. J. and L. J. Katzin	Reported the widespread occurrence of members of the Phacotaceae, including *Pteromonas* and *Phacotus*, in the Ohio River system.
1942	Lackey, J. B.	Described 2 species of *Phacotus* and 1 of *Wislouchiella* from the Cumberland and Duck Rivers in Tennessee.
1944	Jane, F.	Described *Pteromonas varians*, along with other phacotacean species.
1949	Hortobagyi, T.	Described a new species, *Coccomonas eberii*.

TABLE I (Continued)

Date	Author	Contribution
1950	Kampter, E.	Investigated the chemical composition of the lorica of *Phacotus* and noted the lack of iron.
1950	Smith, G. M.	Described 8 phacotacean genera from the United States.
1953	Bold, H. C. and R. C. Starr	Described a new species, *Dysmorphococcus globosus*.
1955	Cole, G. A.	Noted *Phacotus lenticularis* as one of the hardiest forms with respect to stagnation endurance.
1957	Bourrelly, P.	Described the Phacotaceae, including *Phacotus* and *Pteromonas*.
1957	Fott, B.	Described a new species, *Pteromonas protracta*.
1963	Swale, E.	Wrote a brief history and taxonomy of *Pteromonas angulosa*.
1964	Evans, J. H.	Described the taxonomy, occurrence and growth in culture of *Pteromonas varians*.
1965	Peterfi, L. S. and S. Peterfi	Described 5 species of *Pteromonas* with illustrations of 2.
1966	Bourrelly, P.	Provided a complete listing of revision of the known genera of the Phacotaceae.
1967	Belcher, J. H. and E. M. F. Swale	Compared the morphology of *Pteromonas angulosa* and *P. tenius*, using light and electron microscopy.
1970	Prescott, G. W.	Described the 8 phacotacean genera found in the United States.
1976	Porcella, R. A.	Described the ultrastructure and lorica development in *Dysmorphococcus globosus*.
1978	Gerard, D. A. and P. L. Walne	Described general structure and composition of the lorica of *Pteromonas protracta*.

TABLE I (Continued)

Date	Author	Contribution
1979	Gerard, D. A. and P. L. Walne	Described cellular ultrastructure and lorica development in Pteromonas protracta.

reveal that the wall does not contain cellulose as previously suggested (Walne, 1967), but is predominantly composed of a complex glycoprotein rich in hydroxyproline (Roberts et al., 1972; Hills, 1973; Roberts, 1974). Miller (1978) described a similar wall composition for Chlorococcum oleofaciens. Herth et al. (1977) found that the lorica microfibrils of Poteriochromonas stipitata are chitin rather than cellulose, as had been reported earlier (Kramer, 1972; Schnepf, 1968). In the same study the authors pointed out that it no longer can be assumed that a wall or lorica component is cellulosic simply on the basis of a microfibrillar structure. Thus, other microfibrillar loricas (e.g., Epipyxis) previously described as cellulosic on the basis of structure only, need to be re-examined with a variety of biochemical and technical analyses. Chitin has also been discovered in the frustules of at least 2 diatom species (McLachlan et al., 1965; Blackwell et al., 1965, 1967). Sporopollenins, resistant compounds historically associated with the walls of spores and pollen grains, have recently been reported for numerous algal cell coverings (Atkinson et al., 1972; Staehelin and Pickett-Heaps, 1975; Pickett-Heaps and Staehelin, 1975; Marchant, 1977; Good and Chapman, 1978). Recent studies have demonstrated the involvement of the Golgi apparatus in the production of algal cell coverings including the cyst wall in Euglena (Triemer, 1980), and scales in some prasinophytes (Manton and Leedale, 1961; Manton, 1966a, 1966b; Moestrup and Thomsen, 1974; Moestrup and Walne, 1979), chrysophytes (Brown et al., 1970, 1973; Brown and Franke, 1976) and haptophytes (Outka and Williams, 1971; Allen and Northcote, 1975). A list of pertinent literature on algal cell coverings is presented in Table II.

TABLE II

PARTIAL LIST OF PERTINENT LITERATURE ON LORICA OR CELL COVERING DEVELOPMENT, STRUCTURE AND COMPOSITION

Date	Author	Contribution
1950	Kamptner, E.	Reported lack of iron in the lorica of *Phacotus lendneri*.
1950	Middlehoek, A.	Described and illustrated the lorica of *Biocosoeca planktonica*.
1953	Pringsheim, E. G.	Described the lorica of 13 species of *Trachelomonas* and discussed the reliability of taxonomy based on lorica structure.
1956	Singh, K. P.	Discussed the structure of the lorica in 6 species of *Trachelomonas*.
1958	Cronshaw, J., A. Meyers and R. D. Preston	Used paper chromatography, x-ray diffraction and electron microscopy to investigate cell walls of marine algae.
1963	Hilliard, D. K. and B. Asmund	Examined the ultrastructure of *Dinobryon*, *Hyalobryon* and *Epipyxis*, and combined some species on the basis of lorica structure.
1967	Belcher, J. H. and E. M. F. Swale	Described the structure of the lorica of *Pteromonas tenuis* by light and electron microscopy.
1967	Green, J. C. and P. H. Jennings	Reported Golgi apparatus involvement in cell wall scale production *Chrysochromulina chitin*.
1967	Karim, A. G. A. and F. E. Round	Described cellulose-like microfibrils in the lorica of several species of *Dinobryon*.
1968	Belcher, J. H.	Used light and electron microscopy to describe the lorica in *Pseudokephrion pseudospirale*.

TABLE II (Continued)

Date	Author	Contribution
1968	Gold, K.	Reported proteins in the lorica of the ciliated protozoan Tintinnida.
1968	Tappan, H. and A. R. Loeblich	Discussed 2 basic lorica types for Tintinnida.
1969	Brown, R. M., W. W. Franke, H. Kleinig H. Falk and P. Sitte	Reported Golgi apparatus involvement in production of cellulosic wall components in Pleurochrysis scherffelii.
1969	Gold, K.	Used ^{14}C labeling on the lorica of Tintinnida.
1969	Kristiansen, J.	Described the interwoven microfibrillar structure of the lorica of Chrysolykos planktonicus.
1969	Nevo, Z. and N. Sharon	Revealed a non-cellulosic glucan as the predominant cell wall component in Peridinium westii.
1969	Peterfi, L. S.	Characterized the fine structure of the lorica of Poteriochromonas malhamensis as a microfibrillar meshwork.
1969	Wujek, D. E.	Postulated a mechanism for lorica development in Dinobryon sertularia.
1970	Brown, R. M., W. W. Franke, H. Kleinig H. Falk and P. Sitte	Showed cellulosic and non-cellulosic wall components produced by the Golgi apparatus in the Chrysophyceae.
1970	Kramer, D.	Described the fine structure of the lorica fibrils of Ochromonas malhamensis.
1971	Hilliard, D. K.	Discussed 3 possible modes of lorica synthesis in Dinobryon.
1971	Horne, R. W., D. R. Davies, K. Norton and M. Gurney-Smith	Isolated the cell wall from Chlamydomonas.
1972	Belcher, J. H. and E. M. F. Swale	Described the lorica of Chrysococcus cordiformis as thin and unmineralized.

TABLE II (Continued)

Date	Author	Contribution
1972	Kristiansen, J.	Discussed lorica morphology and microfibril arrangement in 5 Chrysophycean algae.
1972	Roberts, K., M. Gurney-Smith and G. J. Hills	Analysed the ultrastructure and chemical composition of the cell wall of Chlamydomonas reinhardi.
1973	Franke, W. W. and W. Herth	Described the structure and possible modes of lorica formation in Dinobryon sertularia.
1973	Hills, G. J.	Demonstrated reassembly of the dissociated cell wall components from Chlamydomonas reinhardi.
1974	Roberts, K.	Demonstrated the crystalline glycoprotein structure of many chlamydomonads.
1975	Gold, K. and E. A. Morales	Examined the mineral content of protozoan loricas.
1975	Leadbetter, B. S. C.	Used electron microscopy to describe 2 loricated protozoans.
1975	Leedale, G. F.	Described lorica development in Trachelomonas.
1975	Rosowski, J. R., R. L. Vadas and P. Kugrens	Described the surface configuration of the lorica of Trachelomonas by scanning electron microscopy.
1976	Porcella, R. A.	Reported sporopollinen in aplanospore loricas of Dysmorphococcus globosus.
1977	Herth, W., A. Kuppel and E. Schnepf	Characterized the microfilaments of the lorica of Poteriochromonas stipitata as chitinous rather than cellulosic.
1977	West, L. K.	Investigated the ultrastructure of Trachelomonas hispida var. coronata and the substructure, composition and biomineralization of the envelope.

TABLE II (Continued)

Date	Author	Contribution
1978	Gerard, D. A. and P. L. Walne	Reported the presence of calcium and silicon and a lack of iron in the lorica of Pteromonas protracta.
1978	Good, B. H. and R. L. Chapman	Described the cell wall of Phycopeltis (Chlorophyta) and reported sporopollenin as the major component.
1979	Donnelly, L. S.	Described the structure and composition of the envelope in 3 species of Trachelomonas.
1979	Gerard, D. A. and P. L. Walne	Described the structure, development and composition of the lorica of Pteromonas protracta, including the involvement of the Golgi apparatus in lorica production.
1979	Good, B. H. and R. L. Chapman	Reported sporopollenin in the lorica of Dysmorphococcus.
1979	Herth, W. and P. Zugenmaier	Reported cellulose I and protein in the lorica of Dinobryon.
1979	Moestrup, O. and P. L. Walne	Demonstrated the involvement of the Golgi apparatus in scale production in Pyramimonas tetrarhynchus.
1980	Porcella, R. A. and P. L. Walne	Described lorica development in Dysmorphococcus globosus.

The terminology used for structures which classically have been termed "loricas" has proliferated with the increased interest in these structures. Following the precedent of Pringsheim (1953), Leedale (1975), West (1977) and Donnelly (1979) elected to use the term "envelope" for the covering of various species of Trachelomonas. The finely fibrillar layer secreted first during envelope formation is referred to as a "skin" by Leedale (1975) and Donnelly (1979). Leedale observed that mineralization occurred interior to this structure, and Donnelly described mineralization exterior to the "skin." West (1977) did not observe a "skin" in his studies on T. hispida. Belcher (1969) described a "distinct outer bounding layer" in loricas of what were thought to be the youngest cells of Chrysococcus ruferscens, but he used no term for that layer. Porcella (1976) adopted the term "immature envelope" for a structure in Dysmorphococcus globosus that is analogous to the "skin" in some Trachelomonas species.

It is evident from the preceding paragraph that there will be difficulties with any terminology selected; therefore, the term lorica, used in most early descriptions of Pteromonas, has been retained to avoid any further proliferation of terminology. In keeping with the terminology adopted by Belcher and Swale (1967) for P. angulosa, the 2 distinct lorica layers in P. protracta will be referred to in the text as the inner (IL) (closer to the protoplast) and outer lorica (OL).

The primary objectives of this study are: 1) to characterize the process of lorica development and biomineralization, 2) to determine the chemical composition of the lorica, and 3) to compare the basic ultrastructure of vegetative cells of Pteromonas protracta with previously described volvocalean genera.

CHAPTER II

MATERIALS AND METHODS

Culture Conditions

Cultures of Pteromonas protracta (Stein) Lemm. (No. LB647) were obtained from the Indiana University Culture Collection of Algae (now at the University of Texas, Austin). Numerous defined media were used to try to attain satisfactory growth and development of cells. Cells were grown in glass petri plates (100x20 mm) containing 15 ml of 1% agarized Modified Bold's Basal Medium (MBBM) with a 10 ml overlay of liquid MBBM and were maintained indefinitely by transferring cells from actively growing cultures (7-10 days old) to new media. Cultures were also maintained for prolonged periods in a modified biphasic soil water medium (MSW) and were used for comparative studies with MBBM cultures (Appendix A). MSW cultures were maintained in 200-ml milk bottles containing 20 g of soil (from Nashville, Tennessee), ammonium phosphate and magnesium phosphate and overlaid with 100 ml of distilled water.

All cultures were maintained in growth chambers (Sherer models RT 18B-SE, RT 46B-SE) or in a modified cold room under 20w cool-white fluorescent illumination of 150-200 ft-c with a 12/12 or 16/8 L/D cycle at 18-20^{o}C.

For growth-curve studies MBBM cultures were grown on a 12/12 L/D cycle at 18-20^{o}C. Glass petri plates containing 15 ml of 1% agarized MBBM overlaid with 19 ml of liquid MBBM were inoculated with 1 ml from an actively growing culture to give a final concentration of 450 cells/ml. At intervals after inoculation, cultures were harvested by centrifugation

and fixed for 1 hr with 2% glutaraldehyde; samples were counted using a hemacytometer. Optical density and percent transmittance of the cultures were measured using a Bausch and Lomb Spectronic 20 Spectrophotometer.

Light Microscopy and Cytochemistry

Wet mounts of living cells, cells fixed with 2% glutaraldehyde in 0.05M cacodylate buffer, air-dried specimens and thick sections of plastic-embedded cells were examined with various optical techniques. These included bright-field, dark-field, phase-contrast, oblique illumination, and Nomarski differential-interference-contrast optics with the following microscope systems: 1) Zeiss WL Research microscope, equipped with bright-field, phase-contrast and Nomarski differential-interference-contrast optics, a Zeiss photographic system and a Leica M4 dark box M35; 2) Olympus VANOX Universal Research Microscope equipped with bright-field optics and an oblique illumination system, and an Olympus PM-10-A 35mm photographic system.

Aliquots of cells were removed from MBBM or MSW cultures and fixed with 2% glutaraldehyde in 0.05M cacodylate buffer for 1 hr, in preparation for cytochemical studies. Cells were gently concentrated by centrifugation, washed twice with distilled water and treated with various cytochemical stains to determine possible lorica constituents. The following cytochemical stains were employed: 1) Alcian blue, 2) Alcian yellow, 3) Methylene blue, 4) Mercuric Bromphenol, 5) Periodic Acid Schiff's Reagent, 6) Potassium ferrocyanide, 7) Ruthenium red, and 8) Toluidine blue. Details of the use and preparation of these stains are found in Appendix B.

Photographic data were recorded on Panatomic X (ASA 32), or Ektachrome (Tungsten, ASA 160) film, using appropriate filters.

Autoradiography

MBBM cultures were grown for 10 days in media containing 10 uC of ^{44}Fe. Cells from these cultures were harvested, washed throughly with unlabeled MBBM, fixed in 2% glutaraldehyde and postfixed in 2% osmium tetroxide both in 0.05M cacodylate buffer, dehydrated, and embedded in Spurr's plastic. Sections 1 um thick were cut with glass knives and mounted onto cleaned glass slides that were coated with Kodak NTB bulk liquid emulsion and exposed in the dark at 4-6^{o}C for 10 days. The slides were developed with Kodak D-19 for 2 min, placed in acid stop bath for 5 sec, fixed with Kodak Hypofixer for 2 min, treated with Kodak hypo-clearning agent for 2 min and rinsed in running water for 15 min. Slides were post-stained with methylene blue and made permanent with diaphane. Data were recorded on Panatomic X (ASA 32) film.

Transmission Electron Microscopy (TEM)

The following procedures were used for samples prepared for TEM. Cells were gently concentrated into a pellet in an International Clinical Centrifuge Model CL. The supernatant was decanted and fixative was added to the cells. Cells were resuspended and kept either at room temperature or 0-4^{o}C, until dehydration. Several fixatives were used: 1) 2% glutaraldehyde in fresh culture medium, pH adjusted to pH of medium with 0.1M NaOH, postfixed with 2% osmium tetroxide buffered with fresh culture medium and 0.025M phosphate buffer (1:1 v/v), pH 7.1; 2) 2% $KMnO_4$ in fresh culture medium, pH 7.1, at ca 4^{o}C (Luft, 1956); 3) 2% glutaraldehyde and 2% osmium tetroxide together in 0.05M cacodylate buffer, pH 7.1, at 0-4^{o}C, 4) 2% glutaraldehyde in 0.05M cacodylate buffer, pH 7.1, postfixed with

2% osmium tetroxide in 0.05M cacodylate buffer. Cells fixed by method 4 at 0-4^{o}C consistently gave superior results, and this procedure was used for most of the TEM preparations. Appendix C contains the fixation, dehydration and embedding schedules, and procedures for preparing the reagents.

Conventional thin sections. Ultrathin sections were obtained with Sorvall (Porter Blum) MT-1 or MT-2 ultramicrotomes or a Reichert OM-U3 ultramicrotome outfitted with either glass or dupont diamond knives. Light gold-to-silver sections (90-120 nm) were mounted on either uncoated or formvar-coated copper grids of various mesh sizes and patterns, then post-stained with aqueous uranyl acetate for 20-30 min and with lead citrate (Reynolds, 1963) for 5 min. Sections were examined and photographed with Zeiss EM9S, JEM 6C, or RCA 3D transmission electron microscopes.

Serial sections. Serial sections were obtained with a Dupont diamond knife mounted on either a Sorvall MT-2 or a Reichert OM-U3 ultramicrotome. Ribbons of 40-60 gold-to-silver sections were picked up on 0.2/0.5mm slot grids coated with formvar and carbon and were post-stained and examined as described above.

Thick sections. Sections of plastic-embedded cells (0.5-1.0 um) were obtained with either glass or Dupont diamond knives on a Sorvall MT-2 ultramicrotome. The sections were flattened with either xylene or chloroform vapors and mounted on clean glass slides for subsequent cytochemical staining and examination with light microscopy. Cells of interest were photographed with light microscopy. Occasionally, the thick sections

were remounted using a modification of the techniques described by Kaplin and Hinds, 1977 (Appendix C). The remounted thick sections were then thin sectioned as previously described, mounted onto formvar-coated slot grids, post-stained and examined with TEM.

Whole mounts. Chemically fixed or unfixed cells, or cell-free lorica preparations (see Analytical Electron Microscopy, p. 19) were washed several times with distilled water and air dried on formvar-coated 300-mesh grids or finder grids. The whole mounts were observed with TEM, and with the finder grids; the same specimen was also examined and analysed with SEM-EDX.

Acetolysis

Cells from MBBM and MSW cultures were concentrated to a pellet in 15-ml culture tubes by centrifugation and subjected to acetolysis to test for the presence of sporopollenin in the loricas of P. protracta (Atkinson et al., 1972). Eight ml of acetic anhydride/1 ml of concentrated sulfuric acid (8:1, v/v) were added to the pelleted cells which were then resuspended and the tube placed in a boiling water bath for 1 hr. After removal from the water bath, the remaining material was centrifuged, washed once with glacial acetic acid and several times with distilled water. A drop of the final pellet material was air dried on formvar-coated finder grids, examined with TEM and subsequently analysed with SEM-EDX.

Glusulase Treatment

Cells of P. protracta produce copious amounts of mucilage that often obscures the external structure of the lorica; therefore, fixed specimens to be shadow cast or examined with SEM were often pretreated with 1%

glusulase for 1 hr to remove excess mucilage from the surface of the loricas (Appendix C). The specimens were then washed 3-4 times with either distilled water or 0.05M cacodylate buffer and processed as were untreated samples.

Shadow-casting

To obtain additional information on the exterior ultrastructure of the lorica, and to enhance visualization of the fine flagellar hairs, fixed cells (either untreated or pretreated with glusulase) were air dried on formvar-coated grids and were shadow cast with a 20 nm coating of gold-paladium evaporated from 5 cm fo 8 mil wire (SPI) at an angel of ca 6^{o} and a distance of 15 cm in a Denton model DV-515 vacuum evaporator. The grids were then examined and photographed with TEM.

Scanning Electron Microscopy (SEM)

Cells were collected from MBBM or MSW cultures and fixed for 1 hr with 2% glutaraldehyde in 0.05M cacodylate buffer at 0-4^{o}C. The cells were then washed 2-3 times with distilled water. Some cells were treated with 1% glusulase for 1 hr and subsequently washed with distilled water. Both untreated and glusulase-treated cells were either air dried on 12-mm circular glass cover slips coated with 0.1% poly-l-lysine (Mazia et al., 1975), or were dehydrated in a graded acetone series in preparation for critical point drying (CPD). While in 100% acetone, dehydrated cells were mounted on 12-mm round cover slips coated with poly-l-lysine, transferred to a Bomar-12-mm cover slip holder (Model 2113) and processed in a Bomar Critical Point Drying apparatus (Model SPC-900/EX), with CO_2 used as the replacement liquid. The cover slips were then mounted onto aluminum SEM

stubs with double-stick tape and coated with ca 20 nm of gold-paladium (40/60, w/w) using a rotating stage in a Denton Model DV-515 vacuum evaporator. The procedure for preparing specimens for SEM is outlined in Appendix D.

Specimens were examined in an ETEC Autoscan or AMR-900 scanning electron microscope. Data were recorded on Polaroid type 55 positive/ negative film.

Analytical Electron Microscopy

Empty loricas were harvested from the bottom of culture vessels and concentrated by centrifugation to yield 80-90% cell-free lorica preparations. By this technique, cell-free loricas from MBBM and MSW cultures of various ages were obtained. These loricas were washed several times with double-distilled water to remove any cellular debris or bacteria Washed loricas were either pretreated with glusulase, 0.01mM EDTA or 0.01mM EGTA or left untreated; subsequently, the loricas were air dried on formvar-coated finder grids. The grids were examined with conventional TEM, and numerous empty loricas were photographed. The same grids were then mounted on spectroscopically pure SEM graphite stubs, modified to hold TEM grids (West, 1978), and the same loricas were analysed for elemental composition by scanning electron microscopy-energy dispersive spectroscopy (SEM-EDX) in an AMR-900 SEM equipped with an Ortec X-ray detector, model 6200 multichannel analyser (MCA) and a Hewlett-Packard X-Y recorder.

A light gold-to-silver section (ca 90 nm) of fixed plastic-embedded cells was cut immediately followed by a 0.5 um thick section from the same block. Both sections were flattened and mounted on separate formvar-coated slot grids. The 90 nm section was post-stained and examined with

conventional TEM to find suitable regions for analytical analysis. The appropriate areas were photographed, and the corresponding regions of the unstained 0.5 um thick section were analysed using a JEOL JEM-100C Analytical Electron Microscope (120 Kv) equipped with a Kevex X-ray detector and data processor (use of this instrument by courtesy of Dr. J. Bentley, ORNL). Chemical analyses of lorica components, cytoplasmic structures and contents were carried out using this technique.

CHAPTER III

RESULTS

Members of the Phacotaceae are distinguished from other volvocalean flagellates by a mineralized covering termed a lorica. In Pteromonas protracta, the lorica is composed of an inner lorica (IL) and an outer lorica (OL), as shown in a diagram of general ultrastructural features of the vegetative cell (Plate I, Figure 1).[1]

Basic Lorica Structure

The lorica is composed of 2 valves that are closely appressed to the protoplast. The valves are fused, forming a wing which laterally circumscribes the cell. The wing extends from the lorica 1.5-2.0 um. The flattened or indented nature of the anterior end of the lorica, as seen also with LM, is explained by the presence of a third, wedge-shaped segment which is fused to both valves. The wedge-shaped segment has 2 centrally located flagellar pores with thickened collars. The lorica surface is covered with slightly raised ridges that form a hexagonal pattern, with each hexagon measuring 0.20-0.25 um in diameter (Plate IV, Figures 13, 14; Plate V, Figures 15, 17).

TEM whole mounts and glancing thin sections show the basic hexagonal surface pattern, but they also reveal a secondary reticulum, which is characterized by numerous puncta, inside the primary hexagonal reticulum

---

[1]All plates and figures hereinafter referred to may be found in Appendix E.

(Plate II, Figures 2-4; Plate IV, Figures 13, 14; Plate VII, Figures 23-24). TEM thin sections through mature loricas show that a typical IL is granulo-fibrillar and closely appressed to the OL which is dense and amorphous with a scalloped margin which corresponds to the raised hexagonal pattern (Plate VII, Figure 22, 27). The IL and OL are joined at the anterior end of the cell to form the flagellar pores which are tightly appressed to the flagella (Plate VI, Inset).

Effects of Media on Lorica Structure

The data on comparative lorica structure and composition from cells grown in MSW and MBBM media are summarized in Table III. Structural differences are shown in Plate II, Figures 5-6; Plate III, Figures 7-12; Plate VII, Figures 22-27. A hexagonal pattern is a constant feature of all loricas from either medium. The pattern on the OL surface is evident on loricas from MSW cultures, whereas in loricas of cells grown in MBBM, the pattern is internal to a copious layer of mucilage and is thus obscured.

Lorica Composition

The elemental composition of loricas from MBBM and MSW cultures of 4 different ages were examined to determine whether the chemical composition varies with differences in the culture medium. Tables IV, V and VI summarize analytical data for all untreated loricas from MBBM and MSW cultures of all ages.

SEM-EDX of untreated loricas. Cell-free loricas from 3-, 7-, 14- and 60-day-old MBBM cultures and 14-day-old and 2-, 5-, and 18-month-old MSW cultures were examined with TEM and subsequently analyzed with SEM-EDX.

TABLE III

COMPARISON OF STRUCTURE AND ELEMENTAL COMPOSITION OF LORICAS FROM MSW AND MBBM CULTURES

Structure	Technique	Lorica Characteristics	
		MSW Cultures	MBBM Cultures
OL Surface	SEM and TEM shadowcast	Raised hexagonal pattern covers surface; little or no mucilage	Hexagonal pattern not evident; copious mucilage coating over surface
OL Interior	TEM whole mounts	Primary hexagonal reticulum evident; secondary reticulum characterized by numerous puncta	Indistinguishable from loricas from MSW cultures
	TEM thin sections	Compact, dense and amorphous with scalloped margin that corresponds to hexagonal pattern	Broad and diffuse with copious mucilage at margins
IL	TEM thin sections	Granulo-fibrillar; closely appressed to OL	Finely granular; often separated from OL
Elemental Composition			
OL	SEM-EDX STEM-EDX	Major peaks: Ca, P, Si. Fe detected in 87% of loricas, minor peaks variable	Major peaks: Ca, P. Si. Fe never detected, minor peaks variable

TABLE IV

SEM-EDX UNTREATED LORICAS

Element	Analysis of 100 MBBM Loricas		Analysis of 100 MSW Loricas	
	% Loricas with Element	CPC $X10^3$	% Loricas with Element	CPC $X10^3$
P	100	1750	100	1700
Ca	100	1600	100	1625
Si	81	1000	95	750
S	51	725	71	425
Cr	41	700	69	450
Fe*	0	--	87	500
Cl	33	650	45	350
Al	8	425	48	400
Mg	16	350	35	250
K	6	200	30	275
Mn	3	200	11	250
Ni	5	175	3	200
Hg	1	225	7	250

*Fe is the only element that appears in loricas from one medium (MSW) and not in loricas from the other (MBBM).

TABLE V

SEM-EDX OF LORICAS FROM 4 AGES OF MBBM CULTURES*

Element	3 Day-Old Culture		7-Day-Old Culture		14-Day-Old Culture		2-Month-Old Culture	
	% Loricas with Element	CPC_3 X10^3	% Loricas with Element	CPC_3 X10^3	% Loricas with Element	CPC_3 X10^3	% Loricas with Element	CPC_3 X10^3
P	100	1800	100	1750	100	1775	100	1650
Ca	100	1650	100	1500	100	1600	100	1625
Si	76	1100	84	1150	72	900	92	1200
S	40	700	48	750	72	650	72	675
Cr	36	650	44	625	36	800	36	650
Fe	--	--	--	--	--	--	--	--
Cl	32	675	32	625	28	725	40	425
Al	--	--	--	--	--	--	32	425
Mg	16	400	12	300	24	350	12	300
K	--	--	--	--	--	--	24	200
Mn	--	--	--	--	--	--	12	200
Ni	--	--	--	--	--	--	20	175
Hg	--	--	--	--	4	225	--	--

*25 loricas were analysed from age culture.

TABLE VI

SEM-EDX OF LORICAS FROM 4 AGES OF MSW CULTURES*

Element	14-Day Old Culture		2-Month-Old Culture		5-Month Old Culture		18-Month-Old Culture	
	% Loricas with Element	CPC_3 X10	% Loricas with Element	CPC_3 X10	% Loricas with Element	CPC_3 X10	% Loricas with Element	CPC_3 X10
P	100	1700	100	1800	100	1600	100	1725
Ca	100	1675	100	1700	100	1650	100	1625
Si	100	700	96	725	100	800	84	875
S	60	400	68	425	76	475	80	450
Cr	72	475	80	400	64	400	60	450
Fe	92	550	88	500	88	425	80	400
Cl	40	375	40	400	52	350	48	300
Al	56	525	48	475	48	200	40	300
Mg	40	350	28	325	48	200	24	200
K	36	275	24	300	32	275	28	300
Mn	--	--	8	200	12	325	24	275
Ni	--	--	--	--	--	--	12	200
Hg	--	--	--	--	12	275	16	250

*25 loricas were analyzed from each age culture.

Major peaks for Ca and P were recorded for all loricas from MBBM and MSW cultures analysed with SEM-EDX. A major peak for Si was recorded for 81% of the loricas from MBBM cultures and for 95% of the loricas from MSW cultures. Thus, Ca, P and Si constitute the major elemental components of loricas, regardless of culture medium (Table IV). Iron was never detected in any loricas from MBBM cultures, while 87% of the loricas analyzed from MSW cultures contained it. Typical spectra for loricas from 14- and 60-day-old MBBM cultures, together with micrographs of the loricas analysed are shown in Plate XIII, Figures 56-57, and Plate XIV, Figures 60-61, respectively; typical spectra for loricas from 14-day-old and 2-month-old MSW cultures are shown in Plate XIII, Figures 58-59, and Plate XIV, Figures 62-63, respectively.

SEM-EDX of glusulase-treated loricas. Cell-free loricas from 3-. 7-, 14- and 60-day-old MBBM cultures and from 14-day-old and 2, 5-, and 18-month-old MSW cultures were treated with 1% glusulase and subsequently examined with TEM and SEM-EDX. The glusulase-treated loricas were indistinguishable from untreated loricas when examined with TEM. The major elements detected with SEM-EDX were P, Ca and Si, but there were fewer total elements present in glusulase-treated loricas when compared with untreated loricas from MBBM or MSW cultures of the same age (Tables VII and VIII). Typical spectra and micrographs of glusulase-treated loricas from 14-day-old and 2-month-old MBBM and MSW cultures are presented in Plate XV, Figures 64-67, and Plate XVI, Figures 68-71, respectively.

TABLE VII

SEM-EDX OF GLUSULASE-TREATED LORICAS FROM 4 AGES OF MBBM CULTURES*

Element	3-Day-Old Culture		7-Day-Old Culture		14-Day-Old Culture		2-Month-Old Culture	
	% Loricas with Element	CPC_3 X10^3	% Loricas with Element	CPC_3 X10^3	% Loricas with Element	CPC_3 X10^3	% Loricas with Element	CPC_3 X10^3
P	100	1900	100	1850	100	1925	100	1800
Ca	100	1450	100	1500	100	1600	100	1625
Si	80	950	90	925	80	1000	70	975
S	40	250	50	250	50	225	60	250
Cr	--	--	40	200	--	--	40	225
Fe	--	--	--	--	--	--	--	--
Cl	40	200	40	275	60	300	50	400

*20 loricas were analysed from each age culture.

TABLE VIII

SEM-EDX OF GLUSULASE-TREATED LORICAS FROM 4 AGES OF MSW CULTURES*

Element	14-Day-Old Culture		2-Month-Old Culture		5-Month-Old Culture		18-Month-Old Culture	
	% Loricas with Element	CPC_3 X10^3	% Loricas with Element	CPC_3 X10^3	% Loricas with Element	CPC_3 X10^3	% Loricas with Element	CPC_3 X10^3
P	100	1825	100	1800	100	1750	100	1825
Ca	100	1600	100	1625	100	1700	100	1600
Si	80	850	90	900	80	1100	100	975
S	40	275	50	200	40	200	50	275
Cr	20	200	40	175	40	225	40	200
Fe	60	250	50	200	60	300	60	250
Cl	--	--	30	225	40	200	30	300

*20 loricas were analysed from each age culture.

EDTA-treated loricas. Loricas from 3- and 14-day-old MBBM cultures and from 14-day-old and 2-month-old MSW cultures were treated for 30 sec with 1uM EDTA, a chelating agent for cations. Examination by TEM showed no visible surface pattern and loricas were less dense than untreated loricas. A Ca peak was negligible in all loricas analysed. Silicon and P were the major elements detected in loricas from MBBM cultures, while Si, P and Fe were major elements detected in loricas from MSW cultures. Sulfur, Cr, Al and Mg were also detected in some loricas (Table IX; Plate XVII, Figures 72-75).

EGTA-treated loricas. Loricas from 3- and 14-day-old MBBM cultures and from 14-day-old and 2-month-old MSW cultures were treated for either 30 sec or 5 min with 1uM EGTA, a chelating agent for cations. Examination with TEM revealed that loricas treated for 30 sec retained a faint hexagonal surface pattern, whereas loricas treated for 5 min were completely devoid of any surface pattern. SEM-EDX analysis of loricas treated for 30 sec revealed that Ca was detected in appreciable amounts, but peaks were considerably lower than untreated loricas of the same age. In loricas from both MBBM and MSW cultures P and Si were the major elements detected while Fe was present in loricas from MSW (Plate XVIII, Figures 76-79). SEM-EDX analysis of loricas treated for 5 min showed essentially the same results, except that a Ca peak was negligible (Plate XIX, Figures 80-83). Tables X and XI summarize the results of SEM-EDX analysis of EGTA-treated loricas.

Cytochemical stains. Loricas from MBBM and MSW cultures of various ages were treated with a variety of cytochemical stains. Positive reactions

TABLE IX

SEM-EDX OF LORICAS TREATED FOR 30 SECONDS WITH 1uM EDTA*

	MBBM Loricas				MSW Loricas			
	3-Day-Old Culture		14-Day-Old Culture		14-Day-Old Culture		2-Month-Old Culture	
Element	% Loricas with Element	CPC_3 X10^3	% Loricas with Elements	CPC_3 X10^3	% Loricas with Element	CPC_3 X10^3	% Loricas with Element	CPC_3 X10^3
P	100	950	100	1000	100	1100	100	1050
Ca	80	150	90	175	90	175	100	200
Si	80	800	80	825	90	950	100	900
S	80	450	70	500	70	475	60	450
Cr	80	500	50	475	60	450	50	450
Fe	--	--	--	--	90	850	90	800
Al	20	450	40	400	40	500	30	500
Mg	20	175	30	175	20	150	30	200

*10 loricas were analysed from each age culture.

TABLE X

SEM-EDX OF LORICAS TREATED FOR 30 SECONDS WITH 1uM EGTA*

	MBBM Loricas				MSW Loricas			
	3-Day-Old Culture		14-Day-Old Culture		14-Day-Old Culture		2-Month-Old Culture	
Element	% Loricas with Element	CPC_3 X10^3	% Loricas with Element	CPC_3 X10^3	% Loricas with Element	CPC_3 X10^3	% Loricas with Element	CPC_3 X10^3
P	100	1050	100	1100	100	1200	100	1150
Ca	100	575	100	625	100	700	100	650
Si	80	850	90	875	80	900	70	925
S	60	400	70	500	40	600	60	450
Cr	50	500	60	450	60	400	50	475
Fe	--	--	--	--	90	575	90	550
Al	40	400	30	450	30	375	50	400
Mg	10	175	30	200	20	150	20	225

*10 loricas were analysed from each age culture.

TABLE XI

SEM-EDX OF LORICAS TREATED FOR 5 MINUTES WITH 1uM EGTA*

	MBBM Loricas				MSW Loricas			
	3-Day-Old Culture		14-Day-Old Culture		14-Day-Old Culture		2-Month-Old Culture	
Element	% Loricas with Element	CPC_3 X10^3	% Loricas with Element	CPC_3 X10^3	% Loricas with Element	CPC_3 X10^3	% Loricas with Element	CPC_3 X10^3
P	100	1150	100	1000	100	1100	100	1200
Ca	100	175	90	150	100	150	100	200
Si	90	850	80	850	80	900	90	1000
S	70	450	60	400	50	450	60	425
Cr	50	475	50	375	60	350	50	450
Fe	--	--	--	--	100	600	90	575
Al	30	300	40	350	30	300	40	300
Mg	--	--	20	200	20	225	30	200

*10 loricas were analysed from each age culture.

to the following stains were elicited in all loricas tested: 1) Methylene blue, 2) Toluidine blue, 3) Alcian blue, 4) Alcian yellow, 5) PAS, 6) Mercuric bromphenol blue, 7) Ruthenium red. LM of loricas from 14-day-old MBBM cultures stained with each of the above reagents are shown in Plate XII, Figures 45-53. Potassium ferrocyanide elicited negative tests in all loricas from MBBM cultures, whereas most loricas from MSW cultures gave at least a weak positive reaction to this stain (Plate XII, Figures 54, 55). The results from cytochemical staining indicate that the mucilage component of the lorica is a mucopolysaccharide with a protein moiety.

Autoradiography. Cells grown for 10 days in MBBM containing ^{55}Fe were harvested and processed for TEM. Thick-sections were examined for the presence of labeled Fe in either cells or loricas. All results from these experiments were negative.

Acetolysis. Cell-free loricas from 3-, 7-, 14- and 60-day-old MBBM and MSW cultures were subjected to acetolysis to test for the presence of a sporopollenin. A small number of loricas from older MSW cultures were intact after treatment. These were larger than loricas from motile vegetative cells, and upon examination by TEM showed only the hexagonal surface pattern and no secondary reticulum. SED-EDX analysis of these loricas yielded a simple spectrum with only P and Ca as detectable elements (Plate XX, Figures 84-85).

Hydrochloric acid treatment. Living cells from 3-, 7- and 14-day-old MBBM cultures and from 2-, 5- and 10-month-old MSW cultures were exposed to dilute (0.25%) HCl during observation with LM. In all cases, loricas dissolved with a bubbling action.

Lorica Development

Lorica development is initiated prior to the cessation of cytokinesis; lorica material being visible in extracellular vesicles between forming daughter cells (Plate XLI, Figure 172). A fine "skin" is visible close to the plasmalemma of forming daughter cells in the initial stages of development (Plate VI, Figures 18-20). As the lorica develops the "skin" moves away from the cell and forms the IL.

Two types of presumptive lorica precursor material (PLPM) are visible in Golgi cisternae, in Golgi-derived vesicles, in presumptive secretory vesicles and in extracellular vesicles or free external to the plasmalemma (Plate VI, Figures 18-21; Plate IX, Figures 32, 33; Plate XLI, Figure 172). The 2 PLPM types are dense cores and wispy fibrillar material. Material, which closely resembles the 2 types of PLPM seen in the Golgi apparatus, is deposited to the outside of the inner lorica and becomes incorporated into the OL. In immature loricas, dense cores somewhat smaller than those in Golgi cisternae, are regularly spaced around the cell external to the IL (Plate V, Figure 16; Plate VIII, Figures 28, 29). As the lorica matures, more dense cores can be seen in the OL and become interconnected by the wispy, fibrillar material (Plate VIII, Figures 30, 31). In some instances very dense loricas are formed around daughter cells prior to their release from the parent lorica (Plate VI, Figure 21); however, lorica development usually continues even after daughter cells are released. In mature loricas juxtaposition of the dense cores results in the formation of the primary hexagonal ridges, while the interconnection of the wispy fibrillar components forms the secondary reticulum (Plate VIII, Figure 31). STEM-EDX analysis of dense core PLPM in OL and in Golgi

cisternae of the same cells produce similar spectra, with Ca, P and Si as major peaks, regardless of culture medium. In contrast, analysis of cytoplasmic regions free of PLPM produces spectra with very low Ca peaks (Plate X, Figures 34-39; Plate XI, Figures 40-45). These data suggest that Golgi-derived PLPM is incorporated into the OL, presumably by reverse pinocytosis.

General Cellular Morphology and Ultrastructure

General morphology. The general morphological features of P. protracta visible with LM are shown in Plate XXI, Figures 86, 88. Vegetative cells are biflagellate and ellipsoidal to nearly spherical in shape. The protoplast varies in size from 8-16 um wide and 18-24 um long; the flagella are ca 26 um in length. A single nucleus lies in the anterior end of the cell. A large cup-shaped chloroplast occupies much of the rest of the protoplast and contains a prominent centrally located pyrenoid surrounded by numerous starch plates and a latero-anterior stigma (Plate XXI, Figure 88). The bivalved lorica, which appears flattened or indented at the anterior end with LM (Plate XXI, Figures 86, 88), is closely appressed to the protoplast and forms a flattened wing where the 2 valves are joined. The wing extends from the cell 1.5-2.0 um and is curved upward on one side of the protoplast and downward on the other side (Plate XXI, Inset; Plate XXII, Figure 91). The recurved nature of the wing accounts for the characteristic spiral swimming motion of the cell.

General ultrastructure and cellular organization. P. protracta exhibits a typical chlamydomonad cellular organization (Plate I, Figure 1; Plate XXIII, Figure 92). The nucleus is positioned in the center of the

anterior portion of the cell and may be surrounded by or in close association with the chloroplast (Plate XXIV, Figure 93). The centrally located pyrenoid is just posterior to the nucleus. The stigma, which immediately subtends the chloroplast envelope and the plasmalemma, lies at the same level in the cell (anterior to posterior) as the nucleus. Mitochondria are located throughout the cytoplasm and are commonly seen near the periphery of the cell and the chloroplast envelope. Dictyosome profiles occur around the nucleus and as an amplexis with ER. RER is often continuous with the outer nuclear membrane (Plate XXIV, Figures 93, 94).

Nucleus. The anteriorly located nucleus is slightly lobed and contains a large, centrally located, darkly staining nucleolus often with gaps in the matrix (Plate XXV, Figure 95). The nucleolus persists during early prophase when condensed chromatin is visible inside the nucleus, sometimes in close association with the inner nuclear membrane (Plate XXV, Figure 96). During prophase microtubules are frequently associated with condensed chromatin (Plate XXV, Figure 96). Nuclear pores are common and extend through both the inner and outer membrane, the latter usually studded with ribosomes (Plate XXV, Figure 98).

Endoplasmic reticulum. RER is generally present in the region of the nucleus and dictyosome profiles and is often continuous with the outer nuclear membrane (Plate XXIV, Figure 94). Proliferation of RER is evident in dividing cells, and closely aligned parallel arrays of 6-12 RER cisternae are often discernible around newly formed daughter nuclei and dictyosome profiles (Plate XXVI, Figure 99). Serial sections of the dictyosomes show blebbing of SER vesicles that coalesce and produce the

cisternae at the forming faces of the dictyosomes (Plate XXVI, Figures 100, 101).

Golgi apparatus and cytoplasmic vesicles. Two to 6 dictyosome profiles can be observed near the nucleus, depending on the plane and angle of section (Plate XXVI, Figure 102). Each profile consists of 6-12 curved cisternae, generally swollen at the lateral margins, with the forming faces oriented toward the interior of the cell (Plate XXVI, Figure 103; Plate XXVII, Figures 104-107). PLPM is often visible in the cisternae near the maturing faces, especially in cells undergoing division (Plate XXVII, Figures 104-107).

Membrane flow. Membrane flow, described as the movement of information and material from one membrane system to another, is a classic biological phenomenon (Morré et al., 1971). Serial sections, especially of dividing cells of P. protracta show this phenomenon as membrane continuity from the outer NM, to RER, to SER, to dictyosome cisternae and then to cytoplasmic vesicles, which may contain PLPM (Plate XXVII, Figures 104-107).

Mitochondria. In transverse section, numerous small, round-to-oval mitochondrial profiles occur at the periphery of the cell, in close proximity to the chloroplast and nucleus (Plate XXVIII, Figure 108), and near the basal bodies (Plate XXVI, Figure 134). Longitudinal sections often show long finger-like mitochondrial profiles, especially near the cell periphery (Plate XXVIII, Figure 109). Glancing sections sometimes show profiles with deeply lobed cristae (Plate XXVIII, Figure 110).

Contractile vacuoles. Two prominent anteriorly located contractile vacuoles, typical of chlamydomonad cells, function to maintain osmotic balance within the protoplast. They are formed by the coalescence of smaller cytoplasmic vesicles and alternately discharge their contents to the outside of the cell, as seen with LM. Fortuitous thin sections show both CV, one in the systolic state (discharged) and the other in the diastolic condition (filled) (Plate XXVIII, Figure 111).

Flagellar apparatus and cytoplasmic microtubules. The 2 isokont flagella are ca 24 um long and 1.2 um in diameter and manifest the typical 9+2 microtubular doublet arrangement in the axoneme. They are bounded by a single unit membrane that is continuous with the plasmalemma (Plate XXIX, Figure 116; Plate XXX, Figure 127). The flagella are surrounded by a barely discernible mucilaginous sheath (Plate XXIX, Figures 115, 116). Two types of flagellar hairs are evident in thin section and shadow-cast preparations (Plate XXIX, Figures 112-114). The first type are continuous with the flagellar membrane and are randomly distributed over the flagellar surface. These hairs are short and thick, measuring 1.0-1.4 um in length and ca 1.0 um in diameter (Plate XXIX, Figures 112-114). The second type are regularly arranged in 2 rows along opposite sides of the flagella and are long (3.0-4.5 um) and very fine. Although their origin is often obscured by the mucilage sheath, they apparently do not penetrate the flagellar membrane (Plate XXIX, Figure 112). The tips of the flagella are usually flattened and sometimes frayed, as axonemal microtubules become discontinuous (Plate XXIX, Figure 117).

Transverse sections at various levels along the flagellum from distal end to the basal body are shown in Plate XXX, Figures 118-127. Transverse

sections show that remnants of the central doublet enter the distal portion of the transition zone (Plate XXX, Figure 122). A ring of dense material connects the outer doublets of the axoneme with the flagellar membrane in the transition region (Plate XXX, Figure 127). In longitudinal section, the ring appears as a dense body on either side of the H-shaped piece (Plate XXX, Figure 122).

The 2 basal bodies lie in a V-configuration in a mitochondrial depression and are interconnected at their distal ends by a striated fiber (Plate XXI, Figures 132-134). Three basal bodies are sometimes seen in fortuitous sections (Plate XXXIV, Figure 144), and in some cases it is obvious that the cell is in the process of cell division, which would explain the extra basal bodies (Plate XXIV, Figure 145). Longitudinal sections of the region between the basal bodies show the distal striated fiber as a curved structure and 2 microtubular bands that originate just posterior to the fiber (Plate XXX, Figure 133). Four microtubular bands extend posteriorly from beneath the distal striated fiber but do not interconnect. Occasional glancing sections through the basal body region show bands of 2 (Plate XXI, Figure 133), 3 (Plate XXI, Figure 129) and sometimes 4 (Plate XXI, Figure 128) microtubules that originate from between the basal bodies. Random sections through that region reveal longitudinal arrays of 2, 3, 4 or 5 microtubules (Plate XXXI, Figures 130, 131; Plate XXXIII, Figures 139-143).

Cytoplasmic microtubules that occur in pairs (Plate XXXII, Figure 138) or as 1-3-1 (Plate XXXII, Figure 135) or as 1-4 (Plate XXXII, Figure 136) configurations are seen in transverse sections near the cell periphery

Cytoplasmic and intra-chloroplastidic microtubules may be in close association with the stigma (Plate XXIV, Figures 146-148). Occasional random sections show numerous microtubular profiles near the plasmalemma (Plate XXXII, Figure 137; Plate XXIV, Figures 149, 150).

Chloroplast, pyrenoid and stigma. The chloroplast contains numerous thylakoids that are arranged in stacks of 3-15 throughout the stroma (Plate XXXVI, Figure 153). Single or paired thylakoids enter the pyrenoids between the starch plates and in some sections are shown to traverse the matrix and to exit between 2 other starch plates (Plate XXXV, Figures 154-155). The stigma is closely appressed to the chloroplast membrane that subtends the plasmalemma, and contains 1, 2 or 3 plates of osmophilic granules, each plate separated by a single thylakoid (Plate XXXIV, Figure 146; Plate XXXVI, Figure 151). Glancing sections through the stigma show hexagonal osmophilic granules a result of tight packing (Plate XXXVI, Figure 152).

Growth curve. Growth studies were carried out with agar/liquid overlay MBBM cultures to determine both the reproductive rate and most advantageous times to harvest cells for subsequent studies of cytokinesis and lorica development. A lag phase of 18 hrs (from 0 time) precedes a log phase of 24-192 hrs (ca 8 days), during which doubling time of the cultures is ca 22 hrs. The following formula was used to calculate the doubling times (Buchanan and Fulmer, 1928):

$$G = \frac{t\ (\log 2)}{\log b - \log B}$$

Although the generation time remains approximately the same, most cells become non-motile toward the end of log phase and remain so during stationary phase. A standard growth curve generated by these studies is shown in Plate XXXVII, Figure 156. Measurement of percent transmittance at 650 nm was used because chlorophyll detection at this wavelength closely corresponds to cell number (Hansmann, 1973), and was carried out until day 8 (192 hrs) when the cultures entered stationary phase.

Life cycle. The stages of the life cycle of P. protracta documented with microscopy are diagramatically represented in Plate XXXVIII, Figure 158. Numbers 1-7 represent the common asexual reproductive cycle, and numbers 8-13 represent presumptive sexual reproduction which occurs almost exclusively in older MSW cultures.

Asexual reproduction. The first morphological indication of asexual reproduction is the production of a second pyrenoid in swimming cells (Plate XXXIX, Figure 159; Plate XL, Figures 164, 165). Observations with LM and TEM results indicate that the second pyrenoid arises from division of the original pyrenoid rather than by formation de novo (Plate XL, Figure 165). After the cell loses its flagella, rounds up and becomes quiescent, the 2 pyrenoids migrate to opposite lobes of the chloroplast (Plate XL, Figure 166). Mitosis occurs rapidly, and TEM thin sections reveal that the nuclear membrane persists at least into metaphase (Plate XLI, Figure 168). Cytokinesis proceeds from the anterior end of the cell through the posterior, with the chloroplast being the last major organelle to divide (Plate XXXIX, Figures 160-162, 164; Plate XLII, Figures 172-

174). TEM thin sections indicate that cytokinesis is accomplished by formation of a phycoplast. At the end of the mitotic process both nuclei lie close to the division plane; MT parallel the division plane; and RER and Golgi profiles occur near the forming phycoplast (Plate XLI, Figures 169,170; Plate XLII, Figure 171). During late cytokinesis PLPM is often visualized between the forming daughter cells (Plate XLII, Figure 172). Usually, asexual reproduction is completed with the production of 2 daughter cells (Plate XXXIX, Figures 162, 163); however, a second division at right angles to the first may be initiated prior to completion of cytokinesis, resulting in the production of 4 daughter cells (Plate XLIII, Figures 176-179). The newly formed daughter cells develop loricas and flagella prior to their release from the parent lorica (Plate XXXIX, Figure 163; Plate XLIII, Figure 178). Daughter cells are released by abcission of the parent lorica at the wing where the 2 valves of the lorica are joined.

Presumptive sexual reproduction. In this investigation, sexual reproduction occurred almost exclusively in older MSW cultures. Isogametes, indistinguishable in morphology from vegetative cells, fuse at their posterior ends and form a cytoplasmic bridge between the 2 gametes (Plate IL, Figures 180, 181). At this stage and during the entire fusion process, the loricas of the 2 gametes persist and eventually fuse and form a single lorica. Fusion continues toward the anterior ends of the cells, resulting in a transitory, two-headed, quadriflagellate stage; the wings of both loricas persist (Plate IL, Figures 185-187). A single pyrenoid is visible at this stage and a stigma is often apparent (Plate L, Figures 182-184).

Fully fused elipsoidal planozygotes manifest 2 wings on their loricas, one from each isogamete lorica (Plate L, Figure 188). Finally, the 4 flagella are lost, and the aplanozygote rounds up and forms the resistant stage in the life cycle (Plate L, Figure 189). Division of the aplanozygote, which is assumed to be meiotic, occurs under favorable conditions and results in the production of 4 biflagellate zoospores.

CHAPTER IV

DISCUSSION

Effects of Culture Conditions on Lorica Structure

Differences in growth media have been shown to have pronounced effects on lorica structure in P. protracta. The outer lorica of cells grown in MBBM are broad and diffuse, whreas the outer lorica of cells from MSW are dense, compact and amorphous, with scalloped edges and are similar to the outer lorica of P. angulosa (Belcher and Swale, 1967). Lorica composition is similar in these 2 outer lorica types, however. The diffuse structures from MBBM medium may represent an unconsolidated state where the mucilage component is not as compressed as in the dense structures from MSW medium. This suggestion is supported by the observation that loricas from MBBM appear to have more mucilage associated with them than do loricas from MSW medium. Further support for the idea is provided by Donnelly (1979) who observed that darker envelopes of Trachelomonas were thinner, and she postulated that they represented a more tightly packed form of the lorica mucilage than the broader envelopes that were lighter in color. Differences in media composition have also been shown to affect lorica structure and development in other phacotacean algae, Dysmorphococcus globosus (Porcella and Walne, 1980) and Phacotus lenticularis (Pocratsky, personal communication). In the latter, differences in lorica color and elemental composition can be correlated with changes in the media. Studies on numerous species of Trachelomonas suggest that envelope structure and development are affected by the environment and/or composition of the medium (Pringsheim, 1953; Singh, 1956; West, 1977; Donnelly, 1979).

A component of the medium that is replenished from the soil in MSW cultures may be rapidly depleted from the MBBM medium which lacks soil. Such a component may be necessary for lorica consolidation and continued development. Studies that involve the selective variation of media constituents would be helpful in determining which components are necessary for lorica consolidation, development and subsequent mineralization.

Lorica Composition

This study provides the first definitive data on lorica composition from P. protracta. SEM-EDX and STEM-EDX analyses demonstrate that P, Ca, and Si are the main elements in loricas analyzed regardless of medium. Although treatment with glusulase removes other elements and mucilage, it does not change the structure and conformation of the loricas when they are observed as TEM whole mounts. The disappearance of Al, Mg, Mn, K and Hg upon glusulase treatment suggests that they are loosely associated with the mucilage and not an integral part of the lorica structure. On the other hand, large amounts of Ca are present in both untreated and glusulase-treated loricas. Those treated with EDTA and EGTA, however, lose nearly all Ca and appear diffuse due to a concomitant disappearance of the hexagonal pattern, results suggesting that Ca may be the major element involved in the mineralization of the lorica and in the production of the hexagonal pattern. The role and form of Ca in lorica structure, development and composition may be further elucidated by studies involving the careful alteration of Ca concentrations and sources in the culture media. The Ca may be present in the form of calcite, as evidenced by the

reaction of P. protracta loricas to dilute HCl. The feasibility of this suggestion is supported by the fact that fossilized Phacotus loricas from lake sediments reacted in the same way to HCl and their main constituent has been found to be calcite (Bradbury, personal communication).

The question of why Fe is never detected in any loricas from MBBM cultures, even though it may be a prominent element in loricas from MSW cultures remains unanswered. Perhaps the form of Fe ($FeSO_4$) in MBBM cultures is not readily available to the cell or cannot be incorporated into the lorica. Pringsheim (1953) contended that reduced metals (Fe and Mn) are first accumulated by Trachelomonas in bottom layers of cultures, then deposited on the envelopes as the cells ascended into oxidizing conditions. Cells of P. protracta grown in MSW, migrate to the air/water interface in the light and return to the bottom of the culture vessel in the dark; however, MBBM cultures grown in petri plates do not allow for such migration, which may be necessary for the incorporation of Fe into the lorica. Future studies involving variations in the Fe salts in MBBM medium and in the types of culture vessels used (e.g., bottles or flasks vs. plates) may be helpful in determining whether the form of Fe is important for its incorporation into the lorica, and whether diurnal migration is necessary for its deposition.

Manganese is seldom detected except in trace amounts in loricas of P. protracta, and a corollary observation is that they never darken. Pringsheim (1953) postulated that Mn may be the element responsible for darkening in Trachelomonas envelopes, and Donnelly's (1979) work on Trachelomonas supports that hypothesis. Moreover, pale loricas of the phacotacean alga Phacotus lenticularis contain little Mn, whereas dark ones contain considerable amounts of Mn (Pocratsky, personal communication).

Since classical taxonomic studies of Pteromonas have reported darkened loricas on cells collected from nature (Pascher, 1927; Jane, 1944), it may be useful to examine the effects, if any, of different concentrations and forms of Mn on lorica color and composition in P. protracta. Since treatment with dilute HCl does not appear to affect cell viability, ultrastructural examination of cells after such treatment would show whether the OL is completely removed by such treatment. If so, and if the OL is subsequently regenerated, then additional studies at various times after treatment would help to clarify the process and sequence of lorica development. Also, the elemental composition of the IL, which is unknown at this time, could be analysed with STEM-EDX after removal of the OL.

Cytochemical stains of the organic constituents of the OL of P. protracta suggest the presence of mucopolysaccharides which are both acidic in nature and negatively charged (Parker and Diboll, 1966; Ramus, 1977). A protein moiety is also present as shown by a positive reaction to mercuric-bromphenol blue. These preliminary data, together with chemical analysis of lorica mucilage from the closely related alga, Phacotus lenticularis (Pocratsky, personal communication), suggest that the basic organic constituents of the lorica of P. protracta may be glycoproteins, which may indicate a closer compositional relationship to the cell wall of other chlorophycean algae than previously thought.

For example, recent studies have questioned the historical assumption that algal coverings contain cellulose as do most higher plants. Extensive research on the wall of Chlamydomonas reinhardi, for example, has shown that cellulose is not present as had previously been suggested (Walne, 1966). The wall is also composed of at least 6 distinct layers, and

chemical analysis reveals that a major wall component is a complex glycoprotein rich in hydroxyproline (Roberts et al., 1972; Hills, 1973; Roberts, 1974). Miller (1978) has recently reported similar findings for the cell wall of Chlorococcum oleofaciens (Chlorophyceae) which is composed mainly of a hydroxyproline-rich glycoprotein with no cellulose present. Chemical analysis of isolated loricas of P. protracta may prove valuable in determining whether the organic component of the lorica is similar to the glycoproteins found in the lorica of Phacotus lenticularis and in the cell wall of Chlamydomonas.

Lorica Development

Lorica development in Pteromonas protracta is distinctly different from that described for Dysmorphococcus globosus (Porcella, 1976; Porcella and Walne, 1980) and for some species of Trachelomonas where an "immature envelope" or "skin" is produced initially and lorica material is subsequently deposited (Leedale, 1975). In some other species of Trachelomonas (Donnelly, 1979) and in P. protracta, deposition of lorica material occurs external to the "immature envelope" or "skin." The initial layer may serve as a template for the development of the mature outer lorica. There is precedence in the literature for this hypothesis, since plasmalemma templates are reportedly associated with wall formation and ornamentation in the desmid Micrasterias, for example, where the primary wall is secreted unevenly in a pattern related to the ultimate form of the secondary wall (Kiermayer, 1970). In another desmid, Cosmarium botrytis, a differential membrane apparently functions in the production of the secondary wall (Pickett-Heaps, 1972). A plasmalemma template has also been implicated in the deposition of plaques of material in the outer wall of Pediastrum

boryanum and P. simplex (Millington and Gawlik, 1975). In Dysmorphococcus globosus the "immature envelope" or "skin" is tightly appressed to the plasmalemma during the first stages of lorica development and may contain a pattern for the incorporation of inorganic compounds (Porcella, 1976; Porcella and Walne, 1980). In P. protracta the dimensions of the hexagonal pattern are constant for all loricas examined and may indicate that production of the pattern is a highly regulated process, perhaps involving a template for the selective deposition of certain components at specific sites.

Involvement of Golgi Apparatus in Lorica Development

This investigation provides the first ultrastructural and chemical evidence for the involvement of the Golgi apparatus in the production of lorica material for any green alga. In P. protracta 2 types of material are visualized in the Golgi cisternae, in Golgi-derived vesicles and as non-vesiculate components of the lorica: i) wispy, fibrillar material and ii) dense cores that are similar in appearance to the scales shown by Stewart and Mattox (1977) for Heteromastix. The intracisternal cores in P. protracta are somewhat larger than those observed in the lorica. The size difference may be an artifact; however, the extracellular cores are more readily accessible to chemicals used in fixation and dehydration and may be affected by them, and/or the intracisternal cores may undergo further processing prior to their release to the outside of the cell. Further evidence that the intracisternal cores are eventually incorporated into the lorica is derived from STEM-EDX analysis of cores in the cisternae and the outer lorica in the same cell. Spectra from both are identical

in elemental composition with P, Ca and Si being the major elements detected. Although no definitive data could be obtained on the chemical nature of the wispy fibrillar material, its size and electron density are similar inside the cell and in the developing lorica.

Involvement of the Golgi complex in the production and processing of materials for secretion from cells is widely documented for numerous other eukaryotic systems. For example, the Golgi apparatus has been implicated in the production of scales in some chrysophytes (Brown 1969; Brown et al., 1969, 1970, 1973; Brown and Frank, 1976; Manton and Leedale, 1961), in some haptophytes (Outka and Williams, 1971; Allen and Northcote, 1975; Manton, 1976a; Manton, 1976b) and in some prasinophytes (Manton and Leedale, 1961; Manton, 1966a, 1966b; Gooday, 1971; Moestrup and Thomsen, 1974). Moestrup and Walne (1978) demonstrated that at least 4 of 6 types of scales produced by Pyramimonas tetrarhynchus are formed in the same cisternae, and that there is intracisternal differentiation, since 2 scale types are formed only at the cisternal periphery and the other scale types are formed in the central region. This type of intracisternal differentiation has not been observed in P. protracta where the 2 types of PLPM are not seen in the same Golgi cisternae or in the same vesicles.

In the euglenoids, mucilage is produced and secreted by subpellicular muciferous bodies that are continuous with the well-developed endoplasmic reticulum. Triemer (1980) has recently shown, however, that the muciferous bodies are not the only source of mucilage produced in Euglena gracilis. Using periodic acid-silver methenamine staining, he showed that the Golgi

complex is involved in the production of mucilage that is secreted through the resevoir during cyst formation.

In the foraminiferan Rosalina floridana, Angell (1979) used ^{45}Ca to trace the calcification process, and Sullivan (1976, 1979) used ^{68}Ge to trace the pathway of Si in the mineralization process of the diatom Navicula pelliculosa. Future studies involving the use of radioactive isotopes and thin-section autoradiography could be valuable in determining the intracellular pathway of lorica precursor material and in correlating lorica development with specific stages in the life cycle of Pteromonas protracta. Also, "en bloc" staining with periodic acid-silver methenamine would be helpful in determining whether the wispy, fibrillar material in the Golgi apparatus and in the outer lorica of P. protracta have comparable staining qualities and may thus be similar in chemical composition.

Biomineralization

Two distinct stages of biomineralization occur in P. protracta. Active biomineralization, involving Ca and perhaps Si, is mediated by the cell with material processed through the Golgi apparatus. That material in the form of dense cores and wispy fibers, is then added to the outer lorica in a specific pattern, and those biomineralizing elements constitute an integral part of the lorica.

Passive biomineralization involves the accrual of cations on the negatively charged organic component(s) of the lorica. The extent of biological control involved in this stage is unclear at present, but it might be inferred that at least some mineralization occurs in cell-free loricas. For example, cell-free loricas harvested from progressively

older cultures have been shown to contain increasingly greater numbers of elements, a result suggesting that elemental accrual may continue even without direct biological regulation. Maintenance of cell-free loricas in various media and monitoring their elemental composition at selected intervals might help to determine whether cellular activity is necessary for secondary mineralization to occur or whether the process is a completely passive one.

The mechanism for primary mineralization of the outer lorica of P. protracta may be similar to that described by Leedale (1975) for Trachelomonas where a "skin" forms a compartment around the cell within which mineralization occurs, possibly under cellular control. Secondary mineralization, however, may involve a second mechanism as described by Isenberg and Lavine (1973), where the organic material to be mineralized is selective for the mineralizing agent. In P. protracta the negatively charged mucopolysaccharide component of the lorica may serve as the organic material and cations as the mineralizing agents.

Lorica Function

Two possible functions are generally recognized for biomineralized structures: physical support and/or protection and biochemical regulation (Isenberg and Lavine, 1973). It is unlikely that the lorica is essential for physical support since cells have a well-developed microtubular cytoskeleton similar to that reported for Chlamydomonas which lacks a lorica (Ringo, 1967; Moestrup, 1978). Protection from predation does not appear to be a likely function either since Pteromonas and other members of the Phacotacean are voraciously grazed upon by zooplankton (personal observation).

It is more likely that the lorica functions as a biological regulator in P. protracta. Members of the Phacotaceae are found in eutrophic habitats (Cole, 1955; and personal observations), and because of its negatively charged nature the lorica may act as a sink for toxic cations that would normally be harmful to the cell. For example, even though Al has been shown to be toxic at relatively low levels to most biological systems tested, it is often detected, sometimes as a major element, in the loricas of P. protracta and Phacotus lenticularis (Pocratsky, personal communication).

General Ultrastructure

The general ultrastructure of P. protracta is compared with the phacotacean species Dysmorphococcus globosus (Porcella, 1976), Pteromonas tenuis and Pteromonas angulosa (Belcher and Swale, 1967), and to previously studied volvocalean algae.

Nucleus. The nucleus is similar in structure to the phacotacean algae mentioned above and its position may be related to the number and position of the pyrenoids. In D. globosus (Porcella, 1976) and P. tenuis (Belcher and Swale, 1967), numerous small pyrenoids are dispersed throughout the chloroplast, and the nucleus is posteriorly located in the hollow of the cup-shaped chloroplast, whereas in P. protracta, P. angulosa (Belcher and Swale, 1967) and Chlamydomonas reinhardi (Ringo, 1967), a large basal pyrenoid extends the central portion of the chloroplast to the middle of the cell and physically limits the nucleus to the anterior region of the cell.

Contractile vacuole (CV). The location and operation of these organelles is similar to that described for other volvocalean genera (Lang, 1963a; Lembi and Lang, 1965; Walne, 1967); however, the phacotacean genera D. globosus (Bold and Starr, 1953; Porcella, 1976) and Haematococcus (Smith, 1950) possess numerous CV randomly located in the cell, and generally in close association with the plasma membrane. Porcella (1976) speculated that CV are involved in the secretion of lorica material in D. globosus. The location of the CV, near the plasmalemma close to dictyosome profiles, and the fact that electron-dense material is occasionally seen in them, suggests that these organelles may be involved in the movement of material from the cytoplasm to the exterior of the cell. Labeling studies with ^{45}Ca and ^{68}Ge should be useful in determining whether the CV are involved in the secretion of lorica material.

Flagella. This study has shown for the first time in any volvocalcean alga, the presence of flagellar hairs that are continuous with the flagellar membrane. These flagellar hairs persist after various treatments and are visualized with different techniques, and therefore are not considered to be artifacts. They are termed here simply "flagellar hairs" because they do not meet a generally recognized definition of mastigonemes as "any essentially filamentous appendages that are clearly distinct from the flagella membrane or its amorphous coverings" (Bouck, 1972). In P. protracta there are also 2 rows of long mastigonemes which are easily dissociated from the flagellum and which are similar to those described for Chlamydomonas (Ringo, 1967; Bouck, 1972; McLean and Brown, 1974). Porcella (1976) described short mastigonemes arranged in 2 rows

along the length of the flagella of D. globosus. Mastigonemes are also common on the flagella of chrysophytes, dinoflagellates, prasinophytes, cryptophytes and euglenophytes, but have seldom been described for any chlorophytes (Bouck, 1972). The elaborate mastigonemes of the euglenoids have been studied extensively, and there is evidence that they are connected to the axonemal microtubules (Bouck et al., 1978). The function of the flagellar hairs described in the present study for P. protracta is questionable but may be the same as that proposed for mastigonemes in general, i.e., operational in the swimming motions of the flagella (Bouck, 1972).

Chloroplast, pyrenoid and stigma. The general ultrastructure of these organelles is similar to that previously described for other chlorophytes (Lang, 1963; Belcher and Swale, 1967; Walne, 1967); however, the present study describes both cytoplasmic and intrachloroplastidic microtubules close to the stigma, an association that may represent a structural connection between the flagellar apparatus and the stigma. This observation provides some support to the speculation that a functional relationship may exist between the stigma and the flagellar apparatus of various algae (Moestrup, 1978). The stigma of volvocalean algae is contained within the chloroplast and historically has not been thought to be associated with the flagella (Dodge, 1969); however, Pickett-Heaps (1975) showed microtubules from a flagellar root in close association with the stigma in Volvox. In euglenoids it has been demonstrated for many species that the large stigma is covered with a layer of evenly spaced microtubules that may represent a connection between the flagellar apparatus and the stigma (Walne, 1971; Moestrup, 1978).

Sexual reproduction. This is the first report of presumptive sexual reproduction of Pteromonas that involves the fusion of loricated isogametes and contradicts a report by Smith (1950) that Pteromonas gametes are naked. This reproductive process is observed only in older MSW cultures, and the aplanozygotes which result may be the resistant stage in the life cycle for P. protracta. In support of this suggestion, Belcher and Swale (1967) mentioned that P. tenuis, commonly found in temporary ponds, never produces resistant stages in defined medium, and they speculated that the resistant stage necessary in nature may be an aplanozygote. Moreover, only large loricas of P. protracta, probably from aplanozygotes from older MSW cultures, are resistant to acetylosis, a test for the presence of sporopollenins (compounds commonly found in walls of resistant cells such as pollen grains, spores and aplanospores). Similar results were obtained by Porcella (1976) when he subjected aplanospores of D. globosus to acetolysis. Research on the conditions which trigger aplanozygote formation and subsequent germination are needed to further elucidate the sexual phase of the life cycle of P. protracta.

Phylogeny and Taxonomy

The present study is the first ultrastructural examination of the flagellar apparatus and features of mitosis and cytokinesis for any phacotacean organisms. Differences in these features have recently been used to separate the green algae into 2 classes (Pickett-Heap, 1969, 1972b; Stewart et al., 1973; Stewart and Mattox, 1975a, 1975b; Moestrup, 1978; Melkonian, 1980).

The flagellar apparatus of P. protracta, typical of that described for members of the Chlorophyceae, has a cruciate microtubular rootlet system which is probably in a 4-2-4-2 configuration, although profiles of 3 or 5 microtubules are sometimes observed. Such odd-numbered rootlets may represent the splitting or termination of a single microtubule near the basal body region as described for Chlamydomonas reinhardi (Moestrup, 1978). The 2 basal bodies of P. protracta are connected by a distal striated fiber similar to that described for C. reinhardi (Ringo, 1967), and Melkonian (1980) observed that a striated fiber connection between basal bodies is common to most members of the Chlorophyceae.

During mitosis P. protracta displays a persistent nuclear membrane, at least into metaphase, and cytokinesis is accomplished by the formation of a phycoplast. Both of these characteristics have been observed for numerous members of the Chlorophycease (Goodenough and Porter, 1968; Goodenough, 1970; Triemer and Brown, 1974; Mattox and Stewart, 1977; Graham and McBride, 1978).

On the basis of this study and that of Belcher and Swale (1967), it is suggested that P. protracta and P. angulosa may be the same species. Cell sizes and ultrastructural features including lorica structure are strikingly similar. Comparative studies on cultures of P. angulosa and P. protracta from the Culture Centre of Algae and Protozoa, Cambridge, England, and the University of Texas Culture Collection should help to resolve the taxonomic disposition of the 2 species.

To find a common ancestor for the 2 classes of the Chlorophyta, recent attention has been focused on members of the Prasinophyceae. Members of this loosely allied class are generally considered to be more

primitive than other green algae. A common feature of most prasinophytes is their possession of scales that cover the protoplast and flagella (Stewart and Mattox, 1975a). The dense cores produced by P. protracta resemble the scales of the prasinophyte, Heteromastix, and it is suggested that Pteromonas may be representative of a transitional group between the more primitive scaly prasinophytes and the non-scaly chlorophyceae. STEM-EDX analysis of the scales of Heteromastix could be useful in determining if their elemental composition is similar to the dense cores of P. protracta. If compositional similarities exist it would imply that there is a similar pathway for the production of scales and dense cores and therefore a possible close phylogenetic relationship between these 2 species.

CHAPTER V

SUMMARY AND CONCLUSIONS

The ultrastructure of the phacotacean flagellate, Pteromonas protracta (Volvocales), was investigated, with special reference to lorica structure, composition and development. The bilayered lorica is composed of 2 valves that are closely appressed to the protoplast. The valves are fused, forming a wing which circumscribes the cell. The wing extends from the lorica 1.5-2.0 um. A third, wedge-shaped lorica segment with 2 flagellar pores is located at the anterior end of the cell and is fused to both valves. The surface of the outer lorica (OL) is covered with a raised hexagonal pattern; a secondary reticulum between the hexagonal ridges, is characterized by numerous puncta. Different culture media affect lorica structure but not basic elemental composition. In mature loricas from modified soil water (MSW) cultures, the OL is dense and amorphous with a scalloped margin which corresponds to the hexagonal surface pattern. The inner lorica (IL) is granulo-fibrillar and closely appressed to the OL. In cells grown in modified Bold's Basal Medium (MBBM), the IL is finely granular, and the OL is broad and diffuse with the hexagonal pattern obscured by a copious mucilaginous layer.

The major elements detected in all loricas analyzed by SEM-EDX and STEM-EDX are P and Ca, and Si is detected in over 85% of the loricas, regardless of culture medium or age. Sulfur is present in over 50% of the loricas from either medium, while Fe is present in 87% of loricas from MSW cultures, but never detected in loricas from MBBM cultures. Other

elements such as Cr, Cl, Al, Mg, K, Mn, Ni and Hg are found in less than 50% of all loricas and are often removed from them by treatment with glusulase, a result suggesting that they are loosely associated with the mucilage component of the loricas. Results of tests with a variety of cytochemical stains indicate that the mucilage is an acidic and negatively charged mucopolysaccaride containing a protein moiety. That Ca is localized in the primary hexagonal pattern and forms the basic structural component of the OL is suggested by analysis of loricas subjected to acetolysis and EDTA and EGTA treatment. Observations of loricas treated with dilute HCl indicate that the Ca might be in the form of calcite.

The Golgi apparatus has been implicated in the production of presumptive lorica precursor material (PLPM) for the first time in any green alga. Two types of PLPM, dense cores and wispy fibrillar material, are visible in the Golgi cisternae and associated vessicles. STEM-EDX analysis of dense cores in the Golgi cisternae and in the OL of the same cell produce strikingly similar spectra, with Ca, P and Si as the major elements detected. Lorica development begins with the production of a fine "skin" which initially is closely appressed to the plasmalemma and which becomes the IL as development proceeds. As the OL matures, juxtaposition of the dense cores forms the primary hexagonal pattern, while interconnection of the wispy fibrillar material forms the secondary reticulum. The presumptive role of the IL as a template for the orderly development of the OL is discussed.

Ultrastructural studies have shown that the structure and cellular organization in P. protracta are generally similar to other volvocalean flagellates. Features documented for the first time in any member of the

Phacotaceae include 2 types of flagellar hairs, one continuous with the flagellar membrane and the other easily dissociated from it, and the presence of a cruciate flagellar rootlet system with a 4-2-4-2 microtubular arrangement. During mitosis a closed mitotic spindle persists at least into metaphase, and cytokinesis is effected by the production of a phycoplast. Both cytoplasmic and intrachloroplastidic microtubules have been observed in close proximity to the stigma.

LITERATURE CITED

LITERATURE CITED

Allen, M. B. 1956. Excretion of organic compounds by Chlamydomonas. Arch. Mikrobiol. 24:163-168.

Angell, R. W. 1979. Calcification during chamber development in Rosalina floridana. J. Foram. Res. 9:341-353.

Atkinson, A. W., B. E. S. Gunning and P. C. L. John. 1972. Sporopollenin in the cell wall of Chlorella and other algae: Ultrastructure, chemistry and incorporation of "C^{14}-acetate," studied in synchronous cultures. Planta 107:1-32.

Belcher, J. H. 1968. Lorica construction in Pseudokephyrion pseudospirale Bourrelly. Br. Phycol. Bull. 3:495-499.

Belcher, J. H. 1969. A morphological study of the phytoflagellate Chrysococcus rufescens Klebs in culture. Br. Phycol. J. 4:105-117.

Belcher, J. H. and E. M. F. Swale. 1967. Observations on Pteromonas tenuis sp. nov. and P. angulosa (Carter) Lemmerman (Chlorophyceae, Volvocales) by light and electron microscopy. Nova Hedwigia 13: 353-359.

Belcher, J. H. and E. M. F. Swale. 1972. Some features of the micro-anatomy of Chrysococcus cordiformis Naumann. Br. Phycol. J. 7:53-59.

Blackwell, J., K. D. Parker and K. M. Rudall. 1967. Chitin fibers of the diatoms Thalassiosira fluviatilis and Cyclotella cryptica. J. Mol. Biol. 28:383-385.

Bold, H. C. 1938. Notes on the Maryland algae. Bull. Torrey Bot. Club 65:293-301.

Bold, H. C. 1942. The cultivation of algae. Bot. Rev. 8:69-138.

Bold, H. C. and R. C. Starr. 1953. A new member of the Phacotaceae. Bull. Torrey Bot. Club 80:178-186.

Bold, H. C. and M. J. Wayne. 1978. Introduction to the Algae. Structure and Reproduction. Prentice-Hall, Inc. Englewood Cliffs. 706 pp.

Bouck, G. B. 1972. Architecture and Assembly of mastigonemes. In: Advances in Cell and Molecular Biology (E. J. DuPraw, Ed.). 237-271.

Bouck, G. B., A. Rogalski and A. Valaitis. 1978. Surface organization and composition of Euglena. II. Flagellar Mastigonemes. J. Cell Biol. 77:805-826.

Bourrelly, P. 1957. Initiation pratique a la systematique des algues d'eau douce V. Bull. Microscopie Appliquee. 6:122-144.

Bourrelly, P. 1966. Les algues d'eau douce: Initiation a la systematique Tome 1: Les Algues Vertes. BouBee & Cie, Paris.

Brinley, F. J. and L. J. Katzin. 1942. Distribution of stream plankton on the Ohio river system. Amer. Mid. Nat. 27:177-190.

Brown, R. M. 1969. Observations on the relationship of the Golgi apparatus to wall formation in the marine Chrysophycean alga, Pleurochrysis scherffelii Pringsheim. J. Cell Biol. 41:109-123.

Brown, R. M., W. W. Franke, H. Kleinig, H. Falk and P. Sitte. 1969. Cellulosic wall component produced by the Golgi apparatus of Pleurochrysis scherffelii Pringsheim. Science 166:894-896.

Brown, R. M., W. W. Franke, H. Kleinig, H. Falk and P. Sitte. 1970. Scale formation in Chrysophycean algae. I. Cellulosic and noncellulosic wall components made by the Golgi apparatus. J. Cell Biol. 45:246-271.

Brown, R. M., W. Herth, W. W. Franke and D. Romanovicz. 1973. The role of the Golgi apparatus in the biosynthesis and secretion of a cellulosic glycoprotein in Pleurochrysis: a model for the system for the synthesis and secretion of structural polysaccarides. In: Biogenesis of Plant Cell Wall Polysaccarides. F. Loewus, Ed. Academic Press, Inc., New York. 207-257.

Brown, R. M. and W. W. Franke. 1971. A microtubular crystal associated with the Golgi field of Pleurichrysis scherffelii. Planta. 96:354-363.

Buchanan, R. L. 1919. Life phases in a bacterial culture. J. Intert. Dis. 23:109-125.

Ciulei, I. and M. Alexandru. 1977. Contributions to identification of mucilage in plant tissues by means of toluidine blue. Bull. Soc. Bot. Fr. 124:45-50.

Cole, G. A. 1955. An ecological study of the microbenthic fauna of two Minnesota lakes. Amer. Midl. Nat. 53:213-230.

Conrad, W. 1930. Flagellates nouveaux ou peu connus. I. Arch. Protistenk. 70:657-680.

Cronshaw, J., A. Meyers and R. D. Preston. 1958. A chemical and physical investigation of the cell walls of some marine algae. Biochim. Biophys. Acta. 27:89.

Dangeard, P. A. 1899. "Memoire sur les Chlamydomonadinees ou l'histoire d'une cellule. Botaniste. 6:65-292.

Dodge, J. D. 1969. A review of the fine structure of algal eyespots. Br. Phycol. J. 4:199-210.

Dodge, J. D. 1973. The Fine Structure of Algal Cells. Academic Press, New York.

Donnelly, L. S. 1979. Comparative Cellular Ultrastructure and Chemical Characterization of Envelopes of Three Species of Trachelomonas. (Euglenophyta). Ph.D. Dissertation, The University of Tennessee, Knoxville.

Evans, J. H. 1964. Pteromonas varians Jane [P. aequicolata (Geckh.) Bourr.]: Notes on its taxonomy, occurrence and growth in culture. Br. Phycol. Bul. 2:317-326.

Foot, B. 1957. The taxonomy of microscopic flora of our ponds. Preslia. 29:278-319.

Franke, W. W., S. Krien and R. M. Brown. 1969. Simultaneous glutaraldehyde-osmium tetroxide fixation with postosmication. Histochemie. 19: 162-164.

Franke, W. W. and W. Herth. 1973. Cell and lorica fine structure of the Chrysomonad alga, Dinobryon sertularia Ehr. (Chrysophyceae). Arch. Mikrobiol. 91:323-344.

Gerard, D. A. and P. L. Walne. 1978. Preliminary observations on lorica structure and composition in Pteromonas protracta (Volvocales). ASB Bulletin 25:305.

Gerard, D. A. and P. L. Walne. 1979. Pteromonas protracta: TEM and SEM-EDX of a loricated green alga (Volvocales). J. Phycol. Supple. 15:15.

Gold, K. 1968. Some observations on the biology of Tintinnopsis sp. J. Protozool. 15:193-194.

Gold, K. 1969. Tintinnida: Feeding experiments and lorica development. J. Protozool. 16:507-508.

Gold, K. and E. A. Morales. 1975. Tintinnida of the New York bight: Loricae of Parafavella gigantia, P. parudentata and Ptychocyclis obtusa. Trans. Am. Micro. Soc. 94:142-145.

Gold, K., R. M. Pfister and V. R. Liguori. 1970. Axenic cultivation and electron microscopy of two species of choanoflagellida. J. Protozool. 17:210-212.

Good, B. H. and R. L. Chapman. 1978. The ultrastructure of Phycopeltis (Chroolepidaceae: Chlorophyta). I. Sporopollenin in the cell walls. Amer. J. Bot. 65:27-33.

Good, B. H. and R. L. Chapman. 1979. A comparison between the walls of Haematococcus cysts and the loricas of Dysmorphococcus, and the possible presence of a sporopollenin. J. Phycol. Supple. 15:17.

Gooday, G. W. 1971. A biochemical and autoradiographic study of the role of the golgi bodies in thecal formation in Platymonas tetrathele. J. Exp. Bot. 23:959-971.

Goodenough, U. W. 1970. Chloroplast division and pyrenoid formation in Chlamydomonas reinhardi. J. Phycol. 6:1-6.

Graham, L. E. and G. E. McBride. 1978. Mitosis and cytokinesis in sessile sporangium of Trentepohlia aurea (Chlorophyceae). J. Phycol. 14:132-137.

Green, J. C. and P. H. Jennings. 1967. A physical and chemical investigation of the scales produced by the golgi apparatus within and found on the surface of the cells of Chrysochromulina chiton Parke et Manton. J. Exp. Bot. 18:359.

Hansmann, E. 1973. Pigment Analysis. In: Handbook of Phycological Methods: Culture Methods and Growth Measurements. (J. R. Stein, Ed.). Cambridge University Press, Cambridge. 359-368.

Hayat, M. A. 1970. Principles and Techniques of Electron Microscopy: Biological Applications I. Van Nostrand Reinhold Comp., New York.

Herth, W., A. Kuppel and E. Schnepf. 1977. Chitinous fibrils in the lorica of the flagellate chrysophyte Poterioochromonas stipitata (syn. Ochromonas malhamensis). J. Cell Biol. 73:311-321.

Herth, W. and P. Zugenmaier. 1979. The lorica of Dinobryon. J. Ultra. Res. 69:262-272.

Hilliard, D. K. 1971. Observations on the lorica structure of some Dinobryon species (Chrysophyceae), with comments on related genera. Oesterr. Bot. Z. 119:25-40.

Hilliard, D. K. and B. Asmund. 1963. Studies on Chrysophyceae from some ponds and lakes in Alaska. II. Notes on the genera Dinobryon, Hyalobryon and Epipyxis with descriptions of new species. Hydrobiol. 22:331-400.

Hills, G. J. 1973. Cell wall assembly in vitro from Chlamydomonas reinhardtii. Planta (Berlin) 155:17-23.

Hills, G. J., M. Gurney-Smith and K. Roberts. 1973. Structure, composition and morphogenesis of the cell wall of Chlamydomonas reinhardtii. II. Electron microscopy and optical diffraction analysis. J. Ultrastruct. Res. 43:179-192.

Horne, R. W., D. R. Davies, K. Norton and M. Gurney-Smith. 1971. Electron-microscope and optical diffraction studies on isolated cell walls from Chlamydomonas. Nature 232:493-495.

Hortobagyi, T. 1949. Coccomonas eberii n. sp. Eine neue phytomonade des Balaton-Sees. Borbasia 9:22-27.

Isenberg, H. D. and L. S. Lavine. 1973. Protozoan calcification. In: Biological Mineralization (I. Zipkin, Ed.). Wiley and Sons, New York. 649-686.

Jane, F. 1944. Studies on the British Volvocales. New Phytol. 43:36-48.

Jensen, W. A. 1962. Botanical Histochemistry. W. H. Freeman and Comp., San Francisco.

Johansen, D. 1969. Plant Microtechnique. McGraw-Hill Book Comp., New York. 523 pp.

Kamptner, E. 1950. Ueber den aufbau kalkgehauses von Phactus lendneri Chod. Oesterneich. Bot. Zeitschr. 97:391-402.

Kaplin, M. S. and J. W. Hinds. 1977. Neutogenesis in the adult rat: Electron microscopic analysis of light radioautographs. Science 197:1092-1094.

Karim, A. G. A. and F. E. Round. 1967. Microfibrils in the lorica of the freshwater alga Dinobryon. New Phytol. 66:409-412.

Kiermayer, O. 1970. Causal aspects of cytomorphogenesis in Micrasterias. Ann. N. Y. Acad. Sci. 175:686-701.

Kramer, D. 1970. Fine structure of growing cellulose fibrils of Ochromonas malhamensis Pringsheim (syn. Poterioochromonas stipitata Scherffel). Z. Naturforsch. 25b:1017-1020.

Kristiansen, J. 1969. Lorica structure in Chrysolykos (Chrysophyceae) Bot. Tidsskr. 64:162-168.

Kristiansen, J. 1972. Studies on the lorica structure in the Chrysophyceae. Sven. Bot. Tidsk. 66:184-190.

Lackey, J. B. 1942. The plankton algae and protozoa of two Tennessee rivers. Amer. Midl. Nat. 27:191-202.

Lacalli, T. 1974. Golgi function and cell wall formation in the conjugales. Rev. Can. Biol. 33:125-133.

Lang, N. J. 1963. Electron microscopy of the volvocaceae and Astrephomenaceae. Amer. J. Bot. 50:280-300.

Leadbetter, B. S. C. and I. Manton. 1974. Preliminary observations on the chemistry and biology of the lorica in a collared flagellate (Stephanoeca diplocostata Ellis). J. Mar. Biol. Ass., U. K. 54: 269-276.

Leedale, G. F. 1975. Envelope formation and structure in the euglenoid genus Trachelomonas. Br. J. Phycol. 10:17-41.

Lembi, C. A. and N. J. Lang. 1965. Electron microscopy of Carteria and Chlamydomonas. Amer. J. Bot. 52:464-477.

Luft, J. H. 1956. Permanganate--a new fixation for electron microscopy. J. Biophys. Biochem. Cytol. 2:799-801.

Manton, I. 1966a. Observations on scale production in Prymnesium parvum. J. Cell Sci. 1:375-380.

Manton, I. 1966b. Observations on scale production in Pyramimonas amylifera Conrad. J. Cell Sci. 1:429-438.

Manton, I. and G. F. Leedale, 1961. Observations on the fine structure of Paraphysomonas vestita, with special reference to the Golgi apparatus and the origin of scales. Phycologia. 50:37-57.

Marchant, H. S. 1977. Cell division and colony formation in the green alga Coelastrum (Chlorococcales). J. Phycol. 131:102-110.

Mattox, K. R. and K. D. Stewart. 1977. Cell division in the scaly green flagellate Heteromastix angulata and its bearing on the origin of the Chlorophyceae. Am. J. Bot. 64:931-945.

Mazia, D., P. A. Brewer and M. Albert. 1953. The cytochemical staining and measurement of protein with mercuric bromphenol blue. Biol. Bull. 104:56-67.

Mazia, D., G. Schatten and W. Sale. 1975. Adhension of cells to surfaces coated with polylysine: applications to electron microscopy. J. Cell Biol. 66:198-200.

McFarland, W. 1969. Critical point drying for scanning electron microscopic study of ciliary motion. Sci. 163:817-820.

McLean, R. J. and R. M. Brown. 1974. Cell surface differentiation of Chlamydomonas during gametigenesis. I. Mating and concanavalin A agglutinability. Dev. Biol. 36:279-285.

Melkonian, M. 1980. Ultrastructural aspects of basal body associated fibrous structures in green algae: A critical review. Biosystems 12:85-104.

Middelhoek, A. 1950. New observations on a species of the genus Bicosoeca. Hydrobiol. 2:356-359.

Miller, D. H. 1978. Cell wall chemistry and ultrastructure of Chlorococcum oleofaciens (Chlorophyceae). J. Phycol. 14:189-194.

Millington, W. F. and S. R. Gawlik. 1975. Cell shape and wall pattern in relation to cytoplasmic organization in Pediastrum simplex. Amer. J. Bot. 62:824-832.

Moestrup, Ø. 1978. On the phylogenetic validity of the flagellar apparatus in green algae and other chlorophyll a and b containing plants. Biosystems 10:117-144.

Moestrup, Ø. and H. A. Thomsen. 1974. An ultrastructural study of the flagellate Pyramimonas orientalis with particular emphasis on Golgi apparatus activity and the flagellar apparatus Protoplasma. 81: 247-269.

Moestrup, Ø. and P. L. Walne. 1979. Studies on scale morphogenesis in the Golgi apparatus of Pyramimonas tetrahynehus (Prasinophyceae). J. Cell Sci. 36:437-459.

Morrė, D. J., H. H. Mollenhauer and C. E. Bracker. 1971. Origin and continuity of the Golgi apparatus. In: Origin and Continuity of Cell Organelles. (J. Reinert and H. Ursprung, Eds.). Springer-Verlag, New York. 82-126.

Nevo, Z. and N. Sharon. 1969. The cell wall of Peridinium westii, a non-cellulosic glucan. Biochim. Biophys. Acta. 173:161.

Outka, D. E. and D. C. Williams. 1971. Sequential coccolith morphogenesis in Hymenomonas carterae. J. Protozool. 18:285-297.

Parker, B. C. and A. G. D. Boll. 1966. Alcian stains for histochemical localization of acid and sulfated polysaccharides in algae. Phycologia 6:37-46.

Pascher, A. 1972a. Die Süsswasser-Flora Deutschlands, Österreichs und der Schweiz. 4: Volvocales (=Phytomonadinae). Fischer. 506 pp.

Pascher, A. 1927b. Neue oder weing bekannte Flagellaten. XVIII. Arch. Protistenk. 58:577-598.

Peterfi, L. S. 1969. The fine structure of Poterioochromonas malhamensis (Pringsheim) comb. nov. with special reference to the lorica. Nova Hedw. 17:93-103.

Peterfi, L. S. and S. Peterfi. 1965. Studies on the taxonomy and ecology of Rumanian Volvocales. I. Nova Hedw. 10:536-563.

Pickett-Heaps, J. D. 1969. The evolution of the mitotic apparatus: An attempt at comparative ultrastructural cytology in dividing plant cells. Cytobios. 1:256-280.

Pickett-Heaps, J. D. 1972a. Cell division in Cosmarium. J. Phycol. 8: 343-360.

Pickett-Heaps, J. D. 1972b. Variation in mitosis and cytokinesis in plant cells: Its significance in the phylogeny and evolution of ultrastructural systems. Cytobios. 5:59-77.

Pickett-Heaps, J. D. 1975. Green Algae. Sinaeur Associates. Sunderlands.

Pickett-Heaps, J. D. and L. A. Stalhelin. 1975. The ultrastructure of Scenedesmus (Chlorophyceae). II. Cell division and colony formation. J. Phycol. 11:186-202.

Porcella, R. A. 1976. Cellular organization and development of the envelope in Dysmorphococcus globosus Bold and Starr. Ph.D. Dissertation, The University of Tennessee, Knoxville.

Porcella, R. A. and P. L. Walne. 1980. Microarchitecture and envelope development in Dysmorphococcus globosus (Phacotaceae, Chlorophyceae). J. Phycol. 16:280-290.

Prescott, G. W. 1970. How to Know the Fresh-Water Algae. Wm. C. Brown Comp., Dubuque. 348 pp.

Pringsheim, E. G. 1953. Observations on some species of Trachelomonas grown in culture. New Phytol. 52:238-266.

Ramus, J. 1977. Alcian blue: A quantitative aqueous assay for algal acid and sulfated polysaccharides. J. Phycol. 13:345-348.

Ravetto, C. 1964. Alcian blue-alcian yellow: a new method for the identification of different acidic groups. J. Histochem. Cytochem. 12:44-45.

Reynolds, E. S. 1963. The use of lead citrate at high pH as an electron-opaque stain in electron microscopy. J. Cell Biol. 17:208-212.

Ringo, D. L. 1967. Flagellar motion and fine structure of the flagellar apparatus in Chlamydomonas. J. Cell Biol. 33:543-571.

Roberts, K. 1974. Crystalline glycoprotein cell walls of algae: Their structure, composition and assembly. Phil. Trans. R. Soc. Lond. 268:129-146.

Roberts, K., M. Gurney-Smith and G. J. Hills. 1972. Structure, composition and morphogenesis of the cell wall of Chlamydomonas reinhardi: Ultrastructure and preliminary chemical analysis. J. Ultrastruc. Res. 40:599-613.

Rosowski, J. R., R. L. Vadas and P. Kugrens. 1975. Surface configuration of the lorica of the Euglenoid Trachelomonas as revealed with scanning microscopy. Am. J. Bot. 62:48-57.

Simionescu, N. and M. Simionescu. 1976a. Galloyglucoses of low molecular weight as mordant in electron microscopy. I. Procedure, and evidence for mordanting effect. J. Cell Biol. 70:608-633.

Simionescu, N. and M. Simionescu. 1976b. Galloyglucoses of low molecular weight as mordant in electron micriscopy. II. The moiety and functional groups possibly involved in the mordanting effect. J. Cell Biol. 70:634-647.

Singh, J. 1941. Soil algae of Lahore. Cur. Sci. 10:29-30.

Singh, K. P. 1956. Studies in the genus Trachelomonas. I. Description of six organisms in cultivation. Amer. J. Bot. 43:258-266.

Skvortzow, B. B. 1925. Wislouchiella planktonica nov. gen. et spec. of Volvocales. Proc. Sungari Riv. Biol. Sta. 1:27-29.

Smith, M. 1950. The Freshwater Algae of the United States, 2nd Ed. McGraw-Hill Comp., New York.

Spurr, A. R. 1969. A low-viscosity epoxy resin embedding medium for electron microscopy. J. Ultrastruct. Res. 26:31-43.

Staehelin, L. A. and J. D. Pickett-Heaps. 1975. The ultrastructure of Scenedesmus (Chlorophyceae). I. Species with the "reticulate" or "warty" type of ornamental layer. J. Phycol. 11:163-185.

Stein, F. R. 1883. Der organismus der infusionsthiere. III abt., II. Hafte. Leipzig.

Stewart, K. D. and K. R. Mattox. 1975a. Comparative cytology, evolution and classification of the green algae with some consideration of the origin of other organisms with chlorophylls a and b. Bot. Rev. 41:104-135.

Stewart, K. D. and K. R. Mattox. 1975b. Some aspects of mitosis in primitive green algae: Phylogeny and function. Biosys. 7:310-315.

Stewart, K. D. and K. R. Mattox. 1978. Structural evolution in the flagellated cells of green algae and land plants. Biosys. 10: 145-152.

Stewart, K. D., K. R. Mattox and G. L. Floyd. 1973. Mitosis, cytokinesis, the distribution of plasmodesmata, and other cytological characteristics in the Ulotrichales, Ulvales and Chaetophorales: Phylogenetic and taxonomic considerations. J. Phycol. 9:128-141.

Sullivan, C. W. 1976. Diatom mineralization of silicic acid. I. $Si(OH)_4$ transport characteristics in Navicula pelliculosa. J. Phycol. 12:390-396.

Sullivan, C. W. 1979. Diatom mineralization of silicic acid IV. Kinetics of soluble Si pool formation in exponentially growing and synchronized Navicula pelliculosa. J. Phycol. 15:210-216.

Swale, E. M. F. 1963. Notes on the taxonomy of Pteromonas angulosa (Carter) Lemmerman. Br. Phycol. Bull. 2:259-261.

Takeda, H. 1916. Dysmorphococcus variabilis, gen. et sp. nov. Ann. Bot. 30:151-156.

Tappan, H. and A. R. Loeblich. 1968. Lorica composition of modern and fossil Tintinnida (ciliate Protozoa), systematics of geologic distribution and some tertiary taxa. J. Paleontol. 42:1378-1394.

Triemer, R. E. 1980. Role of Golgi apparatus in mucilage production and cyst formation in Euglena gracilis (Euglenophyceae). J. Phycol. 16:46-52.

Triemer, R. E. and R. M. Brown. 1974. Cell division in Chlamydomonas moewusii. J. Phycol. 10:419-433.

Walne, P. L. 1967. The effects of colchicine on cellular organization in Chlamydomonas. II. Ultrastructure. Amer. J. Bot. 54:564-577.

Walne, P. L. 1971. Comparative ultrastructure of eyespots in selected euglenoid flagellates. In: Contributions in Phycology. (B. C. Parker and R. M. Brown, Eds.). Allen Press, Lawrence, Kansas. 107-120.

West, L. K. 1977. Cellular organization and biomineralization of the envelope of Trachelomonas hispida var. coronata. Ph.D. dissertation, The University of Tennessee, Knoxville. 245 pp.

Wujek, D. E. 1969. Ultrastructure of flagellated Chrysophytes. I. Dinobryon. Cytologia 34:71-79.

APPENDICES

APPENDIX A

CULTURE MEDIA

Monophasic Media

Modified Bold's Basal Medium (MBBM) (Bold, 1942, 1949; Walne, 1967). To approximately 500 ml double distilled water, 10 ml of each of the following stock solutions was added:

a. $NaNO_3$*. 10.0g/400ml
b. $MgSO_4 \cdot 7H_2O$. 3.0g/400ml
c. $CaCl_2 \cdot 2H_2O$. 1.0g/400ml
d. KH_2PO_4. . . . . 6.0g/400ml
e. K_2HPO_4. . . . . 4.0g/400ml
f. NaCl. 1.0g/400ml

*30 ml of this nutrient added

1 ml of each of the following trace elements or micronutrient solutions was also added:

a. EDTA

EDTA. . . . . .50.0 g
KOH . . . . . .31.0 g
Dist. H_2O . . . . . .1000 ml

b. H-Fe

$FeSO_4 \cdot 7H_2O$. . . . . .4.98 g
Acidified H_2O to. . . . . .1000 ml
(i.e., to 999 ml dist. H_2O add 1 ml conc. H_2SO_4)

c. H-boron

H_3BO_3 . . . . . .11.42 g
Dist. H_2O to. . . . . .1000 ml

d. H-H_5

$ZnSO_4 \cdot 7H_2O$. . . . . .8.82 g
$MnCl_2 \cdot 4H_2O$. . . . . .1.44 g
MoO_3. . . . . .0.71 g
$CuSO_4 \cdot 5H_2O$. . . . . .1.57 g

$Co(NO_3)2 \cdot 6H_2O$. . . . . .0.49 g

Acidified H_2O to . . . . . .1000 ml

e. Vitamin B_{12} (1.0 ml of 0.5 ug/100 ml)

Sufficient distilled H_2O was added to make 1 liter.

Dispensed in appropriate culture containers and autoclaved at 121°C for 15 psi for 20 min.

Biphasic Medium

This medium is a modification of the medium used by Pringsheim (1953), as reported by Starr (1978) (MSW).

The following components are added to a ½ pint milk bottle:

a. Soil (from Nashville, Tennessee). . .20 g

b. Split pea cotyledon 1

c. Ammonium and magnesium phosphate 10X stock slurry* . . . . . .20 ml

d. Double-distilled water. . . . . .180 ml

Autoclaving for 30 min on non-consecutive days (2 or 3 times as needed to achieve sterilization) was followed by standing until clear (5-10 days). A pinch of $CaCO_3$ may be placed in the bottle before the soil is added if desired.

*Ammonium and magnesium phosphate 10X stock slurry:

a. $Mg_c(PO_r)_s \cdot 4H_2O$. . . . . .1 g

b. $(NH_4)H_2PO_4$. . . . . .1 g

c. Distilled water . . . . . .1 liter

For even distribution of the components of this slurry, it was necessary to stir vigorously (with a magnetic stirrer) while 20 ml of aliquots are pipetted into the medium.

APPENDIX B

CYTOCHEMICAL STAINS FOR LIGHT MICROSCOPY

1. Methylene Blue (Johansen, 1940; Lillie, 1969)
   Stains pectin and cellulose--purple

   Methylene blue. . . . . .1 g

   Distilled H_2O . . . . . .100 ml

2. Toluidine Blue (Ciulei and Alexdru, 1977)
   Stains plant mucilage--blue

   Toluidine blue. . . . . .0.1 g

   Distilled H_2O . . . . . .1.0 l

3. Alcian Blue (Parker and Boll, 1966; Ramus, 1977)
   Stains acid and/or negatively charged polysaccharides

   Alcian blue . . . . . .0.5 g

   Distilled H_2O . . . . . .100 ml

   Adjusted to pH 0.5 with 1N HCl

4. Alcian Yellow (Ravetto, 1964)
   Stains acid and/or negatively charged polysaccharides

   Alcian Yellow . . . . . .0.5 g

   Distilled H_2O . . . . . .100 ml

   Adjusted to pH 2.5 with 1N HCl

5. Ruthenium Red (Chambers, 1973)
   Stains pectin and acid mucopolysaccharides

   Ruthenium red . . . . . .0.5 g

   1.34M Na cacodylate*. . . . . .99.5 ml

   *1.34M Na cacodylate:

   Sodium cacodylate . . . . . .57.35 g

   Distilled H_2O . . . . . .200 ml

6. Potassium ferrocyanide (Johansen, 1940)
   Stains iron--blue

   1% aqueous HCl. . . . . .25 ml

   35% aqueous potassium ferrocyanide. .0.5 ml

7. Periodic acid-Schiff (PAS) (Hotchkiss, 1948; Jensen, 1962)
   Stains carbohydrates

   a. Periodate solution

      400 mg of periodic acid is dissolved in 15 ml of distilled water. To this solution is added 135 mg of crystalline sodium acetate dissolved in 35 ml of absolute ethyl alcohol. Prepared just before use.

   b. Reducing rinse

      Potassium iodide. . . . . .1 g

      Sodium thiosulphate . . . . . .1 g

      Distilled water . . . . . .20 ml

   When dissolved, 30 ml of ethyl alcohol and then 0.5 ml 2N HCl are added

   c. Schiff's reagent (Allied Chemical)

   d. Procedure:

      1) Loricas are washed in 70% alcohol
      2) Immerse loricas in periodate solution for 5 min
      3) Wash loricas in 70% alcohol
      4) Immerse loricas in reducing rinse for 5 min
      5) Wash loricas in 70% alcohol
      6) Immerse in Schiff's reagent for 30 min
      7) Wash in distilled water 3X

APPENDIX C

PREPARATIVE PROCEDURES FOR ELECTRON MICROSCOPY

Buffer

Sodium Cacodylate Buffer (0.1M)

Sodium cacodylate (Polysciences, FW:214). . . . .10.23 g

Distilled H_2O . . . . . .500 ml

Dissolve sodium cacodylate in distilled water. Adjust to pH 7.2. To make 0.05M buffer for use in rinsing, dilute 100 ml of buffer stock with 100 ml of distilled H_2O.

Glutaraldehyde Fixative

a. Glutaraldehyde Stock Solution (TAAB, 25% in H_2O)

b. Sodium Cacodylate Buffer (0.1M)

c. Buffered Glutaraldehyde Stock Solution (4%)
Combine 4 ml of glutaraldehyde fixative (a) and 21 ml sodium cacodylate buffer (0.1M). Adjust to desired pH (i.e., 7.1).

d. Buffered Glutaraldehyde Working Solution (2%)
Combine buffered glutaraldehyde stock solution (c) (1:1, v/v) with distilled H_2O.

Osmium Tetroxide Post-Fixative Stain

a. Osmium Stock Solution (4%)

Osmium Tetroxide (Engelhard Industry) . . . . . .1.0 g

Distilled H_2O . . . . . .24 ml

Use of vinyl gloves and fume hood recommended during this procedure. Measure 24 ml of distilled water into a heavy-walled reagent bottle. Drop a vacuum-sealed vial containing 1 g of osmium tetroxide crystals into reagent bottle. Fit bottle with ground glass stopper and swirl vigorously to break vial. Wrap bottle with aluminum foil and store in refrigerator.

b. Osmium Working Solution (2%)

Osmium Stock Solution combined (1:1, v/v) with 0.1M sodium cacodylate buffer to produce a 2% solution in 0.05M buffer.

Embedding Medium

Spurr's Embedding Medium (Spurr, 1969)

ERL 4206 (Union Carbide Corp.). . . . . .10 g

DER 736 (Dow Chemical Co.). . . . . .5 g

NSA (Humphrey Chemical Co.) . . . . . .26 g

S-1 (Conshohocken Chemical Corp). . . . . .0.4 g

Measure all of the above chemicals gravimetrically; mix thoroughly.

Representative Protocol for TEM

1. Harvest cells (by pipetting). Then, pellet them gently by centrifugation (e.g., at ca 1000 x g).
2. Overlay the pellet with glutaraldehyde working solution (2%) and mix well. Fix for 2 hr at 0-4°C.
3. Wash cells 3X with buffer (0.05M sodium cacodylate) ca 5 min each at 0-4°C.
4. Post-fix with the osmium working solution (2%) for 2 hr at 0-4°C.
5. Repeat step 3.
6. Optional. Stain for 30 min with 1% tannic acid w/v in 0.05M sodium cacodylate buffer. Rinse 2X with 1% sodium sulfite in 0.05M sodium sulfite in 0.05M sodium cacodylate buffer followed by 3X rinses with 0.05M sodium cacodylate buffer, all at room temperature (Siminescu, 1977, 1979).
7. Dehydrate with an ethyl alcohol series: 10%, 25%, 50%, 70%, 95%, 100% (2X), ca 15 min each.
8. Complete dehydration in propylene oxide (2X), ca 15 min each.
9. Infiltrate with a propylene oxide/Spurr's plastic series: 1:2, 2:1, 100% plastic, ca 4 hr each.

10. Polymerize at 60-80°C for 24 hr.

11. Trim blocks and section. Post-stain with routine stains (e.g., uranyl acetate followed by lead citrate).

Post-Stains for Ultrathin Sections

1. Uranyl Acetate (7.5% in 25% Methanol; Frasca and Parks, 1965)

   Uranyl acetate (J. T. Baker Chem. Co.). . . . . .1.5 g

   25% Methanol. . . . . .18.5 ml

   Dissolve uranyl acetate crystals in 25% methanol.
   Store in refrigerator but warm solution to room temperature before use.

2. Lead Citrate (0.19%; Venable and Coggeshall, 1965; Reynold's, 1963)

   Lead citrate (K & K Laboratories) . . . . . .0.02 g

   1ON NaOH. . . . . .0.1 ml

   Distilled H_2O . . . . . .10 ml

   Add ingredients to 25 ml volumetric flask and shake vigorously for 1 min.

Thick/thin Section Techniques

This technique is a modification of that described by Kaplin and Hinds, 1977.

1. Sections 2 um thick were cut and placed at spaced intervals on an uncleaned coverslip mounted to a slide with permount.

2. These sections were stained with standard cytochemical stains and photographed with LM.

3. Location of cells of interest was noted for future thin-sectioning.

4. Coverslips were removed from the slide with xylene.

5. A small amount of epon/araldite (Kaplin and Hinds, 1977) was placed in a 100°C oven until it became tacky, ca 15 min.

6. The specimen end of a standard Beem capsule was cut off with a razor blade, and the manufactured end dipped in the epoxy mixture.

7. The Beem capsule cylinder is centered over a section and mounted onto the coverslip.

8. Section with the cylinder is placed in a 100^{o}C oven for 15-20 min.

9. The section and cylinder are removed from the oven and the cylinder filled with the epoxy.

10. The cylinder and section are placed back in the oven overnight.

11. The block is then sectioned and processed as any thin-section.

APPENDIX D

SCANNING ELECTRON MICROSCOPY

CHEMICALS AND TECHNIQUES

Critical Point Drying (McFarland, 1969)

Fixatives are the same as for TEM.

1. Glusulase (2%)

   Glusulase (Endo Laboratories). . . . . .1 ml

   Sodium Cacodylate Buffer . . . . . .49 ml

Procedure:

1. Harvest cells and fix for 30 min with 2% glutaraldehyde working solution.
2. Wash cells 3X with sodium cacodylate buffer (0.05M).
3. Optional: Treat cells for 30-60 min with glusulase (2%).
4. Wash cells 3X with sodium cacodylate buffer (0.05M).
5. Mount cells on poly-lysine coated cover slips (12 mm in diameter), by allowing cells to settle out of a drop of buffer.
6. Dehydrate with an acetone series: 25%, 50%, 70%, 95%, 100% (3X).
7. Coverslips were transferred to Bomar 12mm cover slip holder in 100% acetone and subjected to critical point drying (CPD).

APPENDIX E

PLATES AND FIGURE LEGENDS

Plate I. Diagrammatic Representation of Vegetative Cell Ultrastructure.

Figure 1. Diagrammatic representation of a median longitudinal section of a cell from an actively growing MBBM culture of Pteromonas protracta (Diagram courtesy of Linda Pocratsky).

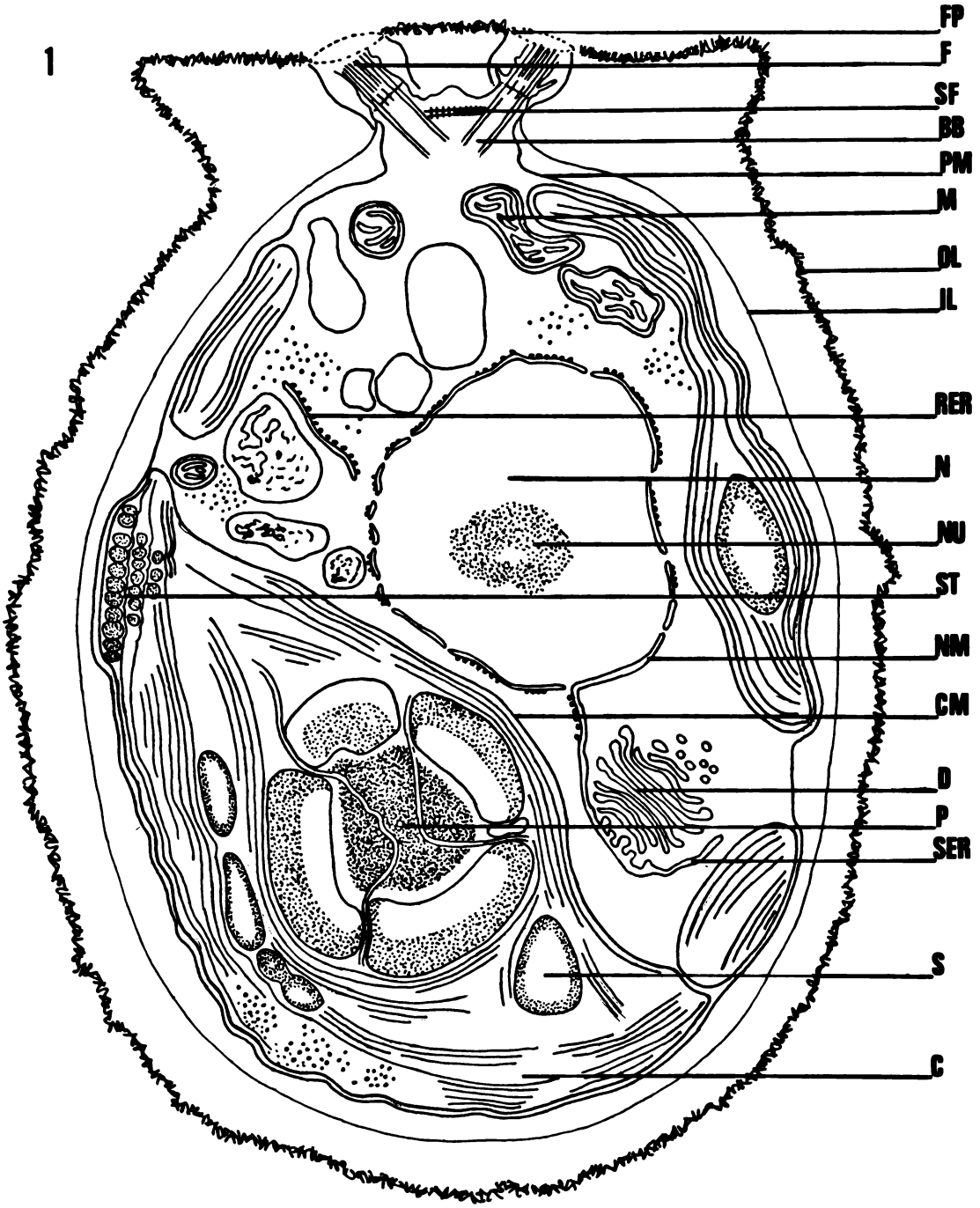


PLATE I

Plate II. TEM: Lorica Surface.

Figure 2. Hexagonal surface is sometimes obscured in loricas from MBBM cultures. This lorica from a 14-day-old culture shows only a faint trace of the hexagonal surface pattern. TEM whole-mount. 15,000x.

Figure 3. Distinctive hexagonal surface pattern is evident in cell-free lorica from 2-month-old MSW culture. TEM whole-mount. 15,000x.

Figure 4. Higher Magnification of lorica shown in Fig. 117 shows a secondary reticulum with numerous puncta within the primary hexagon. TEM whole-mount. 108,000x.

Figure 5. Wing of lorica from 14-day-old MBBM culture shows mucilage on the surface which obscures the hexagonal surface pattern. TEM shadow-cast. 20,000x.

Figure 6. Raised hexagonal surface pattern is evident on wing of lorica from a 14-day-old MSW culture. TEM shadow-cast. 20,000x.

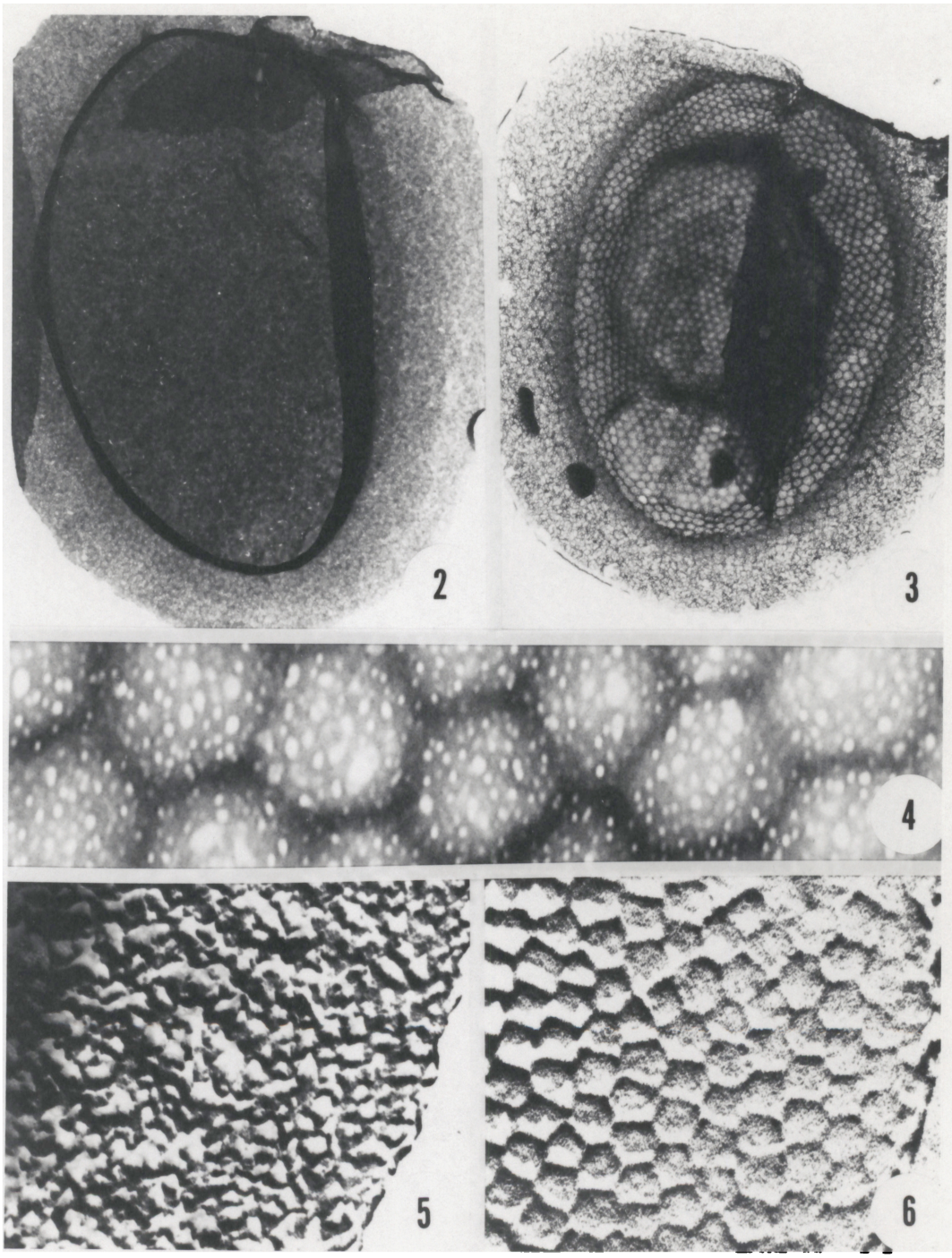


PLATE II

Plate III. SEM: Lorica Surface

Figure 7. Air-dried cell from 14-day-old MSW culture shows wing circumscribing the cell, and raised hexagonal surface pattern. 6000x.

Figure 8. Air-dried cell from 14-day-old MBBM culture shows a smooth lorica surface because of accumulation of mucilage. 5400x.

Figure 9. Glusulase-treated, CPD cell from MSW shows typical hexagonal surface pattern. Wedge-shaped anterior portion of lorica with 2 emerging flagella ia also evident. 6000x.

Figure 10. Glusulase-treated, CPD cell from MBM shows no surface pattern. Lorica collapses even with CPC preparation. 5500x.

Figure 11. Collapsed CPD immature lorica from MSW. Cell was pre-treated with glusulase, but no surface pattern is visible. 6000x.

Figure 12. Untreated, CPD cell from MBBM shows mucilage accumulated on the lorica surface, and no pattern is evident. 7000x.

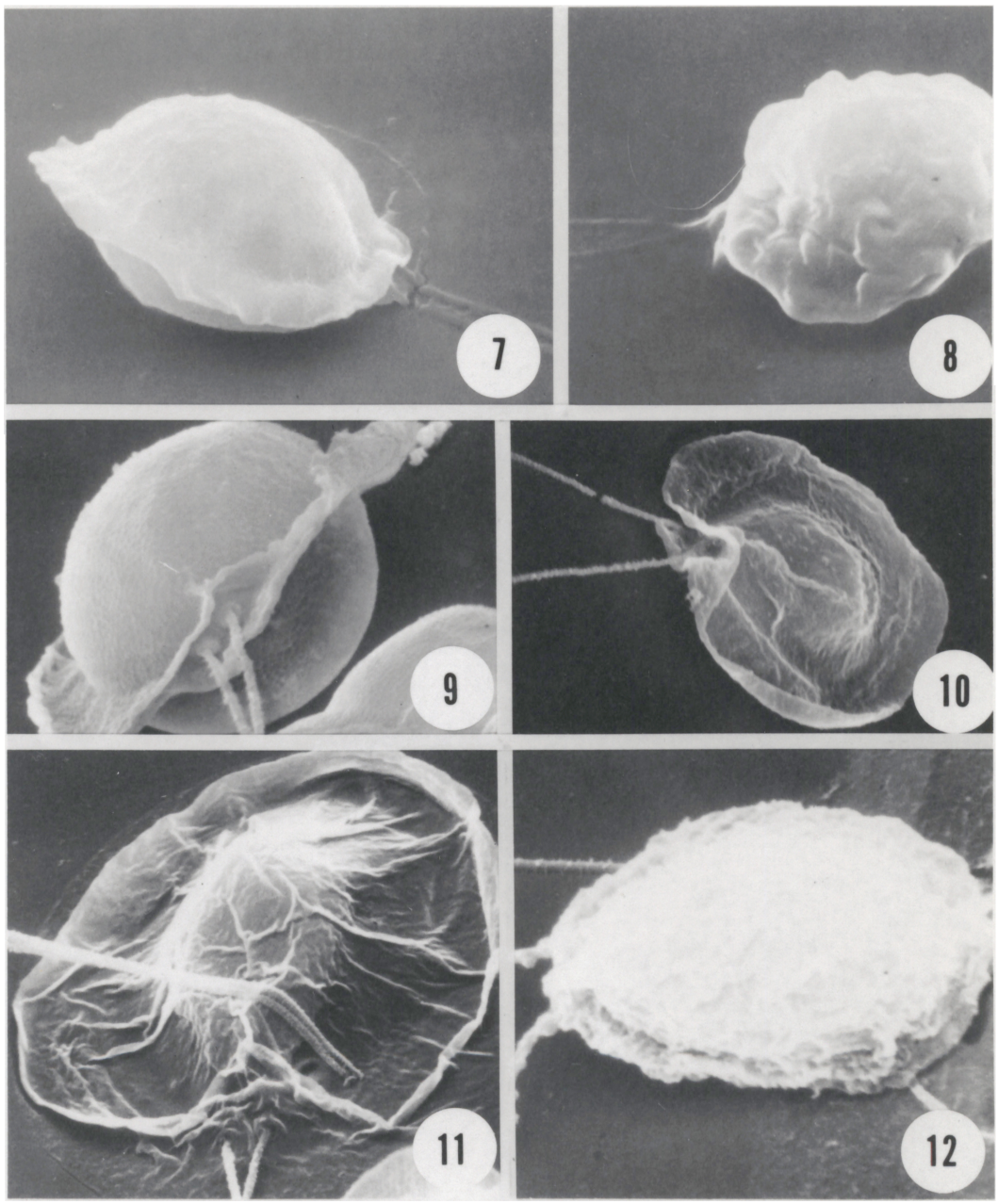


PLATE III

Plate IV. Wedge-shaped Lorica Segment.

Figure 13. Third segment of the lorica, the wedge, with 2 thickened flagellar pores. The primary hexagonal pattern and the secondary reticulum persist on this segment. TEM whole-mount. 17,000x.

Figure 14. Cell from MSW shows collars of the flagellar pores and the positional relationship between the wedge-shaped segment and the 2 valves of the lorica. SEM. 15,000x.

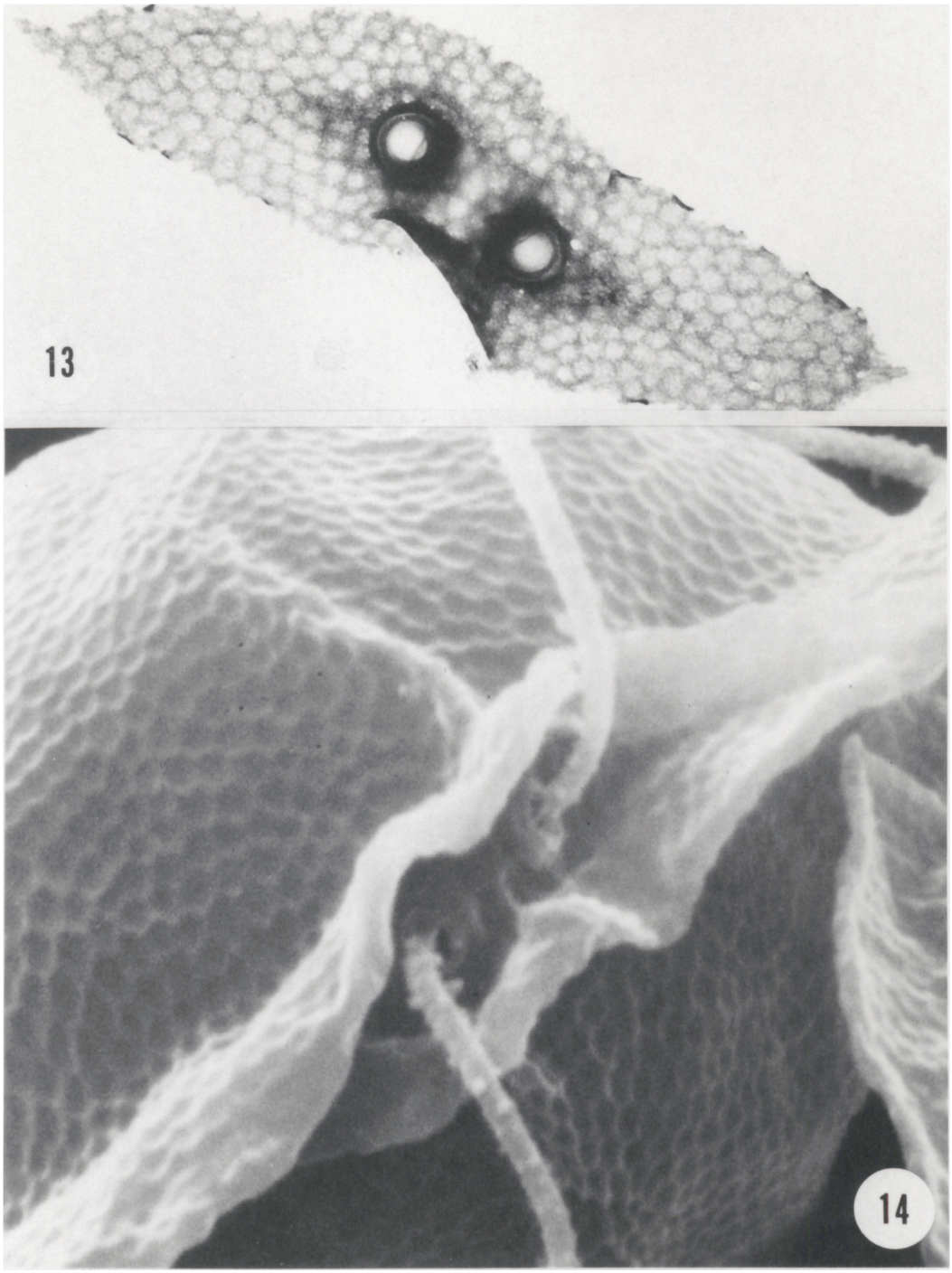


PLATE IV

Plate V. TEM: Lorica Wedge and Flagellar Pore.

Figure 15. Empty lorica shows 2 breaks (arrows) where the wedge-shaped segment separates from the 2 valves of the lorica during asexual reproduction. The thickened collar of 1 flagellar pore is also visible. 57,000x.

Figure 16. Wedge-shaped segment of an immature lorica showing even spacing of the dense cores. 43,000x.

Figure 17. Mature lorica shows both flagellar pores and thickened collars. The proximal portions of the pores are closely appressed to the flagella. 50,000x. Inset. Longitudinal margin is connected to the inner lorica (large arrows). The flagellar ring is connected to the transition zone (small arrows). 103,000x.

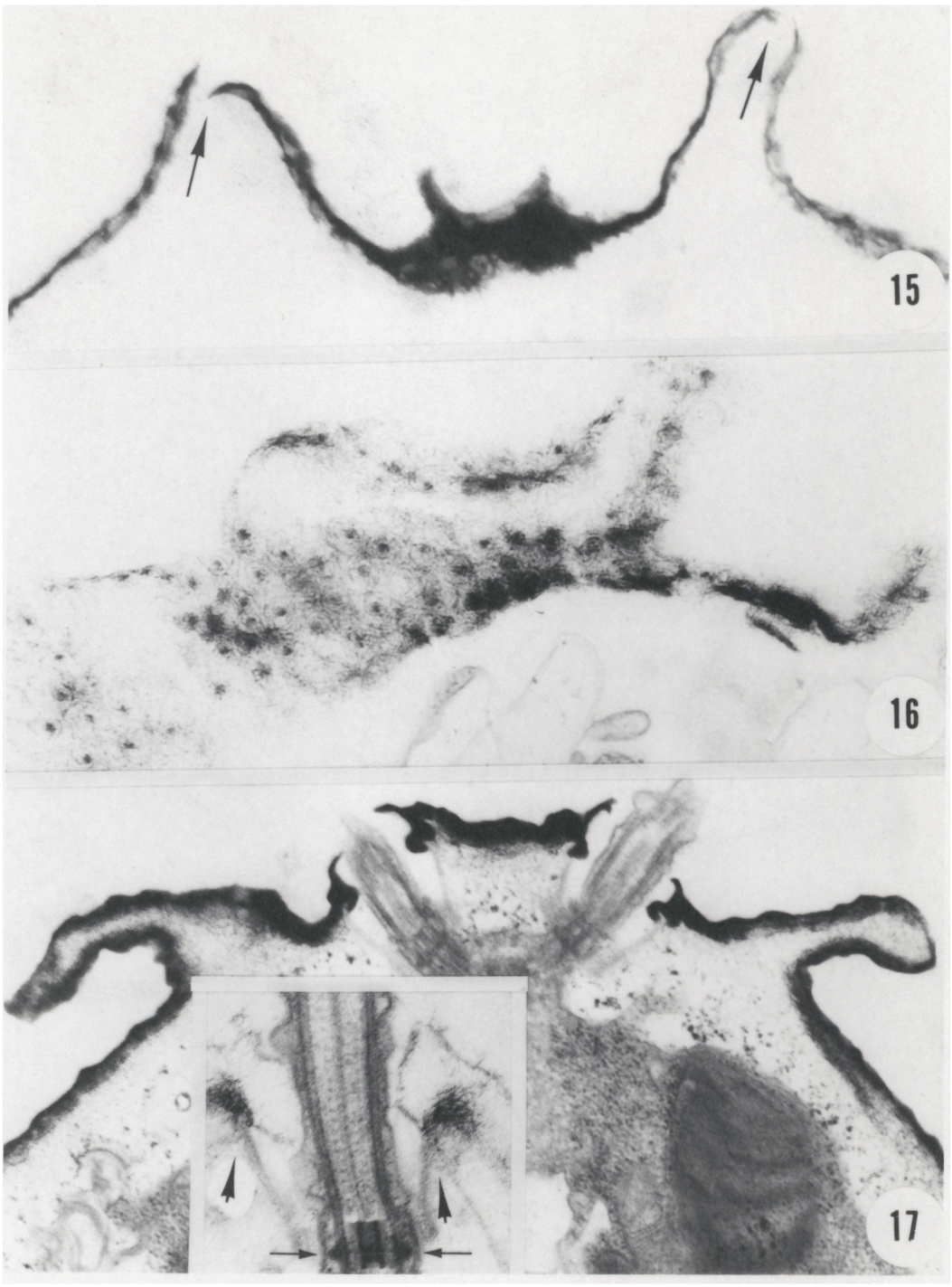


PLATE V

Plate VI. Lorica Development.

Figure 18. Two newly formed daughter cells with incipient loricas close to the plasmalemma (arrows). TEM thin-section. 24,000x.

Figure 19. Diffuse material of incipient loricas is evident around both daughter cells (arrows). TEM thin-section. 26,000x.

Figure 20. Higher magnification of 2 daughter cells shows the beginning of lorica consolidation. PLPM can be seen in Golgi-derived and presumptive secretory vesicles. TEM thin-section. 28,000x.

Figure 21. Fully formed loricas around 2 daughter cells. The hour-glass shape of the protoplast is common at this stage. TEM thin-section. 21,000x.

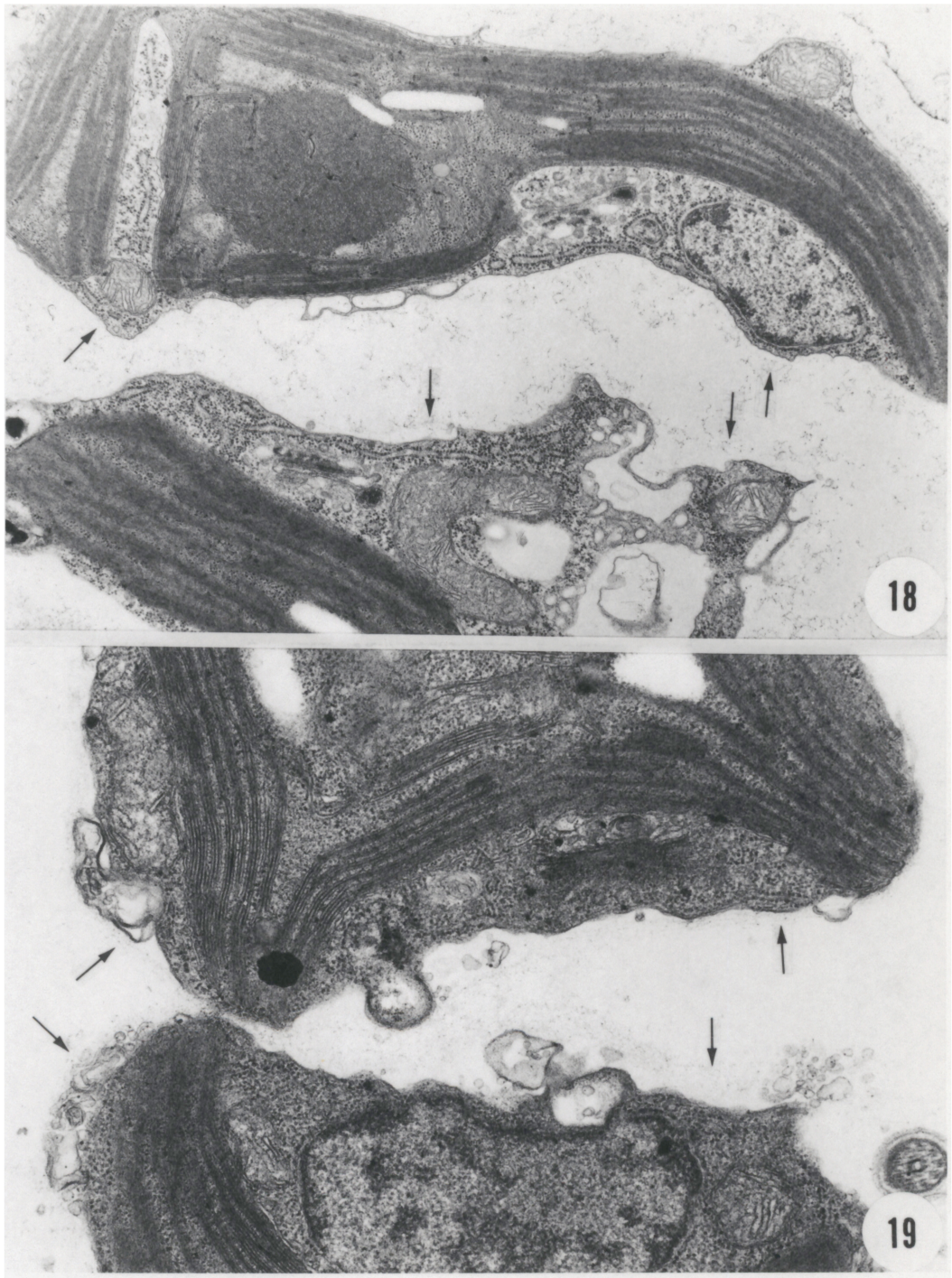


PLATE VI

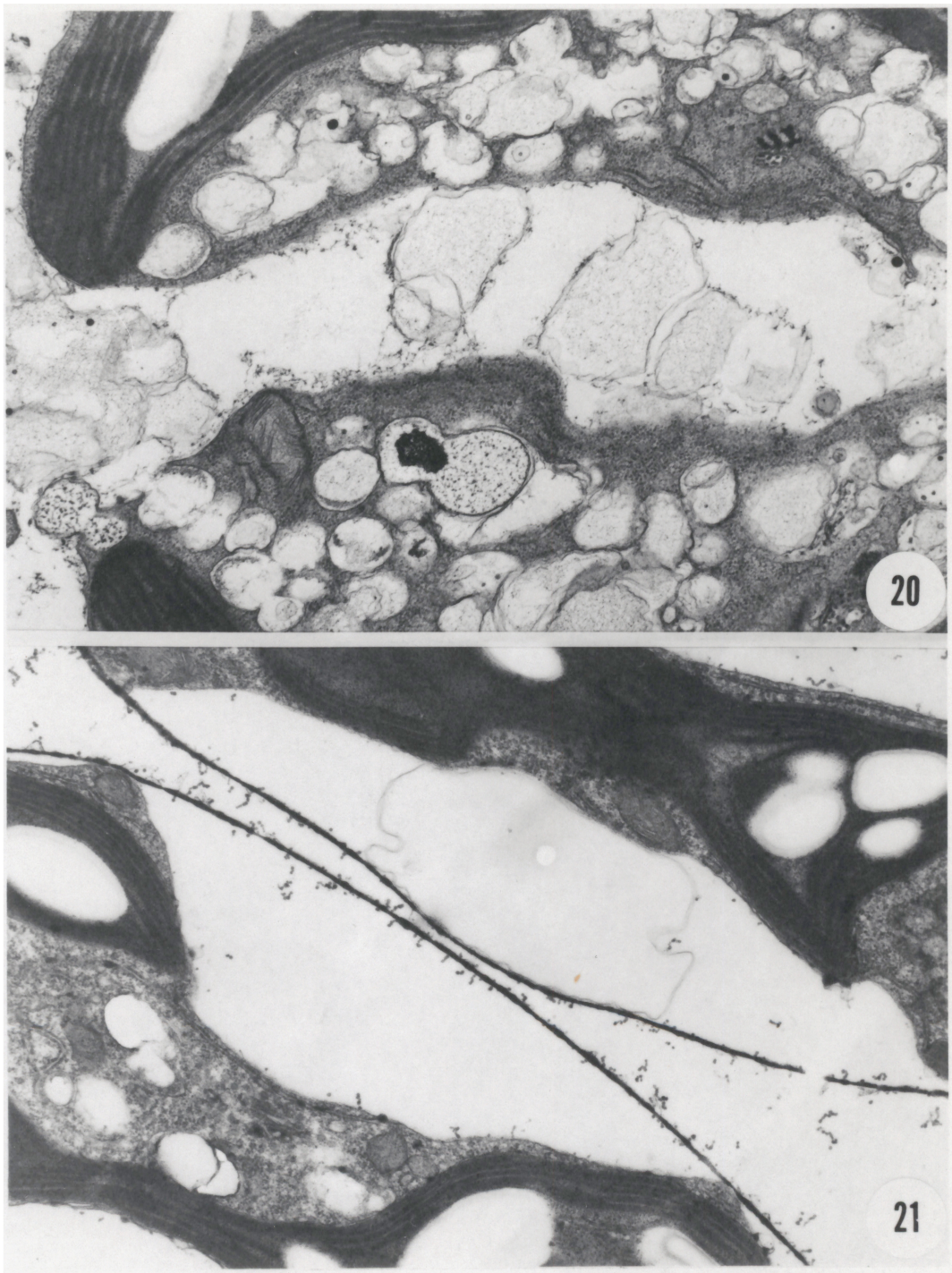


PLATE VI (Continued)

Plate VII. Lorica Structure.

Figure 22. Mature bilayered lorica of vegetative cell grown in MSW shows amorphous outer lorica and granulo-fibrillar inner lorica. Scalloping of the outer lorica corresponds to the hexagonal pattern. TEM thin-section. 34,000x.

Figure 23. Glancing section through the wedge-shaped segment of lorica from MSW culture shows hexagonal pattern. TEM thin-section. 41,000x.

Figure 24. Thick section shows the primary pattern and puncta within the secondary reticulum. TEM thick-section. 42,000x.

Figure 25. Bilayered lorica from cell grown in MBBM shows a fibrillar outer lorica and a finely granular inner lorica. Lorica material can be seen between the plasmalemma and the inner lorica. TEM thin-section. 21,000x.

Figure 26. Higher magnification of lorica from cell grown in MBBM shows the fibrillar nature of the outer lorica. TEM thin-section. 55,000x.

Figure 27. Lorica of cell from 3-day-old MBBM culture is dense and has a scalloped outer lorica. TEM thin-section. 31,000x.



PLATE VII

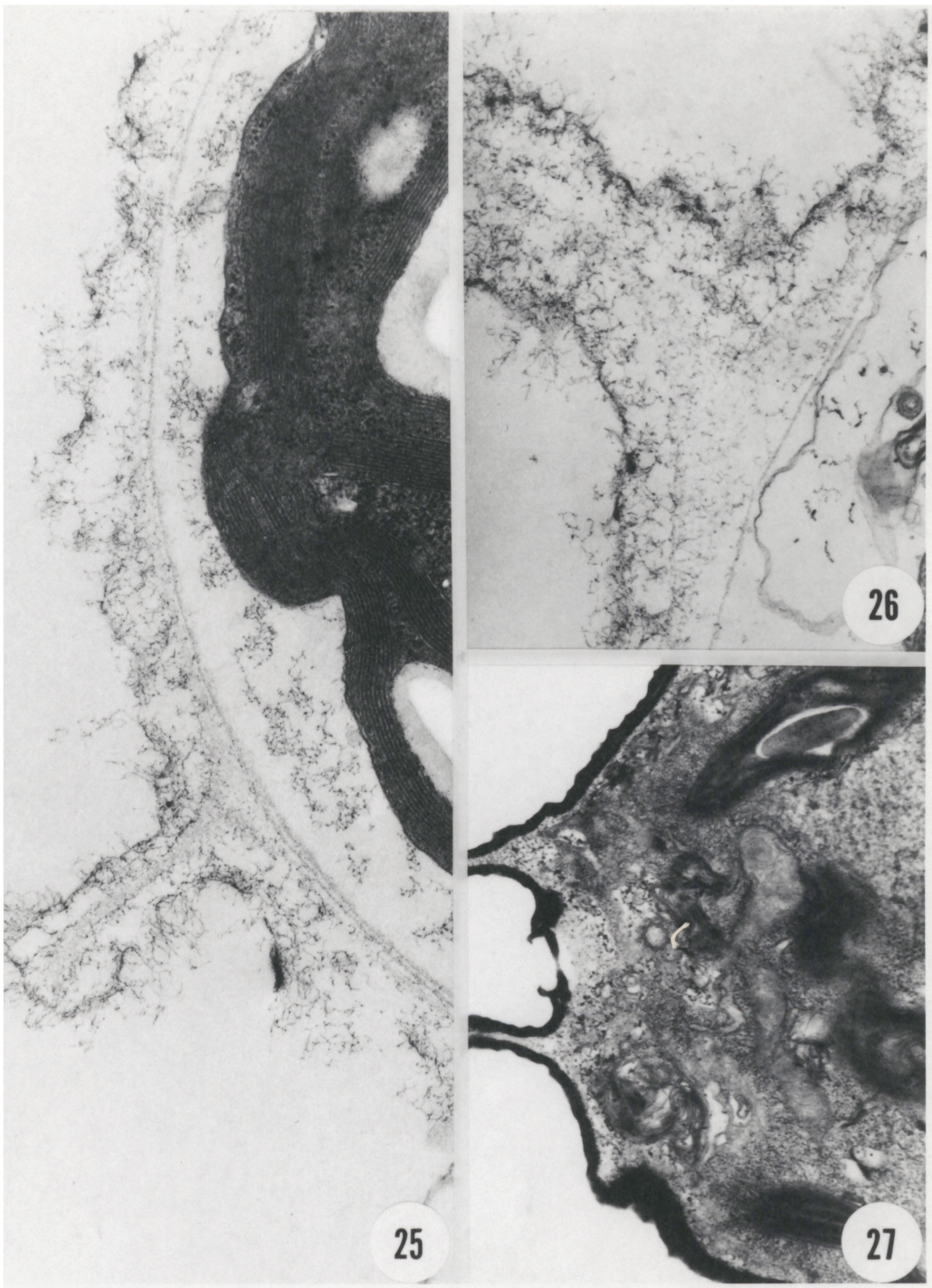


PLATE VII (Continued)

Plate VIII. Lorica Assembly.

Figure 28. Section through daughter cell inside parent lorica. Note regular spacing of the dense cores around the daughter cell (small arrows). The inner lorica is barely visible (large arrows). TEM thin-section. 27,000x.

Figure 29. An earlier stage of lorica development than shown in Fig. 28. Dense cores are regularly spaced around this daughter cell. TEM thin-section. 33,000x.

Figure 30. A mature lorica from a 9-day-old MBBM culture shows dense cores interconnected with fibrillar mucilaginous material. TEM thin-section. 30,000x.

Figure 31. Empty lorica from the same culture as the lorica shown in Fig. 30. Dense cores adjoin (arrow) and form the primary hexagonal pattern and are interconnected by fibrillar mucilaginous strands. TEM thin-section. 96,000x.

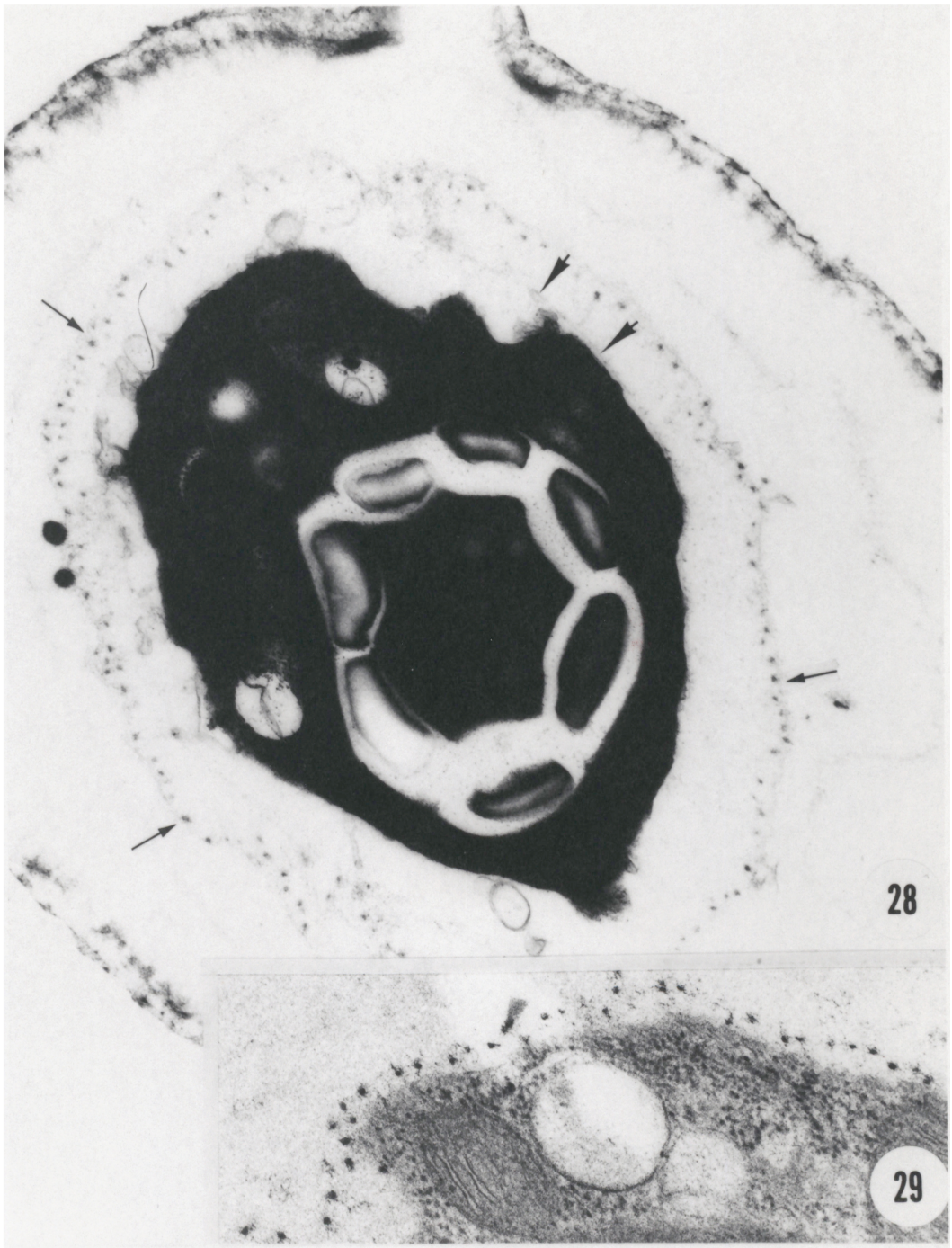


PLATE VIII

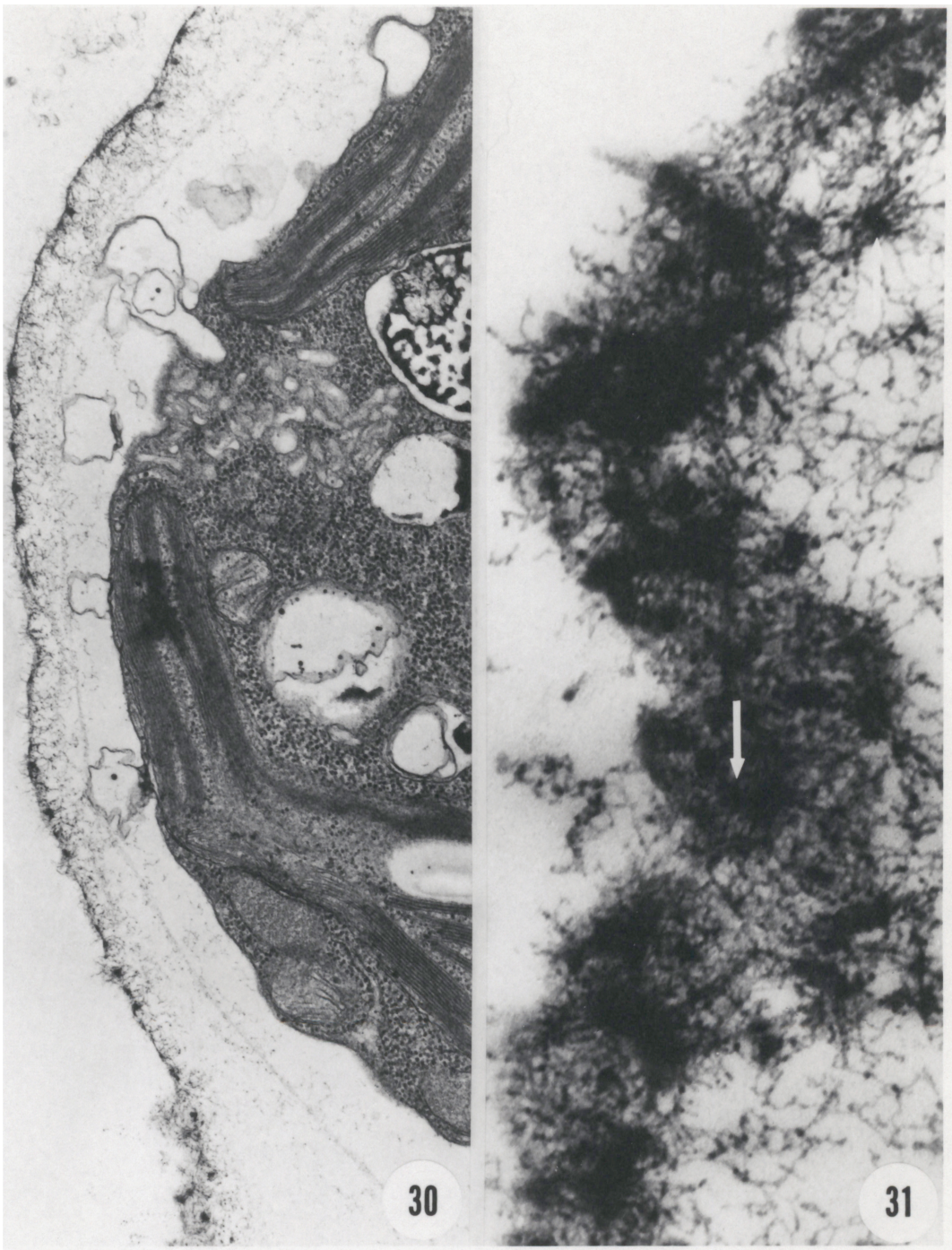


PLATE VIII (Continued)

Plate IX. Golgi Involvement in Lorica Production.

Figure 32. Two dictyosome profiles in a dividing cell show PLPM in the cisternae at the maturing faces and in nearby vesicles. TEM thin-section. 55,000x.

Figure 33. Young zoospore shows proliferation of RER, SER vesicles at dictyosome forming face and 2 types of PLPM in Golgi cisternae and Golgi-derived vesicles; dense cores (small arrows) and wispy, fibrillar components (large arrows). TEM thin-section. 56,000x.

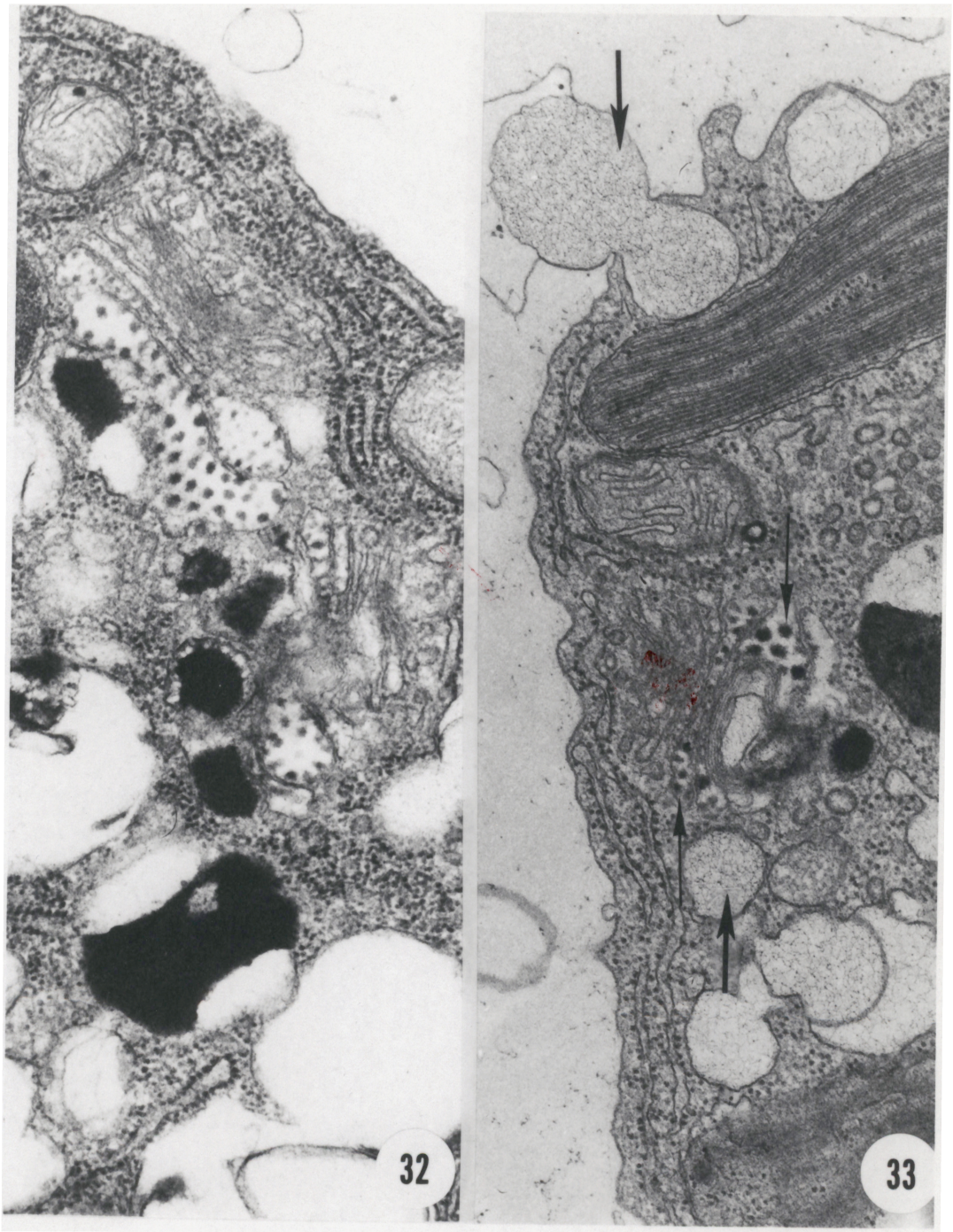


PLATE IX

Plate X. STEM-EDX of MSW Grown Cell.

Figure 34-39 show spectra from 50-nm-thick section of a single cell from 14-day-old MSW culture and TEM thin-sections showing regions analysed. Circles indicate regions analysed.

Figure 34. Spectrum from analysis of longitudinal section through lorica shows P, Ca and Si as major elements detected with some Fe, S and Cl present.

Figure 35. Micrograph shows region analysed to produce spectrum shown in Fig. 34. 50,000x.

Figure 36. Spectrum from analysis of PLPM in Golgi cisternae of cell is almost identical to that shown in Fig. 34, except for the absence of Cl.

Figure 37. Micrograph showing region analysed to produce spectrum shown in Fig. 36. 52,000x.

Figure 38. Spectrum of region of cytoplasm free of PLPM shows lower Ca peak but is otherwise similar to spectrum shown in Fig. 36.

Figure 39. Region analysed in Fig. 38 is shown in this micrograph. 52,000x.

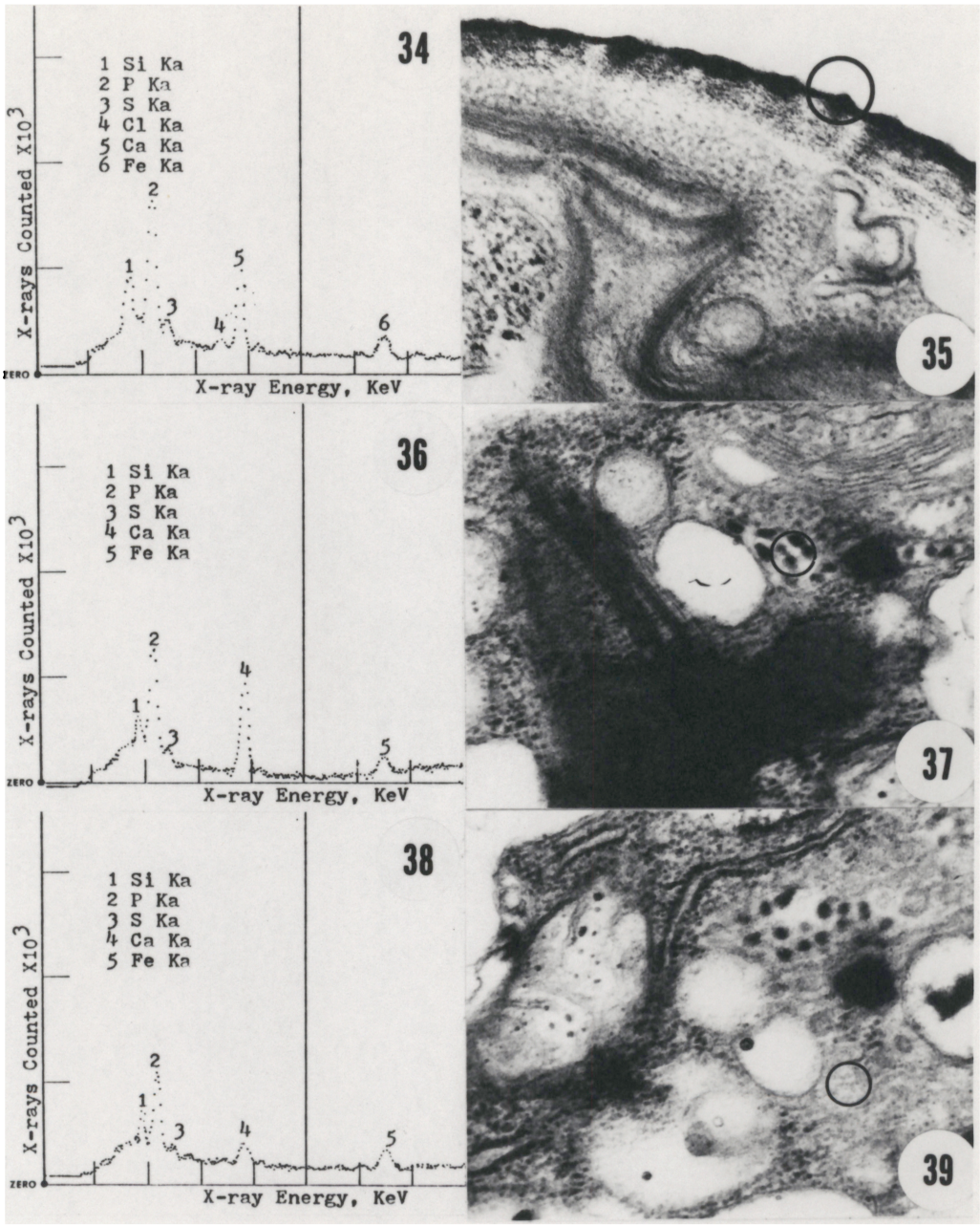

34
1 Si Ka
2 P Ka
3 S Ka
4 Cl Ka
5 Ca Ka
6 Fe Ka
X-rays Counted X10³
ZERO
X-ray Energy, KeV
35
36
1 Si Ka
2 P Ka
3 S Ka
4 Ca Ka
5 Fe Ka
X-rays Counted X10³
ZERO
X-ray Energy, KeV
37
38
1 Si Ka
2 P Ka
3 S Ka
4 Ca Ka
5 Fe Ka
X-rays Counted X10³
ZERO
X-ray Energy, KeV
39

PLATE X

Plate XI. STEM-EDX of MBBM Grown Cell.

Figures 40-45. STEM-EDX spectra of 50-nm-thick section of a single cell from 7-day-old MBBM culture and TEM thin sections showing regions analysed. Circles indicate regions analysed.

Figure 40. Spectrum from analysis of longitudinal section of lorica shows P, Ca and Si as major peaks with no detectable Fe.

Figure 41. Micrograph showing region analysed in Fig. 40. 40,000x.

Figure 42. Spectrum of PLPM in Golgi cisternae is similar, with regard to the major elements, to that shown in Fig. 40. 45,000x.

Figure 43. Micrograph of region analysed in Fig. 42.

Figure 44. Spectrum of region of cytoplasm free of PLPM shows smaller peak for CA but is other wise similar to spectrum shown in Fig. 42.

Figure 45. Micrograph shows region analysed in Fig. 44. 45,000x.

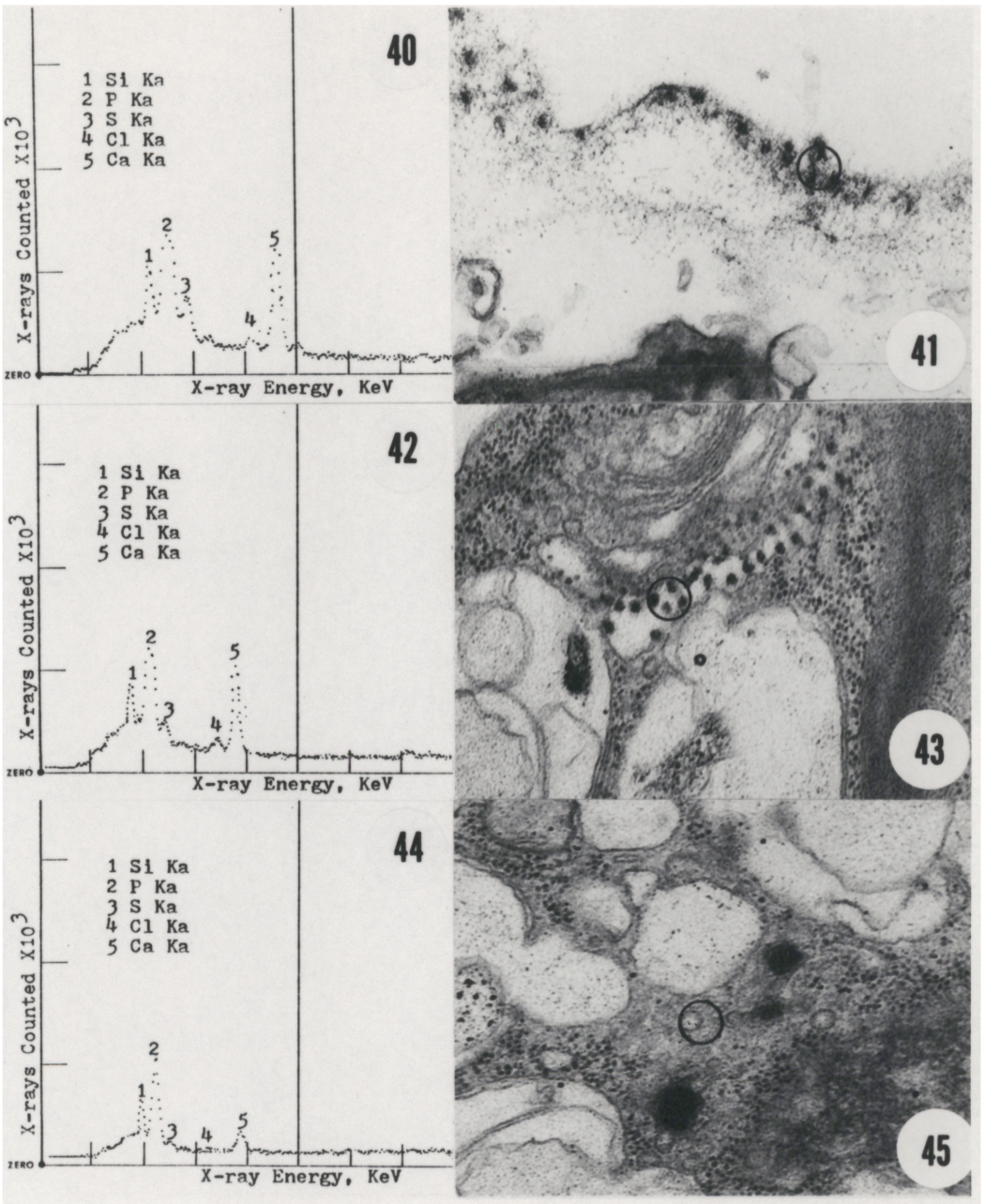

40
1 Si Ka
2 P Ka
3 S Ka
4 Cl Ka
5 Ca Ka
X-rays Counted X10³
ZERO
X-ray Energy, KeV
41
42
1 Si Ka
2 P Ka
3 S Ka
4 Cl Ka
5 Ca Ka
X-rays Counted X10³
ZERO
X-ray Energy, KeV
43
44
1 Si Ka
2 P Ka
3 S Ka
4 Cl Ka
5 Ca Ka
X-rays Counted X10³
ZERO
X-ray Energy, KeV
45

PLATE XI

Plate XII. Cytochemical Stains.

Figures 46-55. Reaction of loricas from 14-day-old MBBM culture (except where noted) to various cytochemical stains. LM bright-field optics.

Figure 46. Lorica shows strong reaction to methylene blue, indicating the presence of mucins. 2700x.

Figure 47. Positive reaction to toluidine blue indicates the presence of acidic polysaccharides. 2700x.

Figure 48. Alcian blue gives positive reaction indicating the presence of mucins and/or acid mucopolysaccharides. 2700x.

Figure 49. Lorica shows a positive reaction to Alcian yellow, indicating the presence of acid and/or negatively charged polysaccharides. 2700x.

Figure 50. Ruthenium red elicits a positive response, indicating the presence of pectins and/or mucopolysaccharides. 2700x.

Figure 51. Positive reaction to PAS indicates the presence of carbohydrates. 2700x.

Figure 52. Mercuric bromphenol blue positive reaction, indicating the presence of protein in lorica from MBBM. 2700x.

Figure 53. Positive reaction to mercuric bromphenol blue indicating the presence of protein in lorica from MSW. 2700x.

Figure 54. Negative reaction with potassium ferrocyanide in lorica from MBBM, which tests for the presence of Fe. 2700x.

Figure 55. Weak reaction to potassium ferrocyanide which indicates the presence of Fe in lorica from MSW. 2700x.

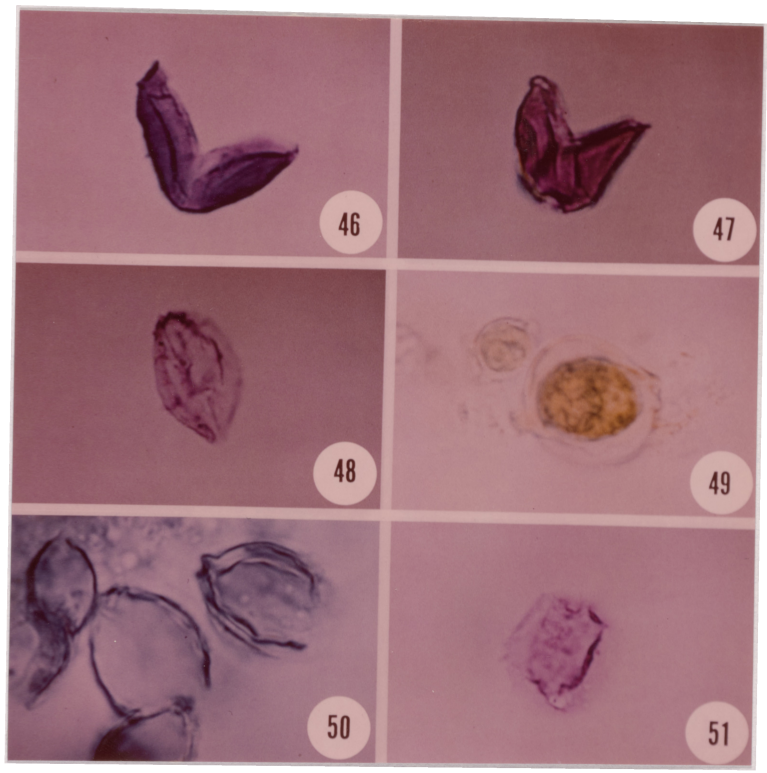


PLATE XII

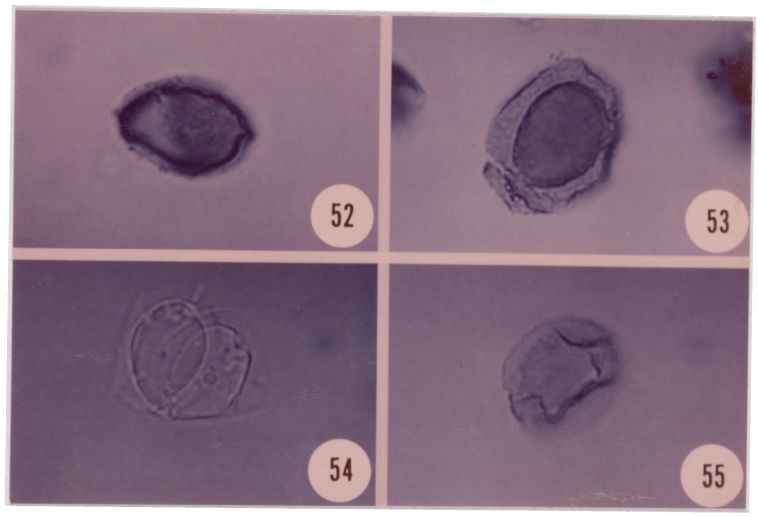


PLATE XII (Continued)

Plate XIII. SEM-EDX: Loricas from 14-Day-Old Cultures.

Figure 56. P, Ca and Si are the major elements recorded in this spectrum of a lorica from MBBM culture.

Figure 57. Lorica analysed in Fig. 56 is shown in this micrograph. TEM whole-mount. 18,000x.

Figure 58. Spectrum of lorica from MSW culture shows P, Ca and Si as major elements and a definite Fe peak.

Figure 59. Micrograph of lorica analysed in Fig. 58. TEM whole-mount. 14,000x.

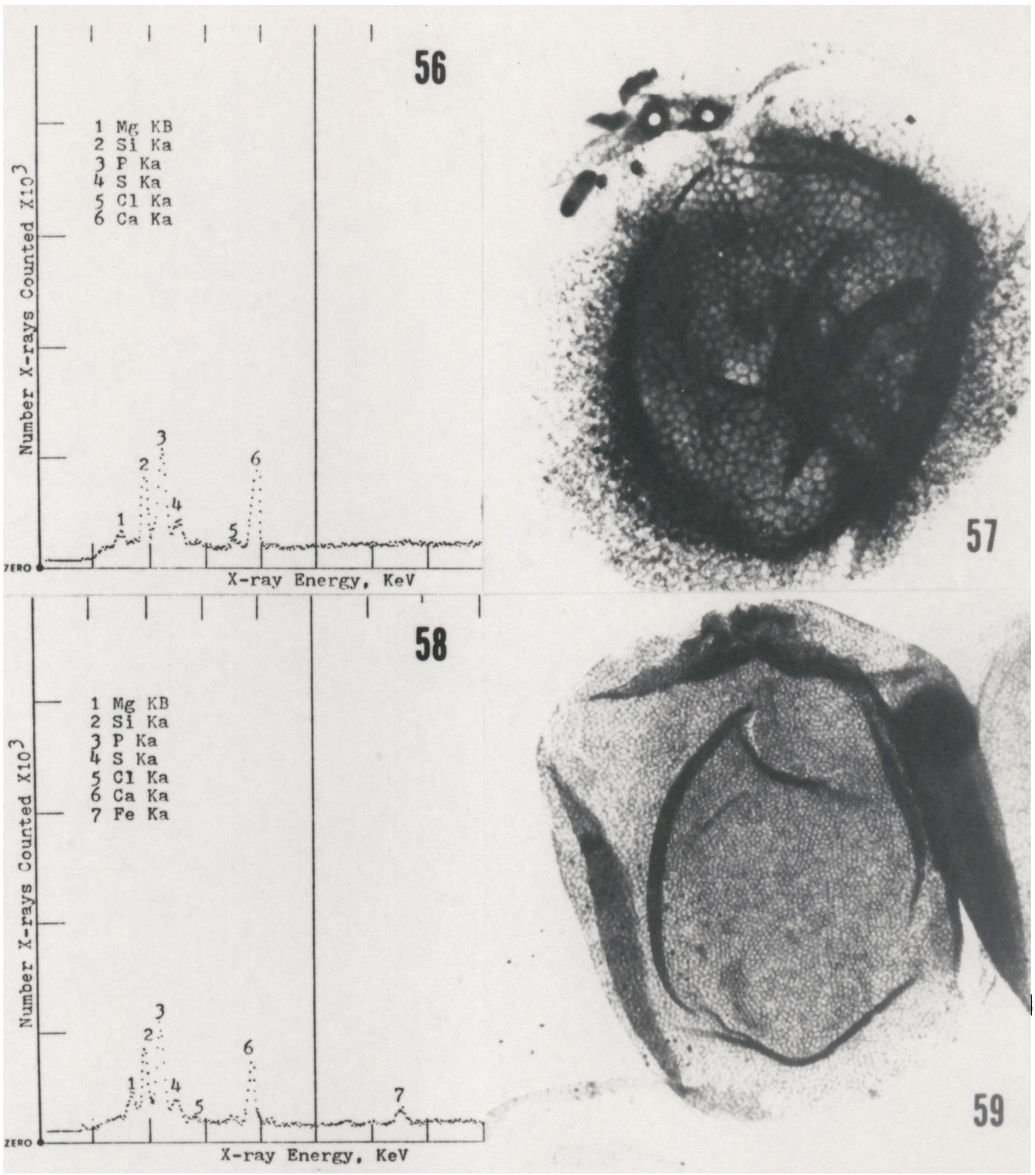

56
1 Mg KB
2 Si Ka
3 P Ka
4 S Ka
5 Cl Ka
6 Ca Ka
Number X-rays Counted X10³
ZERO
X-ray Energy, KeV
57
58
1 Mg KB
2 Si Ka
3 P Ka
4 S Ka
5 Cl Ka
6 Ca Ka
7 Fe Ka
Number X-rays Counted X10³
ZERO
X-ray Energy, KeV
59

PLATE XIII

Plate XIV. SEM-EDX: Loricas from 2-Month-Old Cultures.

Figure 60. An increased number of elements is seen in this spectrum of lorica from MBBM culture, cf. Fig. 57.

Figure 61. Micrograph of lorica analysed in Fig. 60. TEM whole mount. 15,000x.

Figure 62. P, Ca and Si are the major elements indicated in this spectrum of a lorica from MSW along with a noticeable peak for Fe.

Figure 63. Micrograph of lorica analysed in Fig. 62. TEM whole mount. 17,000x.

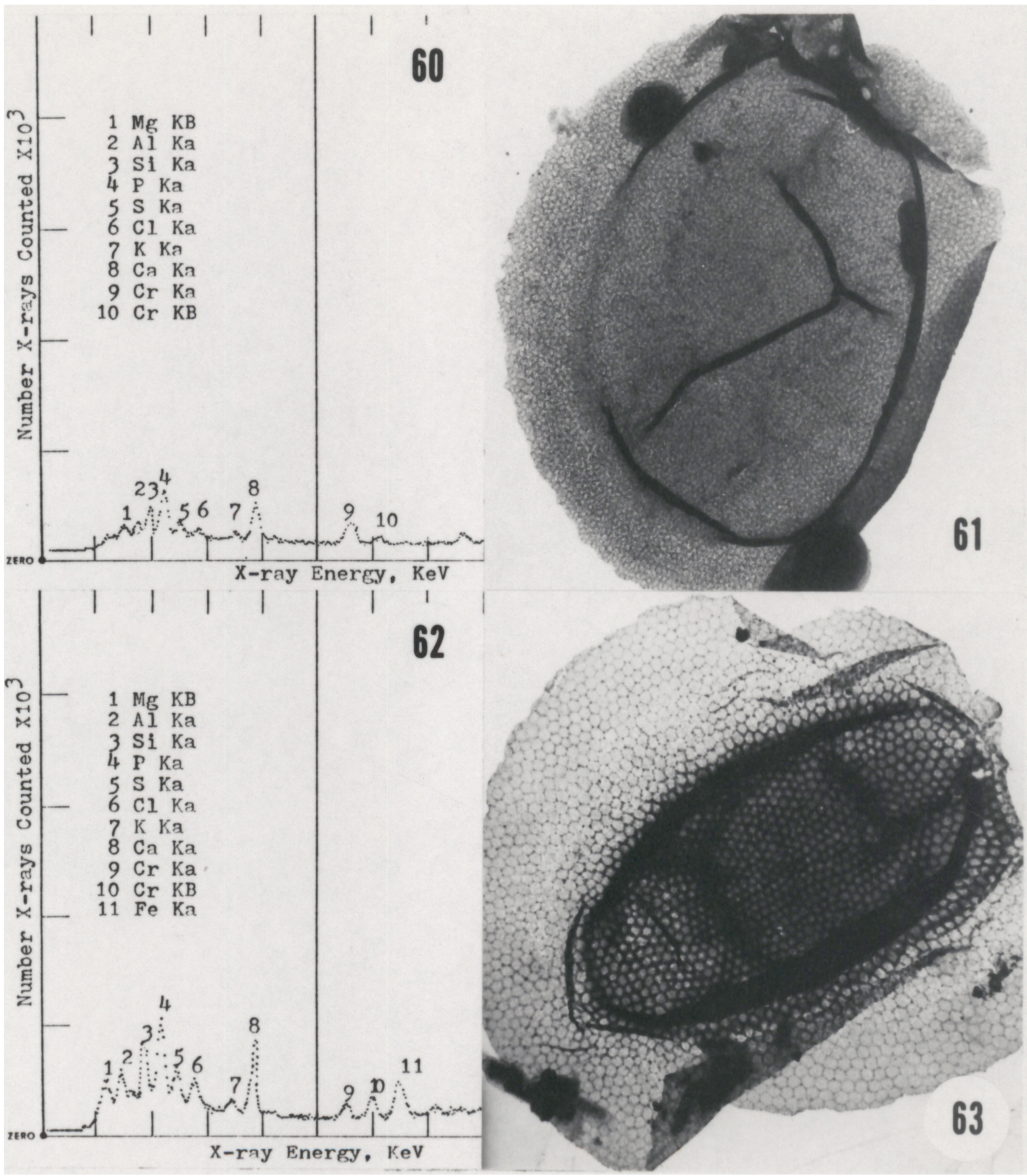

60
1 Mg KB
2 Al Ka
3 Si Ka
4 P Ka
5 S Ka
6 Cl Ka
7 K Ka
8 Ca Ka
9 Cr Ka
10 Cr KB
Number X-rays Counted X10³
ZERO
X-ray Energy, KeV
61
62
1 Mg KB
2 Al Ka
3 Si Ka
4 P Ka
5 S Ka
6 Cl Ka
7 K Ka
8 Ca Ka
9 Cr Ka
10 Cr KB
11 Fe Ka
Number X-rays Counted X10³
ZERO
X-ray Energy, KeV
63

PLATE XIV

Plate XV. SEM-EDX: Glusulase Treated Loricas from 14-Day-Old Cultures.

Figure 64. P, Ca and Si are the major elements shown in this spectrum of a lorica from MBBM.

Figure 65. Lorica analysed in Fig. 64 is shown. Hexagonal surface pattern is visible. TEM whole-mount. 15,000x.

Figure 66. Spectrum of lorica from MSW culture shows much smaller peak for Fe than in untreated loricas of the same age, but P, Ca and Si are still the major elements detected.

Figure 67. Micrograph of lorica analysed in Fig. 66 shows hexagonal surface pattern. TEM whole-mounts. 16,000x.

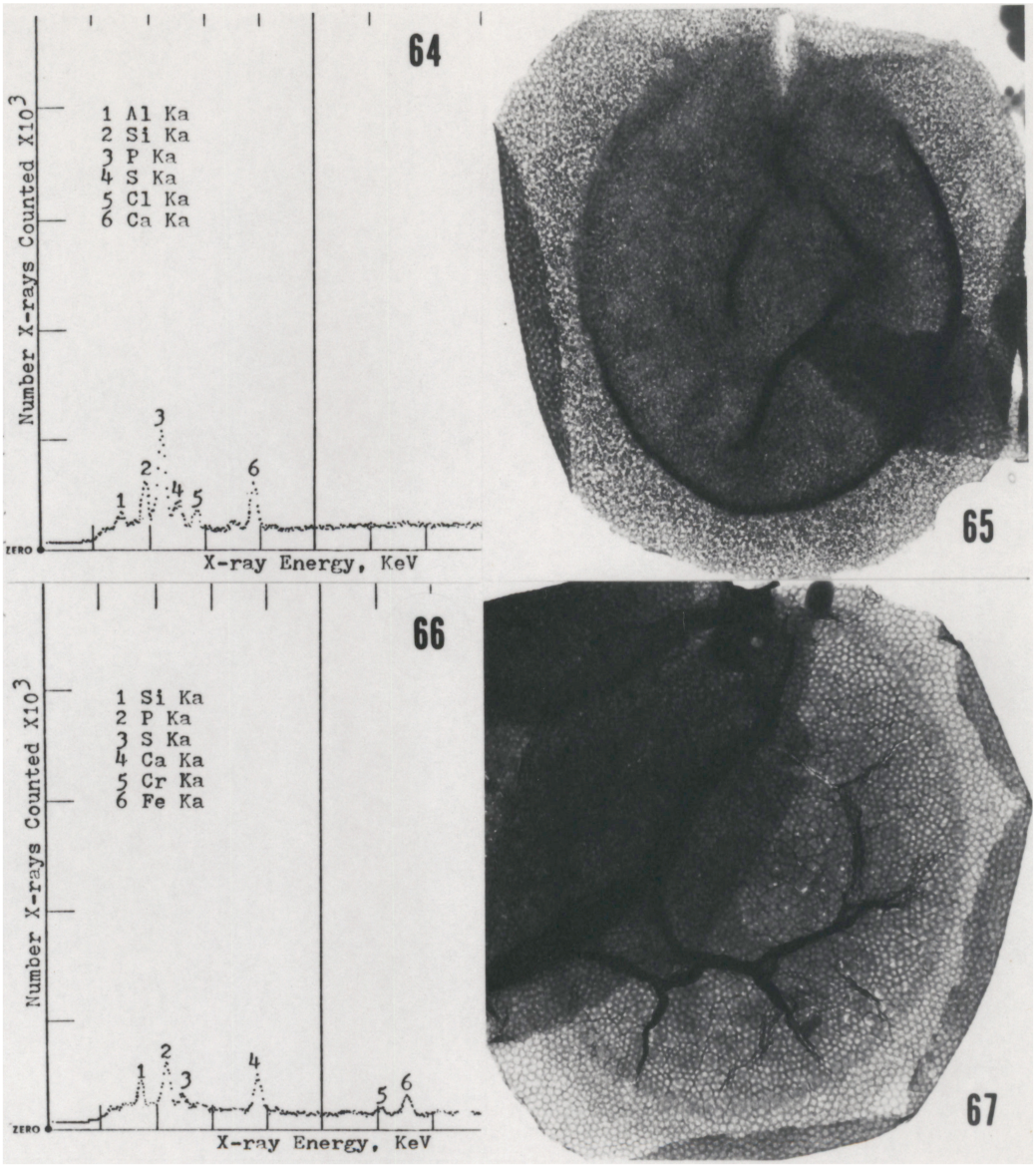

64
1 Al Ka
2 Si Ka
3 P Ka
4 S Ka
5 Cl Ka
6 Ca Ka
Number X-rays Counted X10³
ZERO
X-ray Energy, KeV
65
66
1 Si Ka
2 P Ka
3 S Ka
4 Ca Ka
5 Cr Ka
6 Fe Ka
Number X-rays Counted X10³
ZERO
X-ray Energy, KeV
67

PLATE XV

Plate XVI. SEM-EDX: Glusulase-Treated Loricas from 2-Month-Old Cultures.

Figure 68. Spectrum of lorica from MBBM culture shows P, Ca and Si as the major elements.

Figure 69. Micrograph of lorica analysed in Fig. 68; hexagonal surface pattern is visible. TEM whole-mount. 15,000x.

Figure 70. Spectrum of lorica from MSW culture shows P, Ca and Si peaks; Fe peak is lower than in untreated loricas of the same age.

Figure 71. Micrograph of lorica analysed in Fig. 70. TEM whole-mount. 15,000x.

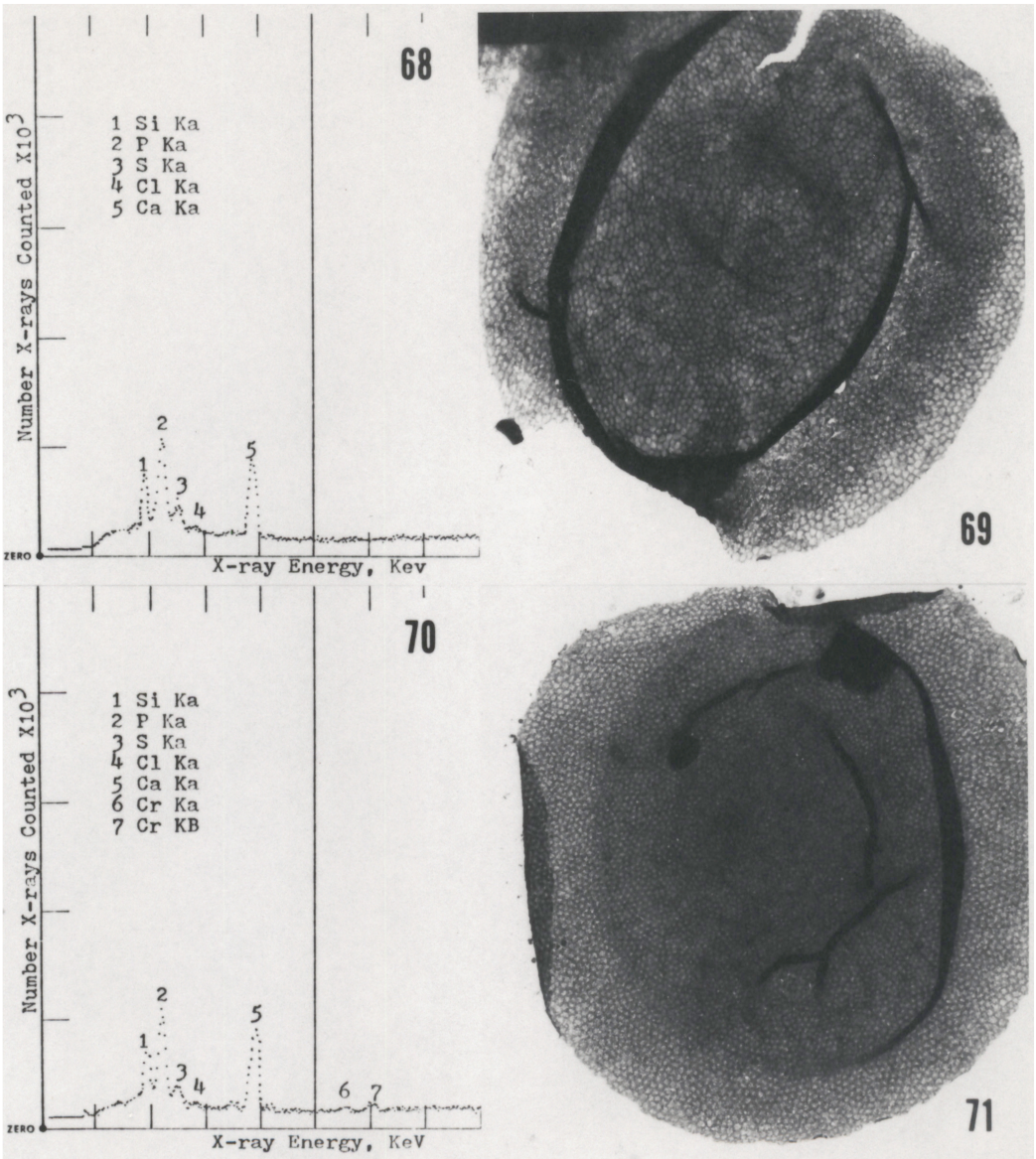

68
1 Si Ka
2 P Ka
3 S Ka
4 Cl Ka
5 Ca Ka
Number X-rays Counted X10³
ZERO
X-ray Energy, Kev
69
70
1 Si Ka
2 P Ka
3 S Ka
4 Cl Ka
5 Ca Ka
6 Cr Ka
7 Cr KB
Number X-rays Counted X10³
ZERO
X-ray Energy, KeV
71

PLATE XVI

Plate XVII. SEM-EDX: Loricas from 14-Day-Old Cultures After 30 Sec Treatment with EDTA.

Figure 72. Si and P are major elements indicated in this spectrum of a lorica from MBBM culture; Ca is barely detectable.

Figure 73. Lorica analysed in Fig. 72 is devoid of typical hexagonal surface pattern. TEM whole-mount. 14,000x.

Figure 74. Si, P and Fe are the major elements shown in this spectrum of a lorica from MSW culture; Ca is barely detectable.

Figure 75. Micrograph shows lorica analysed in Fig. 74 with no discernible surface pattern. TEM whole-mount. 15,000x.

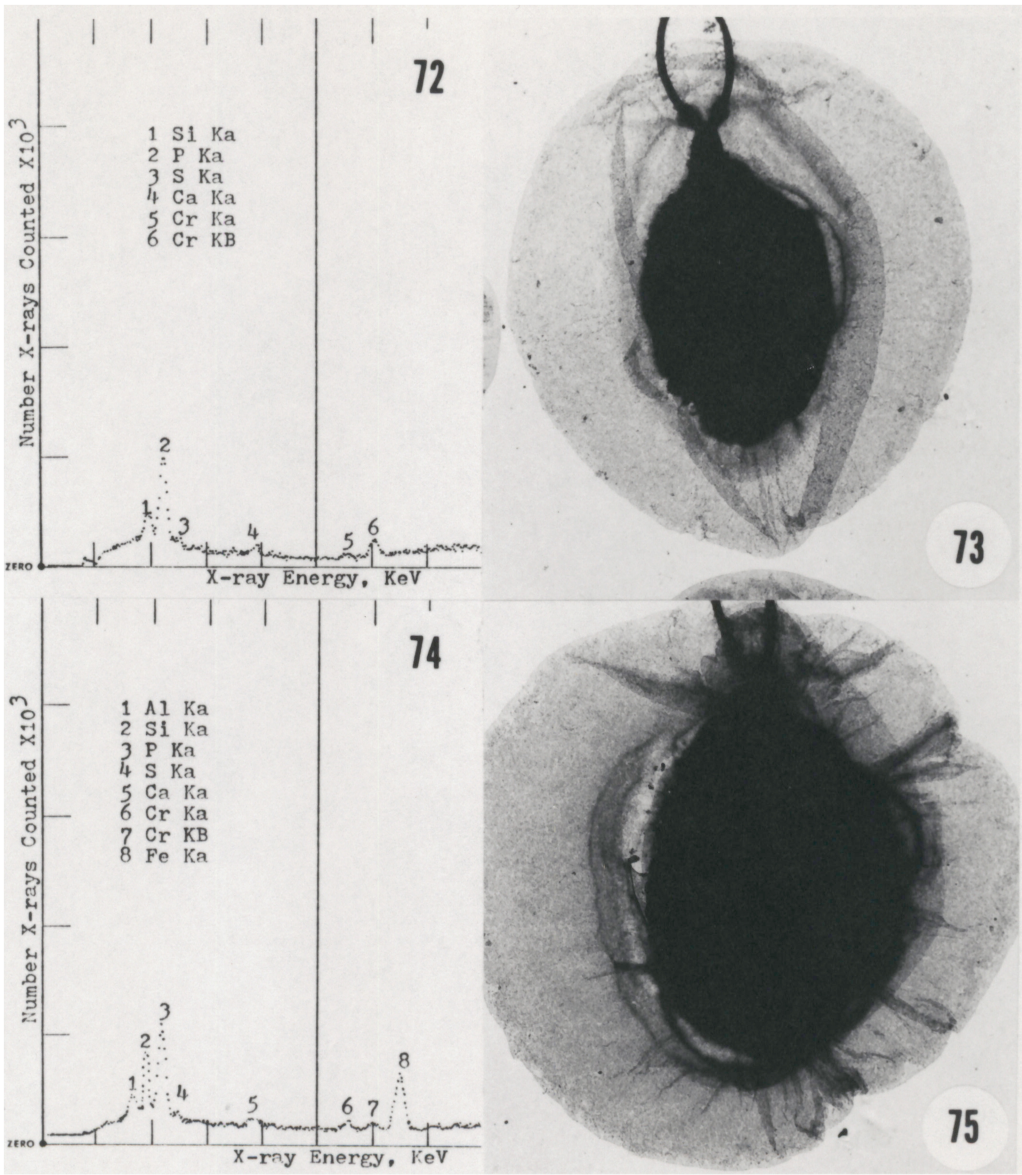

72
1 Si Ka
2 P Ka
3 S Ka
4 Ca Ka
5 Cr Ka
6 Cr KB
Number X-rays Counted X10³
ZERO
X-ray Energy, KeV
73
74
1 Al Ka
2 Si Ka
3 P Ka
4 S Ka
5 Ca Ka
6 Cr Ka
7 Cr KB
8 Fe Ka
Number X-rays Counted X10³
ZERO
X-ray Energy, KeV
75

PLATE XVII

Plate XVIII. SEM-EDX: Loricas from 14-Day-Old Cultures After 30 Sec Treatment with EGTA.

Figure 76. Spectrum of lorica from MBBM culture shows P and Si as major peaks and with a Ca peak intermediate in height between untreated and EDTA-treated loricas of the same age.

Figure 77. Micrograph of lorica analysed in Fig. 76 shows a faintly visible hexagonal surface pattern. TEM whole-mount. 15,000x.

Figure 78. P, Si and Fe are the major peaks in this spectrum of a lorica from MSW; however, Ca peak is considerably lower than in untreated loricas of the same age.

Figure 79. Hexagonal surface is discernible in this micrograph of lorica analysed in Fig. 78. TEM whole-mount. 15,000x.

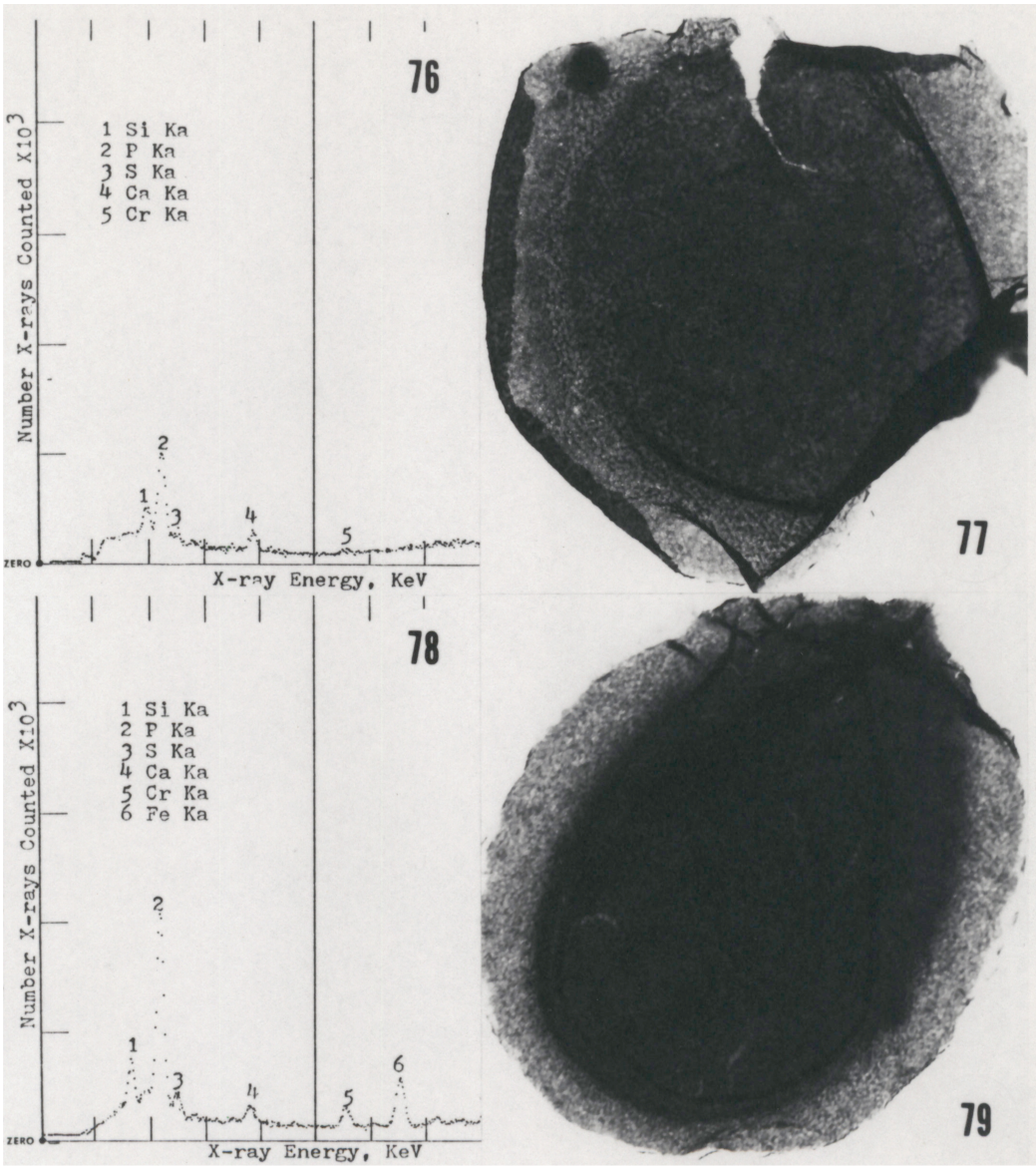

76
1 Si Ka
2 P Ka
3 S Ka
4 Ca Ka
5 Cr Ka
Number X-rays Counted X10³
ZERO
X-ray Energy, KeV
77
78
1 Si Ka
2 P Ka
3 S Ka
4 Ca Ka
5 Cr Ka
6 Fe Ka
Number X-rays Counted X10³
ZERO
X-ray Energy, KeV
79

PLATE XVIII

Plate XIX. SEM-EDX: Loricas from 14-Day-Old Cultures After 5 min EGTA Treatment.

Figure 80. Si and P are major elements shown in this spectrum of lorica from MBBM culture; Ca is a minor element.

Figure 81. Lorica analysed in Fig. 80 shows no discernible surface pattern. TEM whole-mount. 14,000x.

Figure 82. Spectrum of lorica from MSW shows Si and P as major elements detected; Ca is a minor element.

Figure 83. Lorica analysed in Fig. 82 shows no discernible surface pattern. TEM whole-mount. 14,000x.

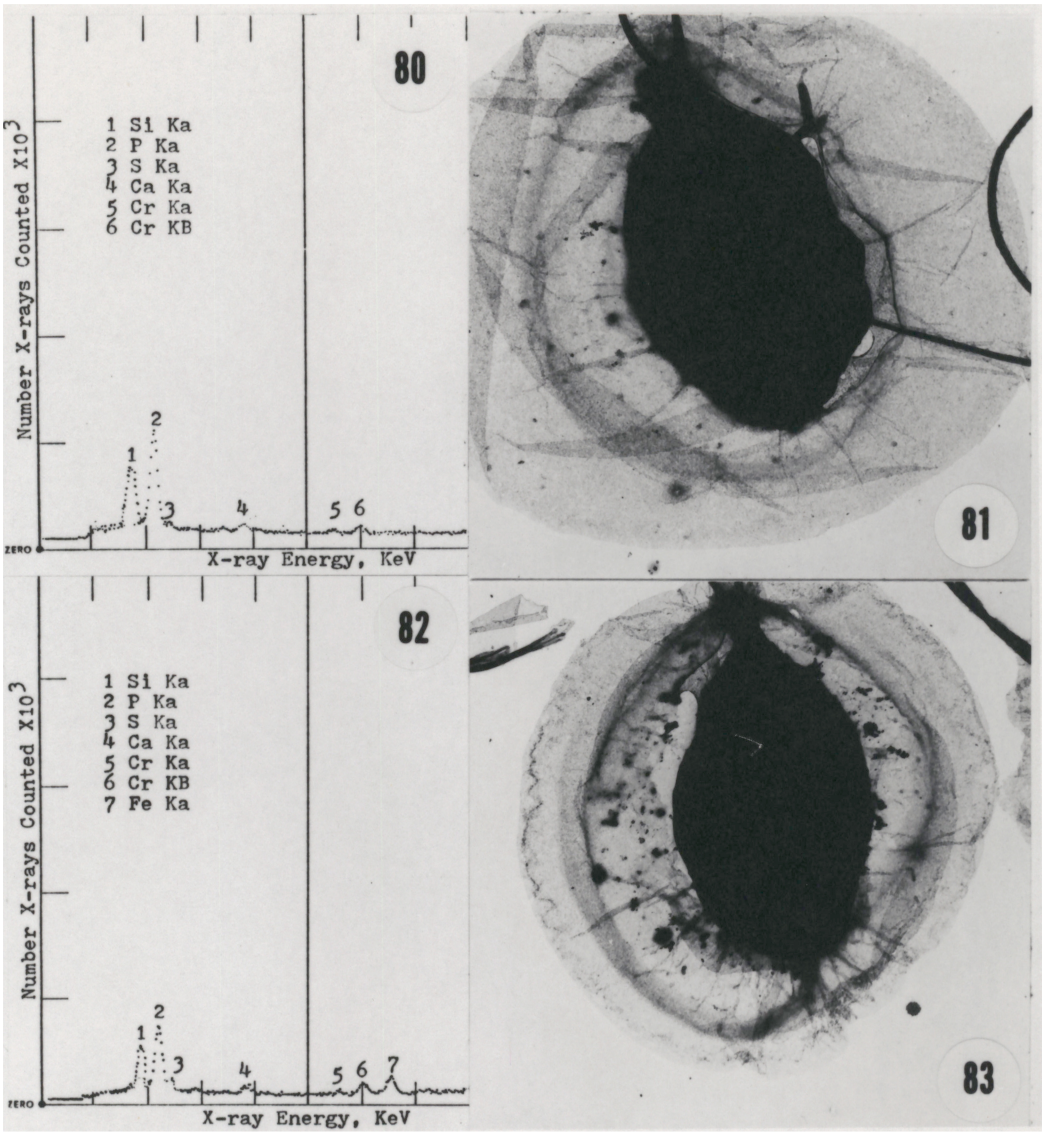

80
1 Si Ka
2 P Ka
3 S Ka
4 Ca Ka
5 Cr Ka
6 Cr KB
Number X-rays Counted X10³
ZERO
X-ray Energy, KeV
81
82
1 Si Ka
2 P Ka
3 S Ka
4 Ca Ka
5 Cr Ka
6 Cr KB
7 Fe Ka
Number X-rays Counted X10³
ZERO
X-ray Energy, KeV
83

PLATE XIX

Plate XX. SEM-EDX: Acetolysis Treated Loricas.

Figure 84. Ca and P are the only elements detected in this spectrum of an MSW lorica which was resistant to acetolysis.

Figure 85. Lorica analysed in Figure 84 shows only the hexagonal pattern with no material visible in the region of the secondary reticulum.

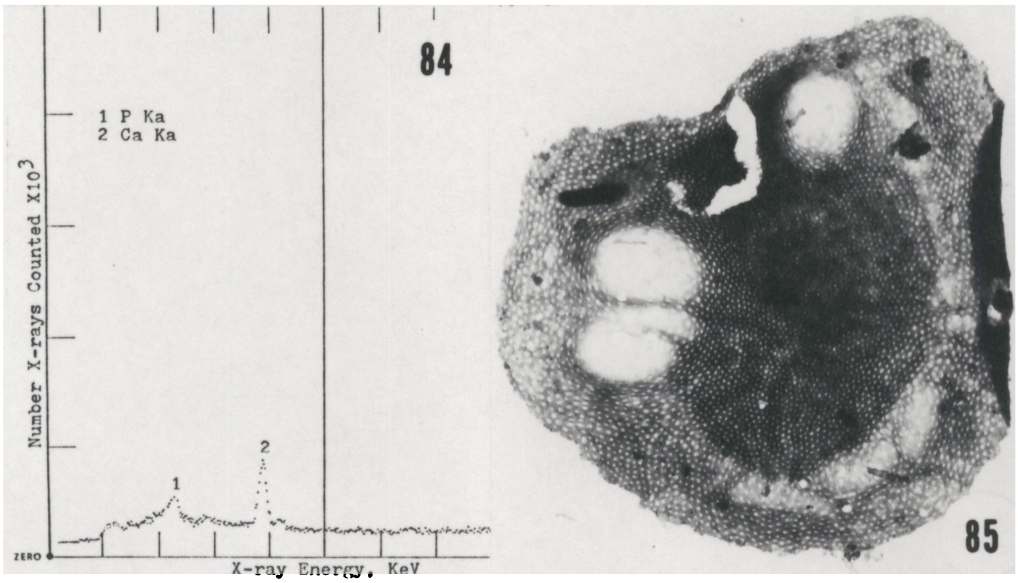

84
1 P Ka
2 Ca Ka
Number X-rays Counted X10³
1
2
ZERO
X-ray Energy, KeV
85

PLATE XX

Plate XXI. General Morphology.

Figure 86. Vegetative cells from MBBM culture show variations in size and shape. Distinctive characteristics at LM level include the winged lorica (arrows), 2 flagella and a single centrally located pyrenoid. LM oblique illumination. 4000x. Inset. Anterior view vegetative cell shows the recurved nature of the lorica wing. LM bright-field, reverse image. 4500x.

Figure 87. Vegetative cell showing the winged lorica with its hexagonal pattern, and 2 isokont flagella ca 1½ times as long as the protoplast. TEM whole-mount. 5300x.

Figure 88. Higher magnification with LM of a vegetative cell shows numerous starch plates around the pyrenoid and a lateral stigma (arrow). 4900x.

Figure 89. Vegetative cell showing that hexagonal pattern is raised above the lorica surface. Flagellar hairs are visible in this preparation. TEM shadow-cast. 5500x.

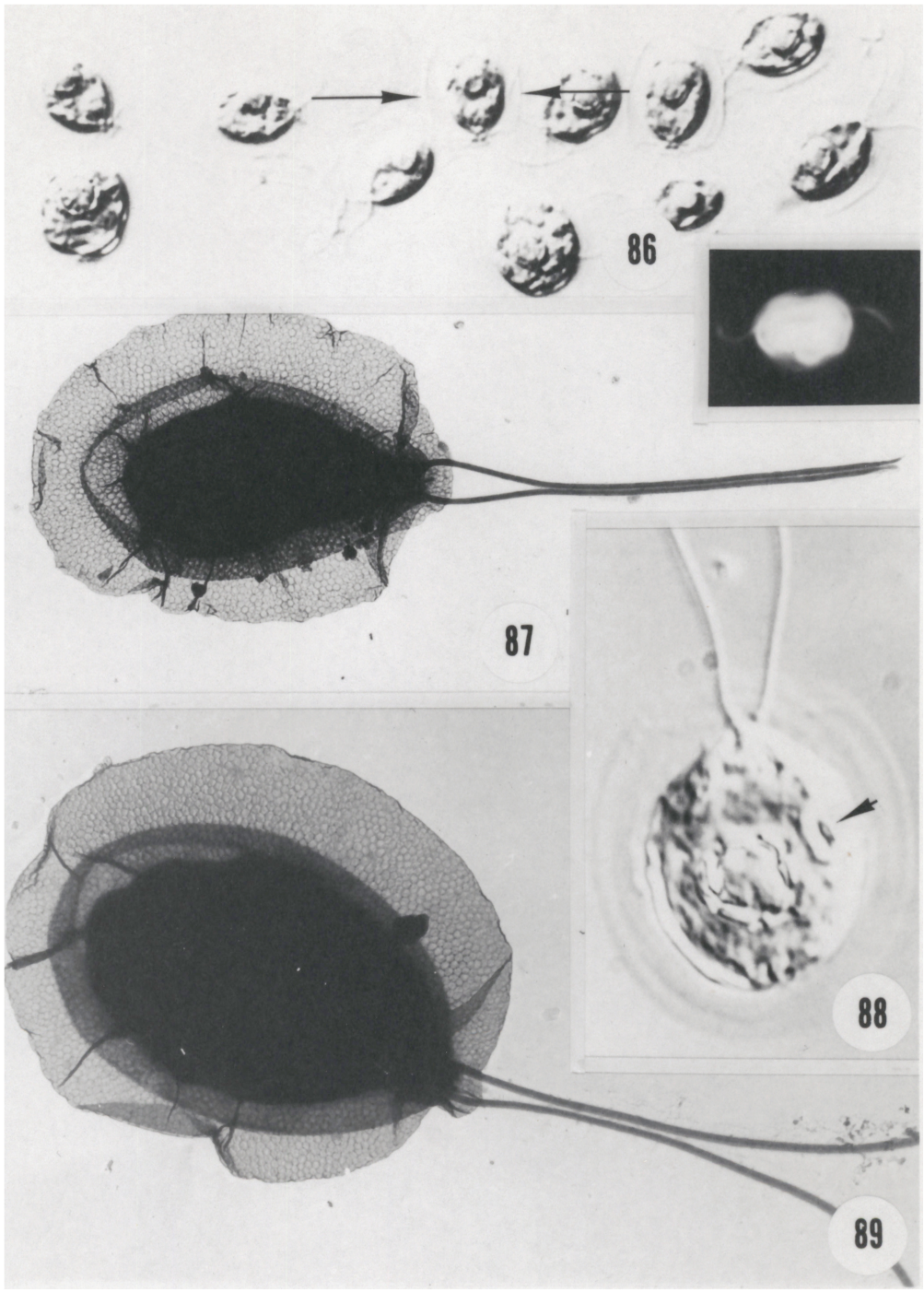


PLATE XXI

Plate XXII. SEM: Vegetative Cell.

Figure 90. Anterior view of vegetative cell grown in MSW shows lorica wing where the 2 valves are appressed together, and the wedge-shaped segment through which the 2 flagella emerge. The raised hexagonal surface pattern is also visible. 9000x.

Figure 91. Micrograph showing the S-shaped configuration of the lorica wing which accounts for the spiral swimming motion of the cell. 3000x.

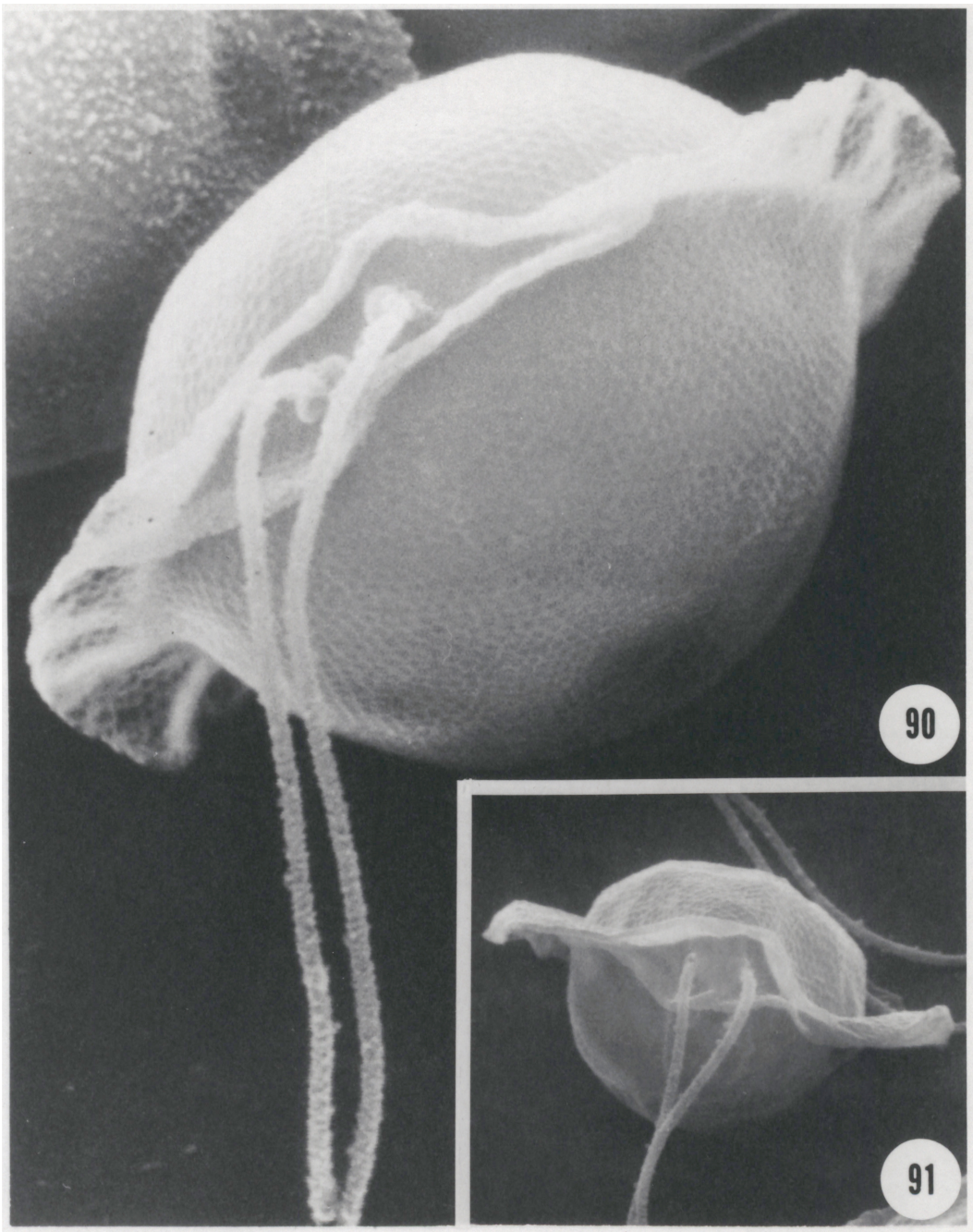


PLATE XXII

Plate XXIII. Vegetative Cell Ultrastructure.

Figure 92. Near median longitudinal section through a vegetative cell shows most major organelles in their typical locations. TEM thin-section. 30,000x.



PLATE XXIII

Plate XXIV. Organelle Relationships.

Figure 93. Portion of vegetative cell shows positional relationships of some organelles, e.g., amplexis of ER and dictyosome, close association of the nuclear membrane and chloroplast membrane. TEM thin-section. 33,000x.

Figure 94. Section of an interphase cell showing RER continuous with the outer nuclear membrane that is also studded with ribosomes. TEM-thin section. 42,000x.

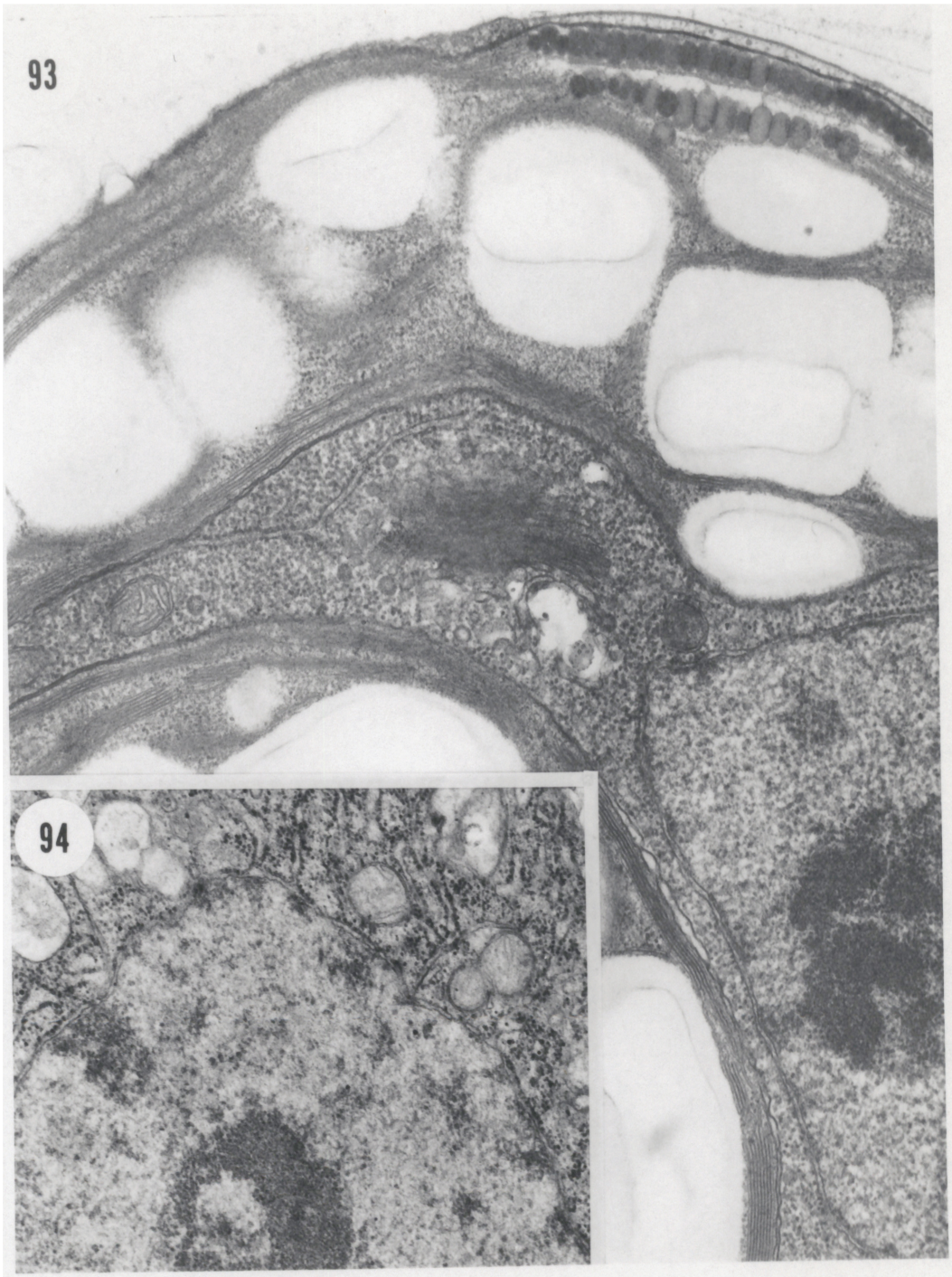


PLATE XXIV

Plate XXV. Ultrastructure of Nucleus.

Figure 95. Transverse section through slightly lobed interphase nucleus with centrally located nucleolus. TEM thin-section. 32,000x.

Figure 96. Early prophase nucleus shows condensation of the chromatin material, some positioned very close to the nuclear membrane. TEM thin-section. 33,000x.

Figure 97. High magnification of a prophase nucleus shows numerous condensed chromosomes, some in close proximity to the nuclear membrane, and associated with microtubules (arrows). TEM thin-section. 125,000x.

Figure 98. High magnification shows nuclear pores. Ribosomes are visible on the surface of the outer nuclear membrane. TEM thin-section. 122,000x.

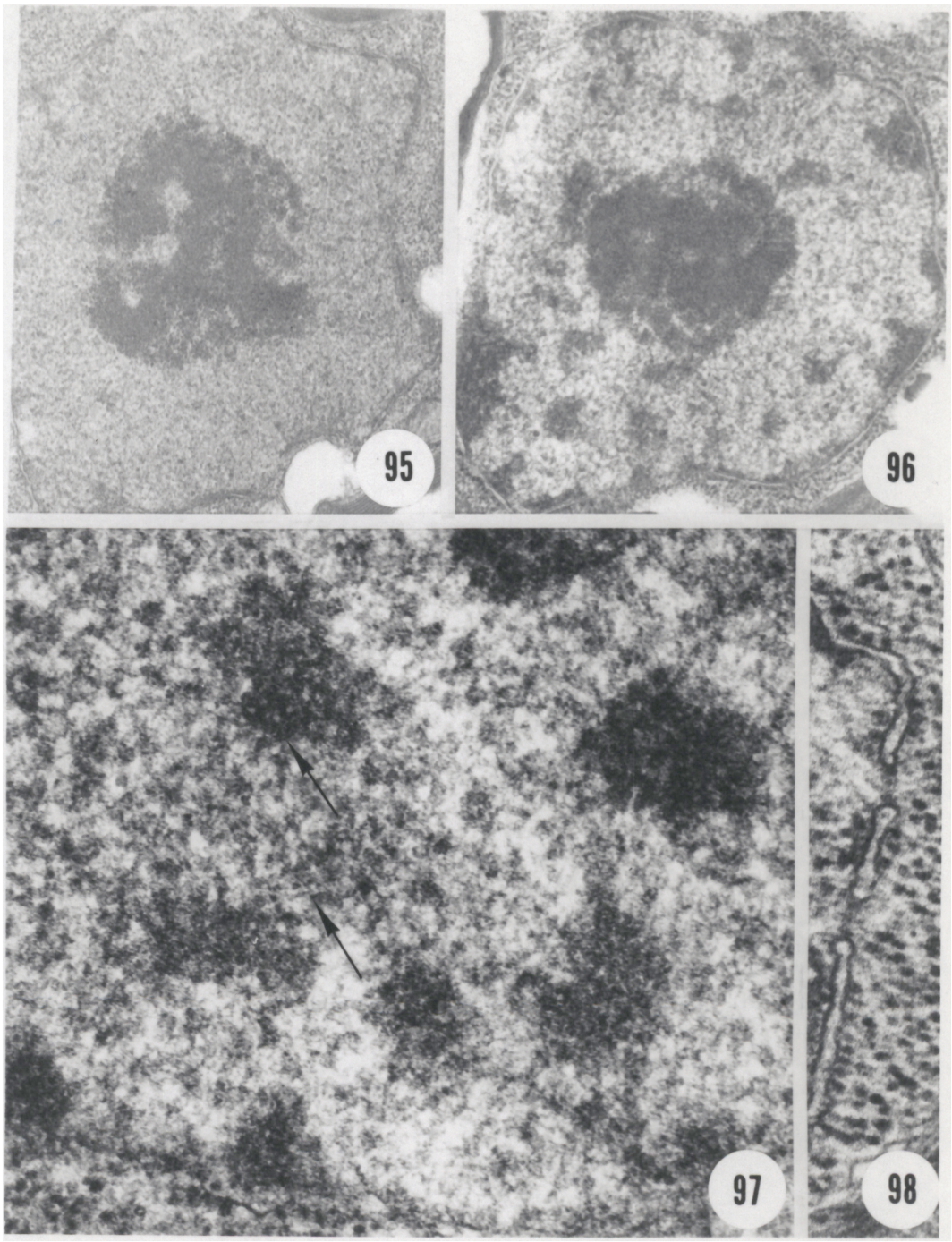


PLATE XXV

Plate XXVI. Endoplasmic Reticulum and Golgi Apparatus.

Figure 99. Proliferation of RER (arrows) is characteristic of dividing cells. TEM-thin section. 46,000x.

Figures 100-101. Serial sections of a dividing cell show RER near the area of the division plane at cell periphery. TEM thin-section. 46,000x.

Figure 100. SER is close to the forming face of dictyosome profile (arrows). 22,000x.

Figure 101. Close to the forming face of dictyosome profile, SER is visible (arrows). 22,000x.

Figure 102. Transverse section at the level of the nucleus shows dictyosome profiles (d) in characteristic locations close to the nucleus. TEM thin-section. 21,000x.

Figure 103. Section through formative cell shows dictyosome profile on either side of the nucleus with PLPM in the cisternae (arrows). TEM thin-section. 22,000x.

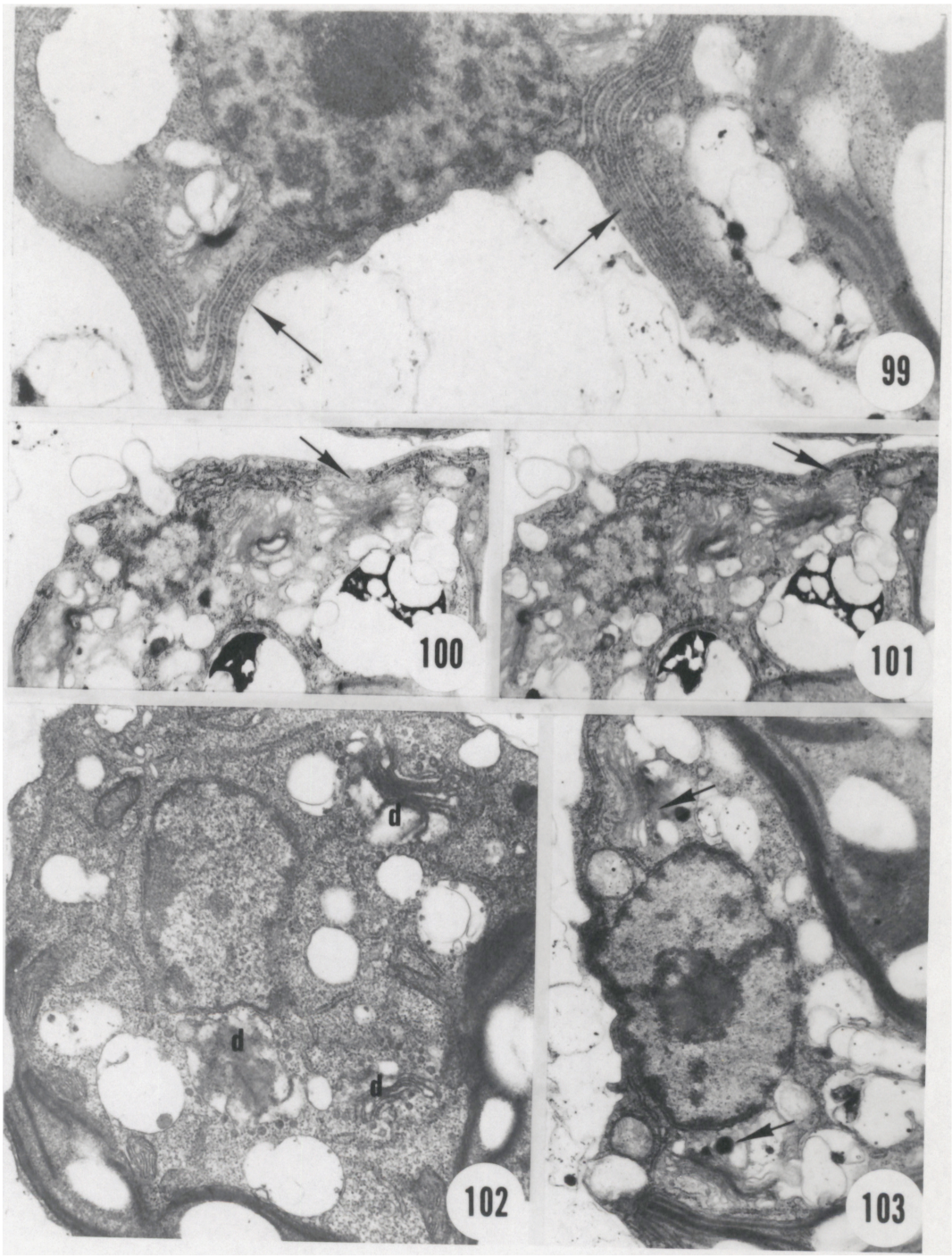


PLATE XXVI

Plate XXVII. Membrane Flow.

Figures 104-107. Serial sections through newly formed daughter cell at the level of the nucleus shows the nuclear membrane-ER-Golgi apparatus relationship. Section number indicated in parentheses.

Figure 104. Dictyosome profile to the left of the nucleus shows SER vesicles at the forming face of the dictyosome. A profile of RER is visible below the dictyosome, but no connection to the nuclear membrane is apparent (1). TEM-thin-section. 30,000x.

Figure 105. Dictyosome to the left of the nucleus shows numerous SER vesicles at the forming face. The dictyosome to the right shows PLPM in the cisternae at its maturing face (4). TEM-thin section. 30,000x.

Figure 106. The outer nuclear membrane is continuous with the RER at the left of the nucleus and SER vesicles at the forming face and PLPM is visible in vesicles at the maturing face of the dictyosome to the right of the nucleus (6). TEM-thin section. 30,000x.

Figure 107. No connection between RER and nuclear membrane is apparent (cf. Fig. 104). Note that both dictyosome profiles have their forming faces toward the outside of the cell and their maturing faces toward the interior of the cell (7). TEM-thin. 30,000x.

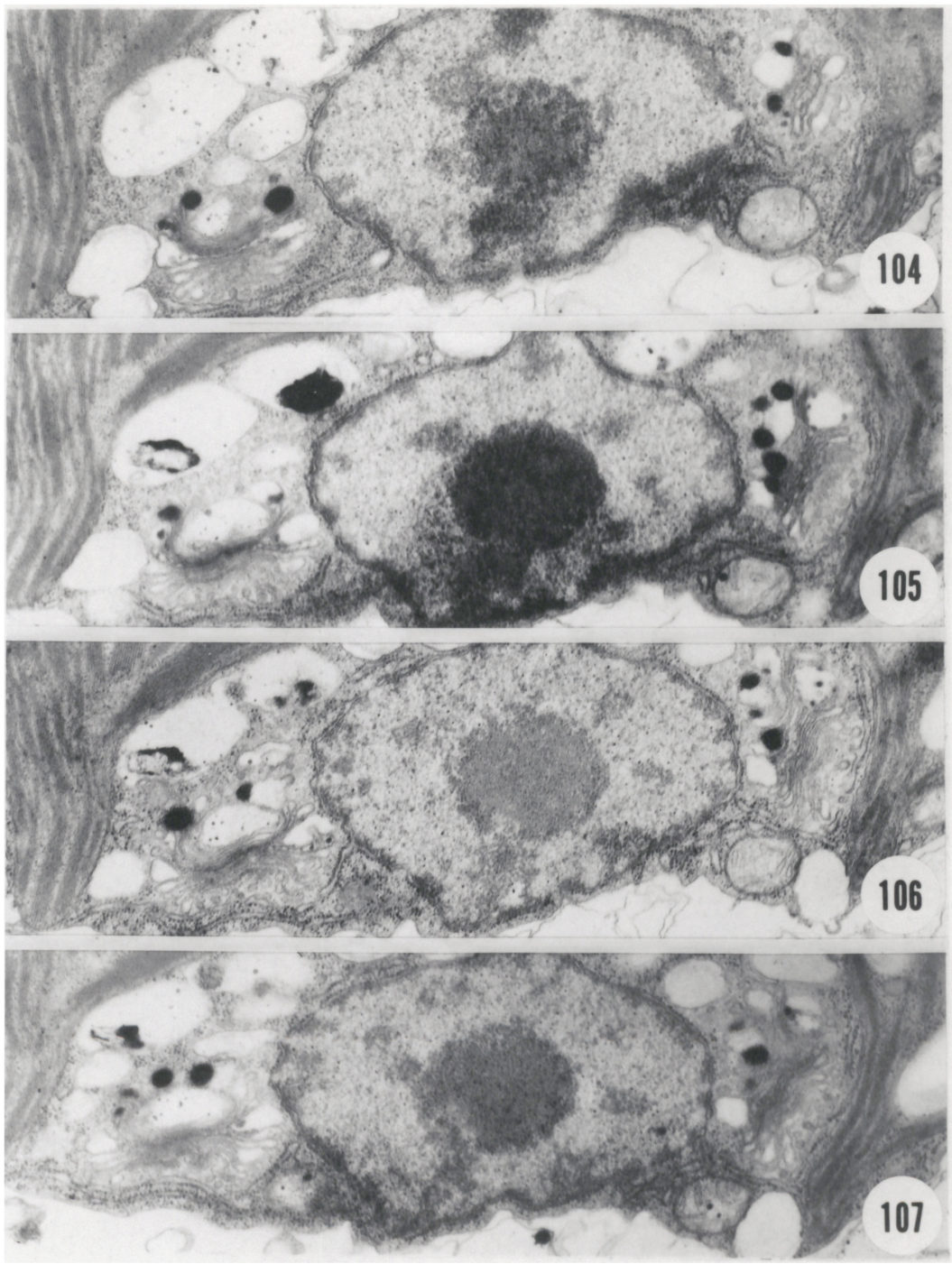


PLATE XXVII

Plate XXVIII. Mitochondria and Contractile Vacuoles.

Figure 108. In transverse section, mitochondria (arrows) are commonly found at the periphery of the cell in close proximity to the chloroplast and nucleus. TEM thin-section. 38,000x.

Figure 109. Longitudinal section shows a long, cylindrical mitochondrial profile. TEM thin-section. 42,000x.

Figure 110. High magnification of a mitochondrion shows the characteristic deeply lobed cristae. TEM thin-section. 69,000x.

Figure 111. Section through the anterior end of a vegetative cell shows both CVs, one expanded and one contracted. TEM thin-section. 41,000x.

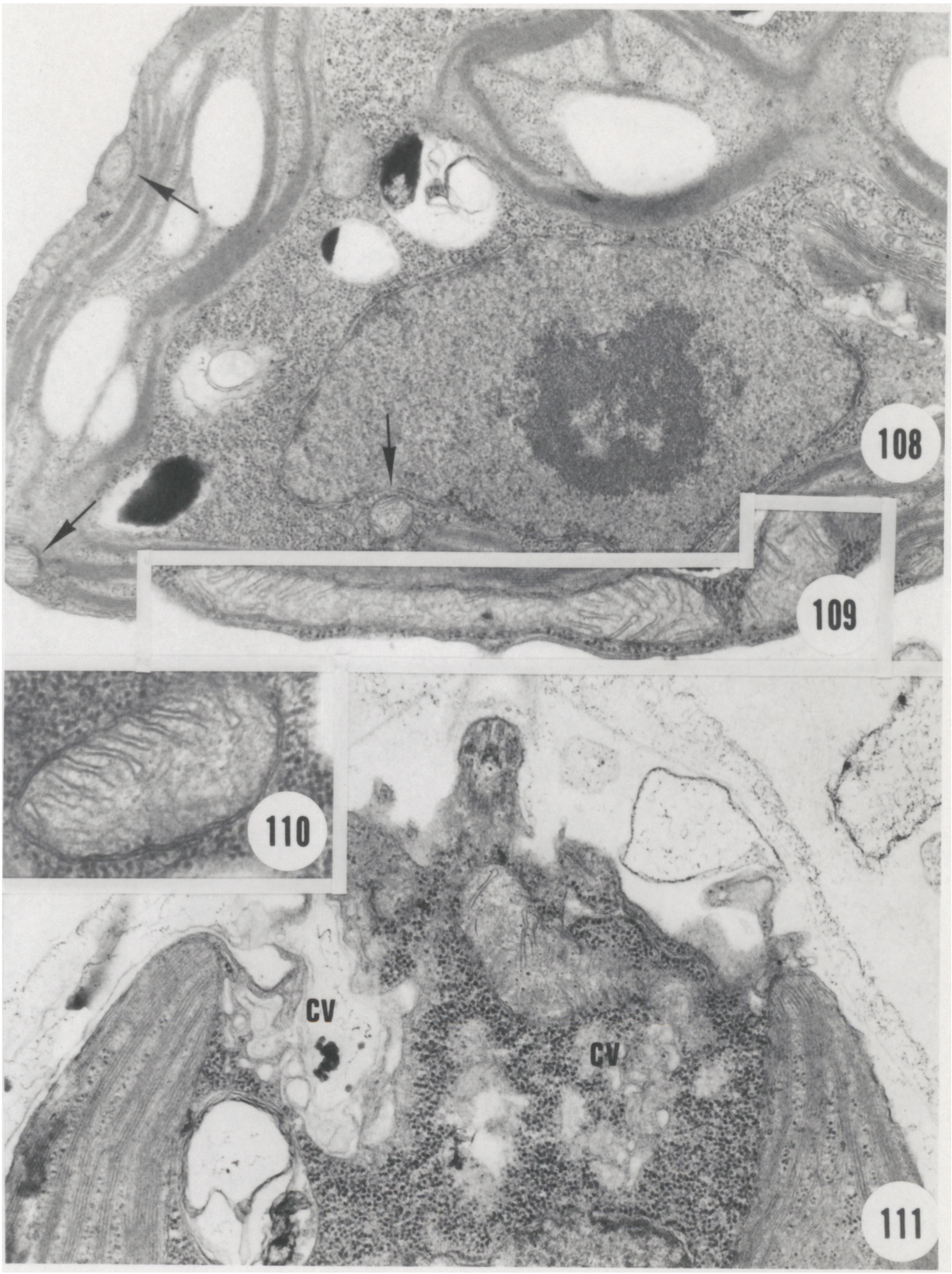


PLATE XXVIII

Plate XXIX. Flagella Ultrastructure.

Figure 112. Longitudinal section through flagellum shows axonemal microtubules and 2 types of flagellar hairs. Short, thick hairs are extensions of the flagellar membrane (large arrows), whereas the fine mastigonemes appear to be attached to the flagellar membrane (small arrows). TEM thin-section. 57,000x.

Figure 113. The long-fine mastigonemes and the short flagellar hairs can be seen in this shadow-cast preparation. 50,000x.

Figure 114. A row of mastigonemes is apparent on either side of 2 flagella. TEM shadow-cast. 54,000x.

Figure 115. High magnification of longitudinal section of flagellum shows axonemal microtubules, the mucilage sheath surrounding the flagellum, and the flagellar membrane. TEM thin-section. 55,000x.

Figure 116. Transverse section of a flagellum shows the typical 9+2 doublet microtubular arrangement, and a fine mucilaginous sheath which surrounds the flagellum. The flagellar membrane is also evident (arrows). TEM thin-section. 69,000x.

Figure 117. The flagellar tips are often flattened like a paint brush allowing observation of individual axonemal microtubules. TEM shadow-cast. 51,000x.

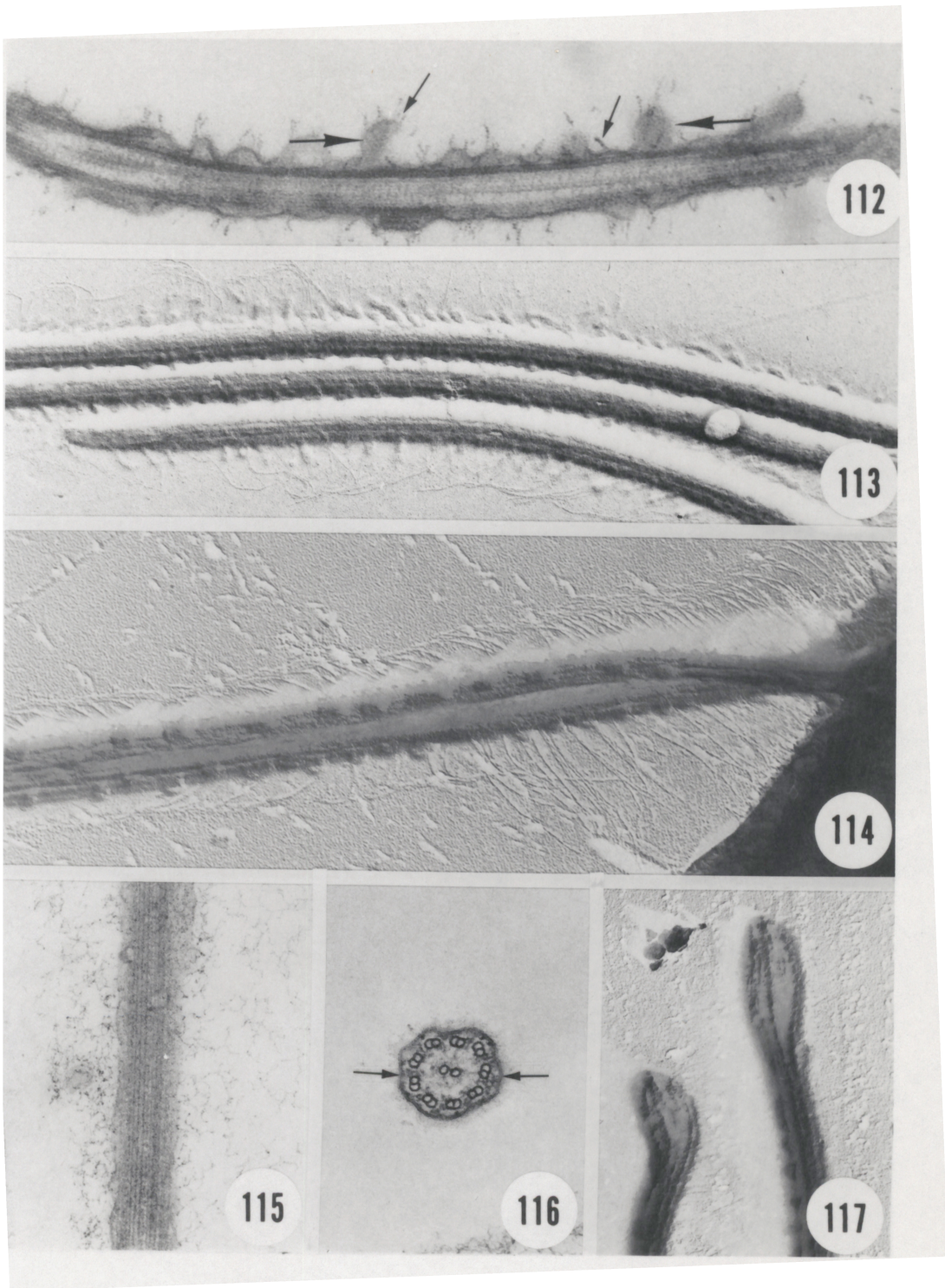


PLATE XXIX

Plate XXX. Flagella Transverse Sections.

Figures 118-126 correspond to levels 1-9, respectively, as shown in Figure 127. TEM thin-sections.

Figure 118. Section external to the lorica. 60,000x.

Figure 119. Section external to the lorica and through flagellar hairs. 60,000x.

Figure 120. Section through the flagellar collar of the lorica. 60,000x.

Figure 121. Section through flagellar pore distal to the transition zone. 60,000x.

Figure 122. Section through the distal portion of the transition zone. Note remnants of the inner microtubular doublets. 65,000x.

Figure 123. Section through distal portion of the H-piece, flagellar pore is still present but the central doublets are no longer evident. 62,000x.

Figure 124. Section through the proximal region of the transition zone. Flagellar pore no longer present. 71,000x.

Figure 125. Section through basal body showing the outer doublets but no central doublet or H-piece. 60,000x.

Figure 126. Section showing triplet region of the basal body. 70,000x.

Figure 127. Longitudinal section through a flagellum. 50,000x.

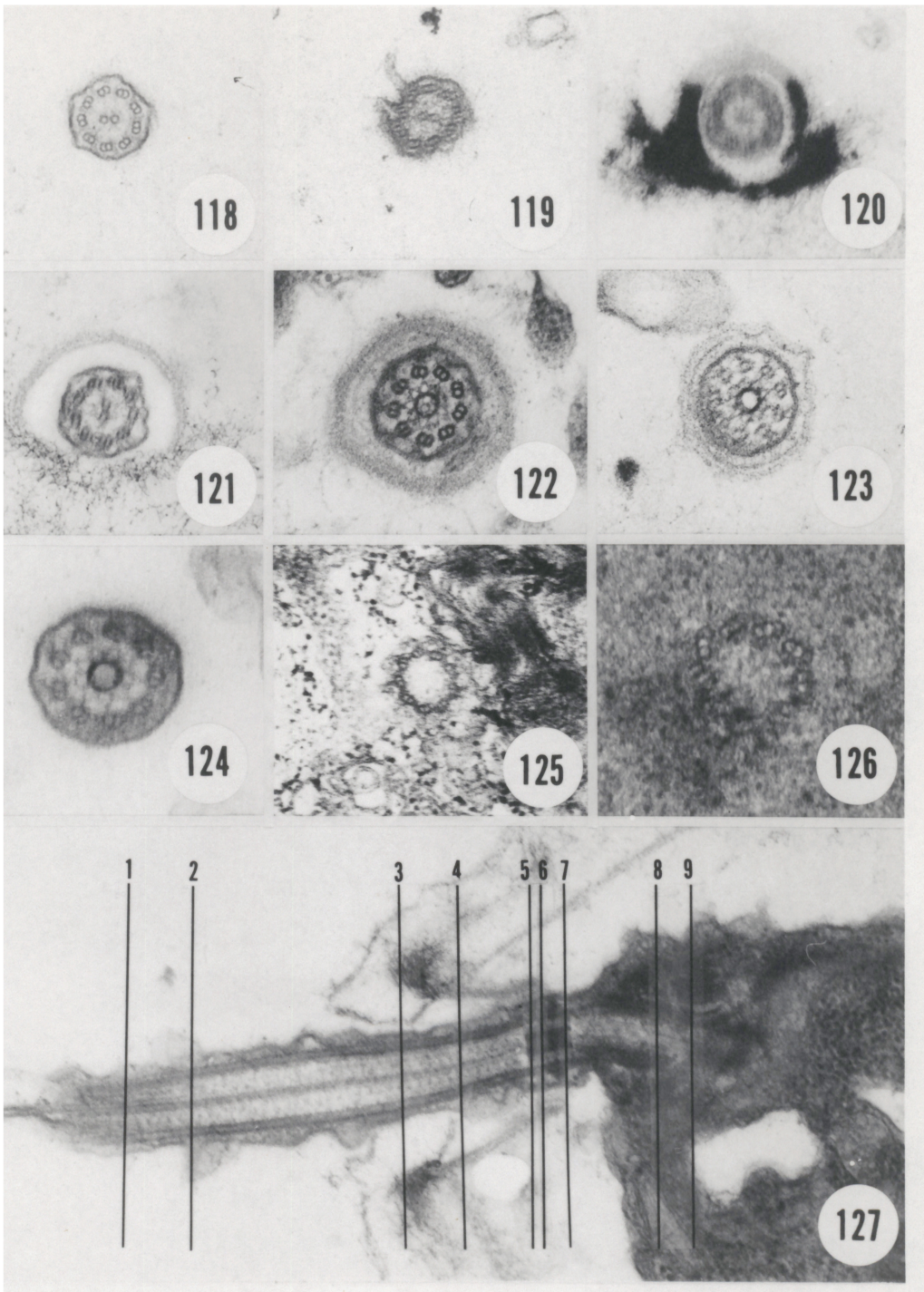


PLATE XXX

Plate XXXI. Flagellar Apparatus.

Figure 128. Transverse section through anterior end of cell shows 4 cruciate microtubular bands (numbered) of the cytoskeleton that originate between the basal bodies. 83,000x.

Figure 129. Tangential section shows 3 microtubular bands (numbered), one flagellar base and second basal body. TEM thin-section. 80,000x.

Figure 130. Transverse section through both basal bodies showing 2 microtubular bands (numbered), one with 4 microtubules (arrow). TEM thin-section. 82,000x.

Figure 131. Longitudinal section through both basal bodies showing the distal striated fiber. TEM thin-section. 26,000x.

Figure 132. High magnification of longitudinal section showing both basal bodies and the distal striated fiber (arrow). TEM thin-section. 78,000x.

Figure 133. Longitudinal section between basal bodies shows the distal striated fiber (arrow head) and 2 microtubular roots originating just posterior to the fiber (arrows). TEM thin-section. 30,000x.

Figure 134. Longitudinal section through both basal bodies shows them in a mitochondrial (M) depression. TEM thin-section. 28,000x.

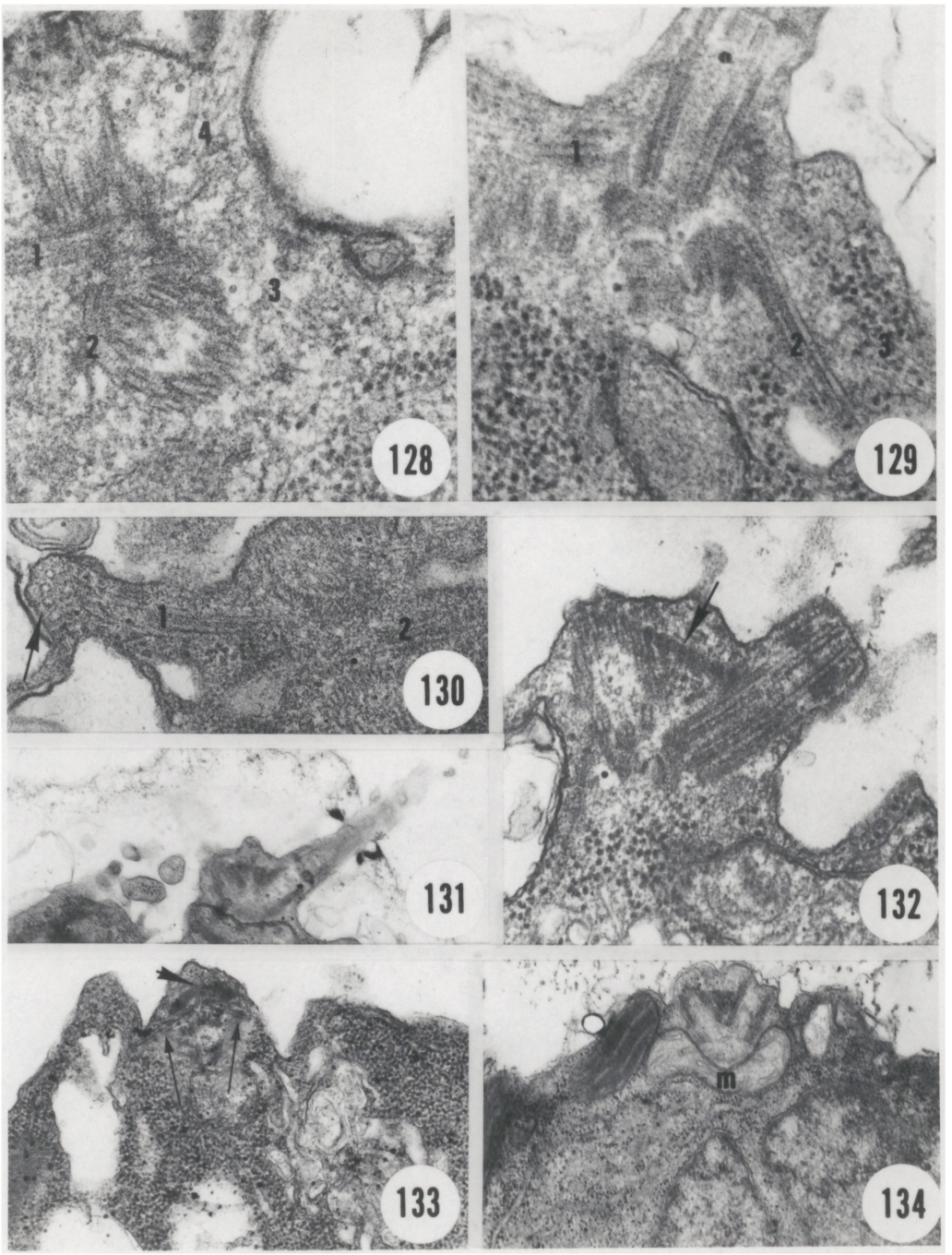


PLATE XXXI

Plate XXXII. Cytoplasmic Microtubules.

Figure 135. Transverse section posterior to level of the nucleus shows 5 microtubules in a 1-3-1 configuration (arrows), just below the plasmalemma. TEM thin-section. 165,000x.

Figure 136. Section through formative zoospores shows a 3-1 cytoplasmic microtubular arrangement (arrows). TEM thin-section. 160,000x.

Figure 137. Transverse section through median region of cell shows at least 7 microtubules (arrows). TEM thin-section. 80,000x.

Figure 138. Section through posterior region of the cell shows 2 microtubules close to the chloroplast membrane. TEM thin-section. 162,000x.

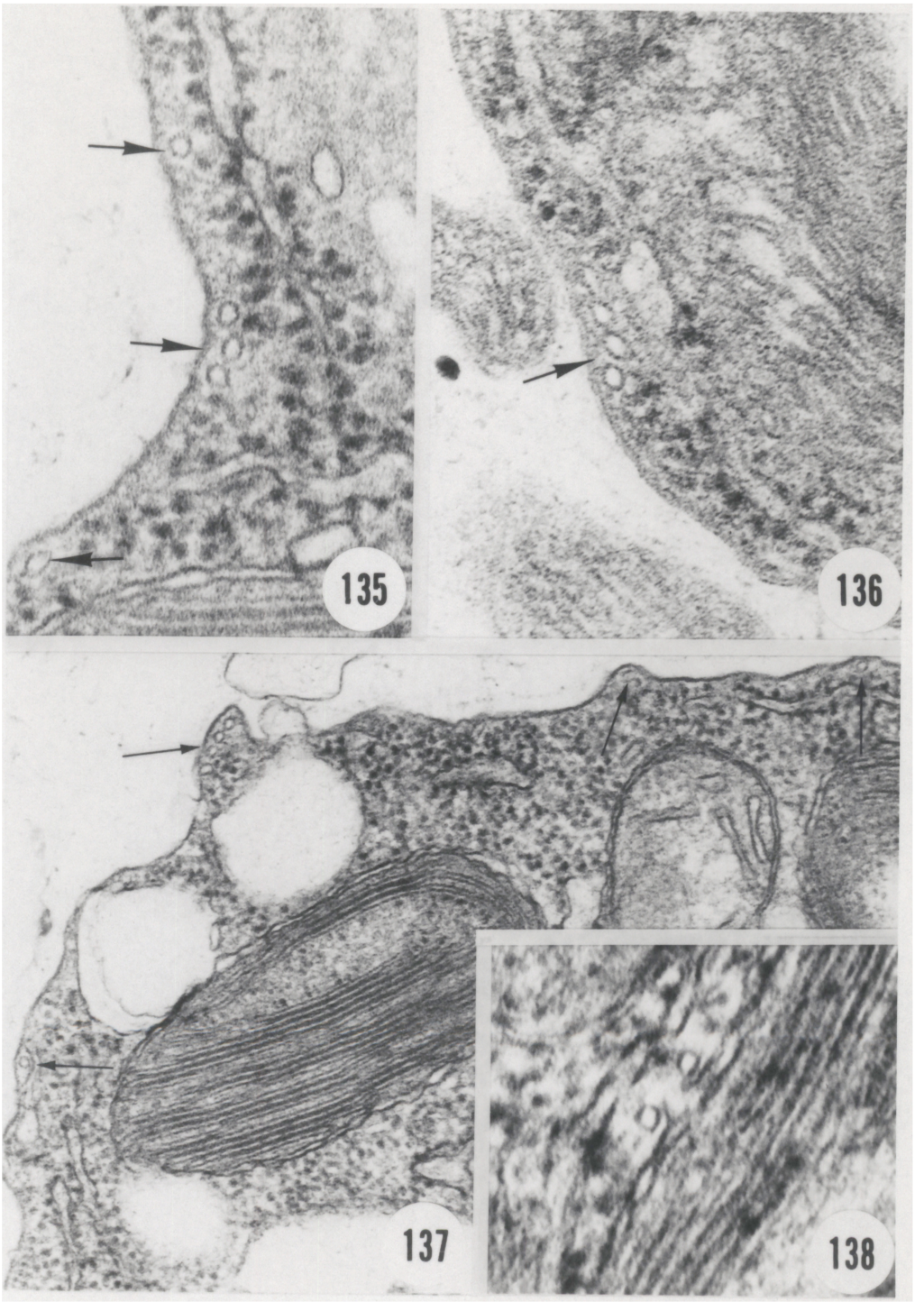


PLATE XXXII

Plate XXXIII. Flagellar Roots.

Figure 139. Section shows 2 bands of 2 microtubules (arrows), one close to a basal body. TEM-thin section. 45,000x.

Figure 140. Section through a basal body showing a root of 2 microtubules (arrow). TEM thin-section. 49,000x.

Figure 141. Transverse section through a microtubular band with a 3-over-1 configuration. TEM thin-section. 110,000x.

Figure 142. Section near the basal body showing a 3-over-1 microtubular root. TEM thin-section. 100,000x.

Figure 143. Longitudinal section through anterior end of the cell shows a 4-over-1 microtubular root. TEM thin-section. 115,000x.

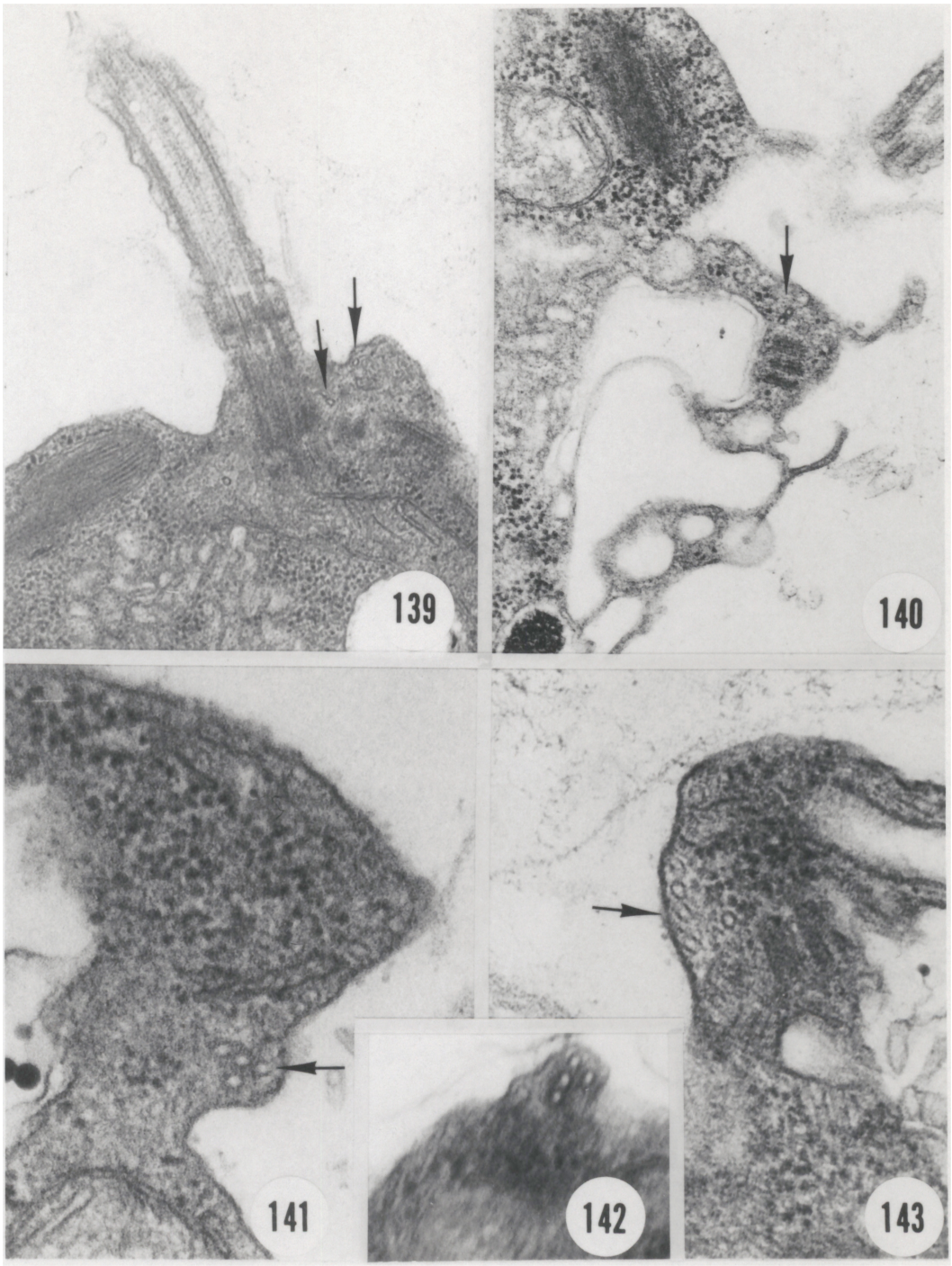


PLATE XXXIII

Plate XXXIV. Extra Basal Bodies and Microtubules Associated with the Chloroplast or Stigma.

Figure 144. Tangential section showing 3 basal bodies (numbers) and 2 microtubular roots. TEM thin-section. 125,000x.

Figure 145. Longitudinal section shows 3 basal bodies (numbers) in formative daughter cell. TEM thin-section. 55,000x.

Figure 146. Section shows microtubule (arrow) inside the chloroplast close to the stigma, which consists of 3 rows of osmophilic granules. TEM thin-sections. 76,000x.

Figure 147. Cytoplasmic microtubules (arrows) are visible near the stigma in this young zoospore. TEM thin-section. 59,000x.

Figure 148. Portion of anterior end of zoospore shows intrachloroplastidic and cytoplasmic microtubules (arrows). TEM thin-section. 58,000x.

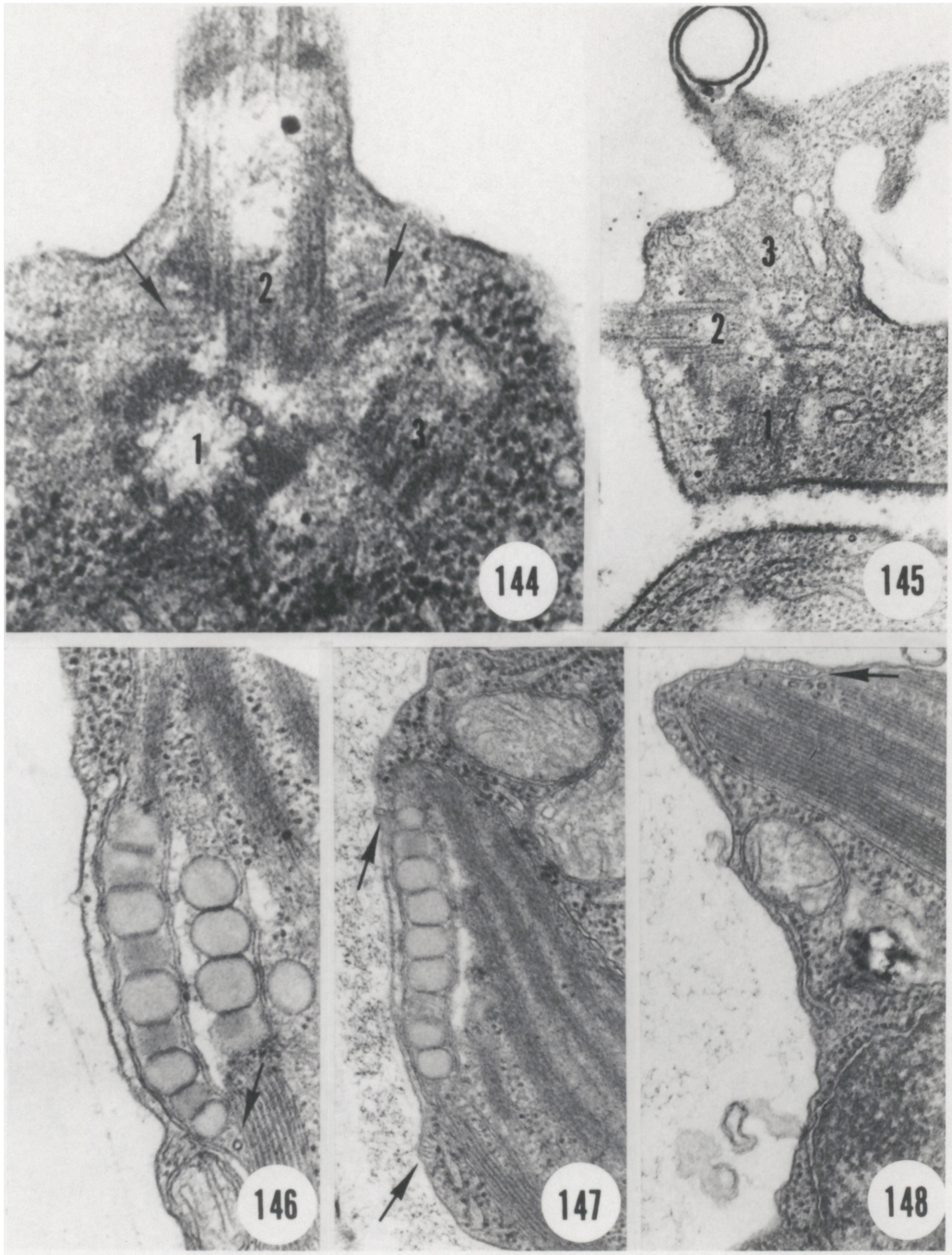


PLATE XXXIV

Plate XXXV. Microtubules.

Figure 149. Transverse section through numerous microtubules beneath the plasmalemma. TEM thin-section. 60,000x.

Figure 150. Longitudinal section through vegetative cell shows more cytoplasmic microtubules (arrows) than can be accounted for by a 4-2-4-2 cruciate root system. TEM thin-section. 62,000x.

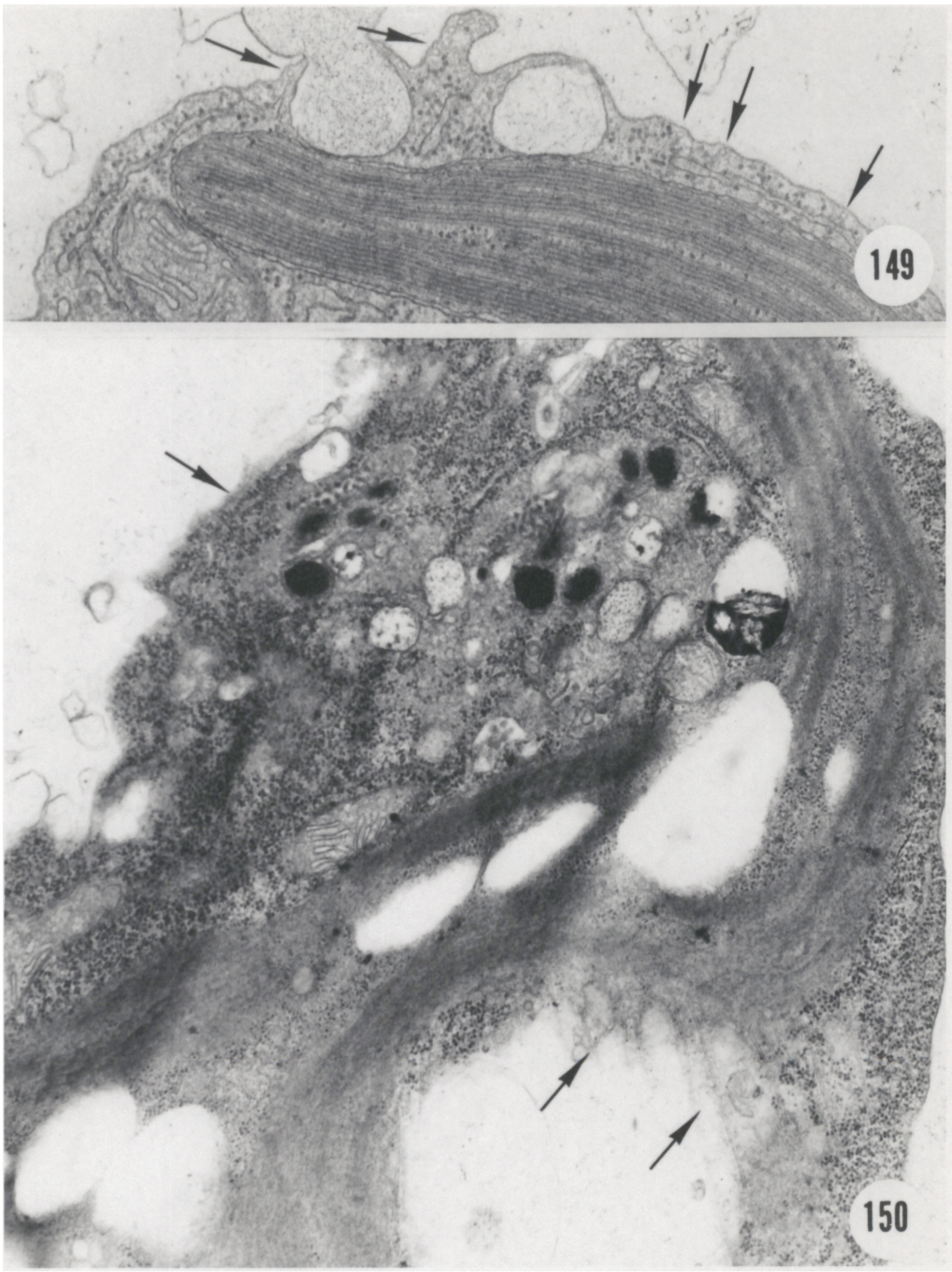


PLATE XXXV

Plate XXXVI. Chloroplast, Pyrenoid and Stigma.

Figure 151. The stigma is commonly closely appressed to the chloroplast membrane and plasmalemma (arrows). A single thylakoid separates each row of osmophilic granules. TEM thin-section. 75,000x.

Figure 152. Glancing section through stigma shows hexagonal osmophilic granules. TEM thin-section. 55,000x.

Figure 153. Longitudinal section shows chloroplast thyalkoids in stacks of 3 to 15 around the pyrenoid. Single thyalkoids enter the pyrenoid between the starch plates, and the chloroplast and nuclear membranes are in close proximity (arrows). TEM thin-section. 35,000x.

Figure 154. Longitudinal section showing thyalkoid that traverses the pyrenoid. TEM thin-section. 14,000x.

Figure 155. Micrograph showing paired thyalkoids in the pyrenoid matrix (arrow). TEM thin-section. 14,000x.

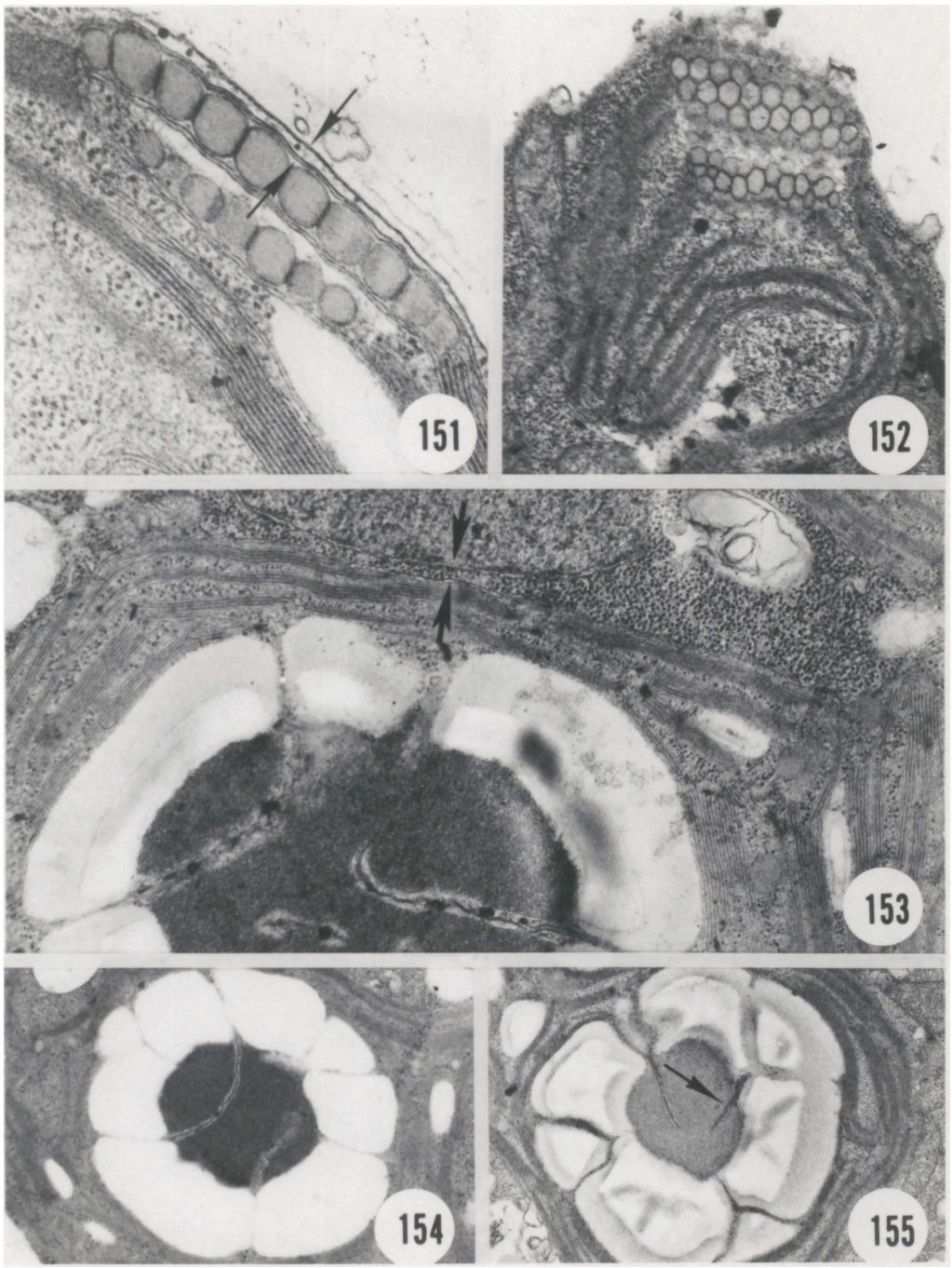


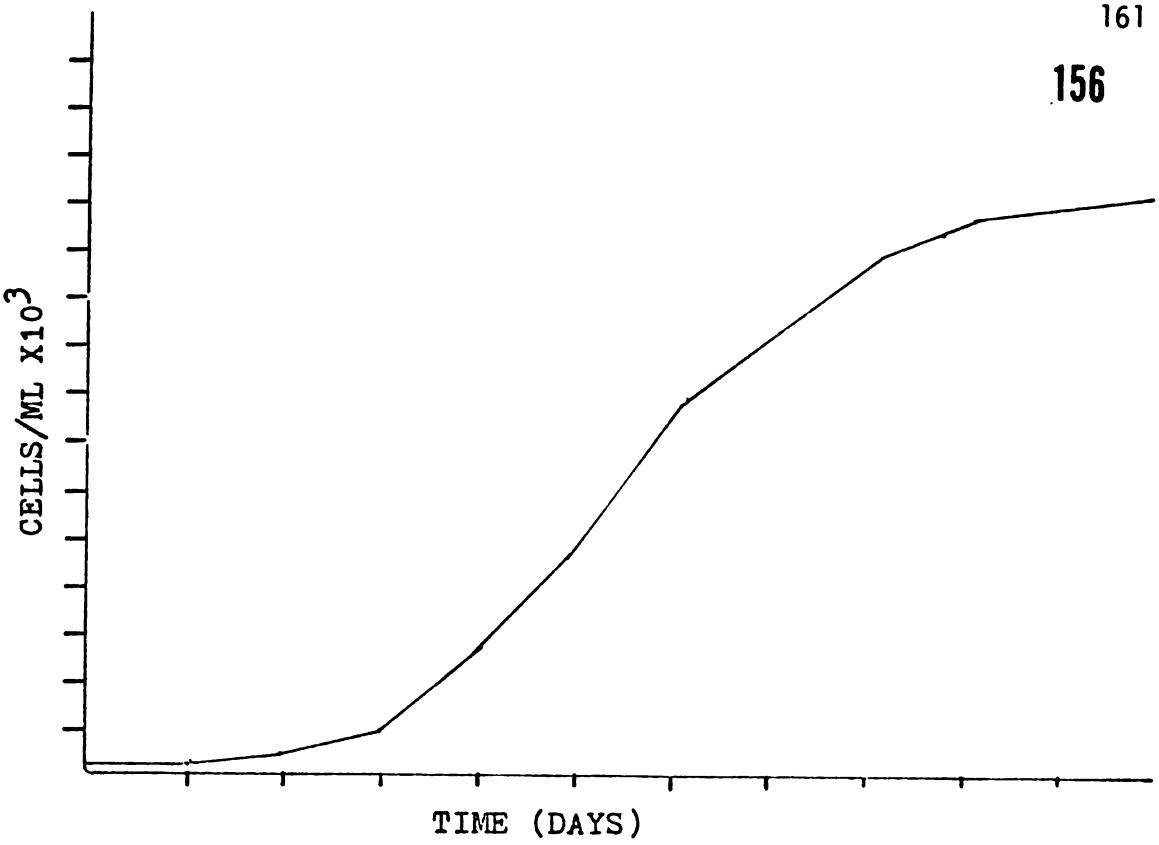
PLATE XXXVI

Plate XXXVII. Growth Studies.

Figure 156. Growth curve of MBBM cultures. Lag phase ca. 18 hr; log phase ca. 144 hr (6 days); stationary phase begins ca. 192 hr (8 days).

Figure 157. Relative chlorophyll content, indicative of cell number, of cultures used to generate growth curve shown in Fig. 156.

156



157

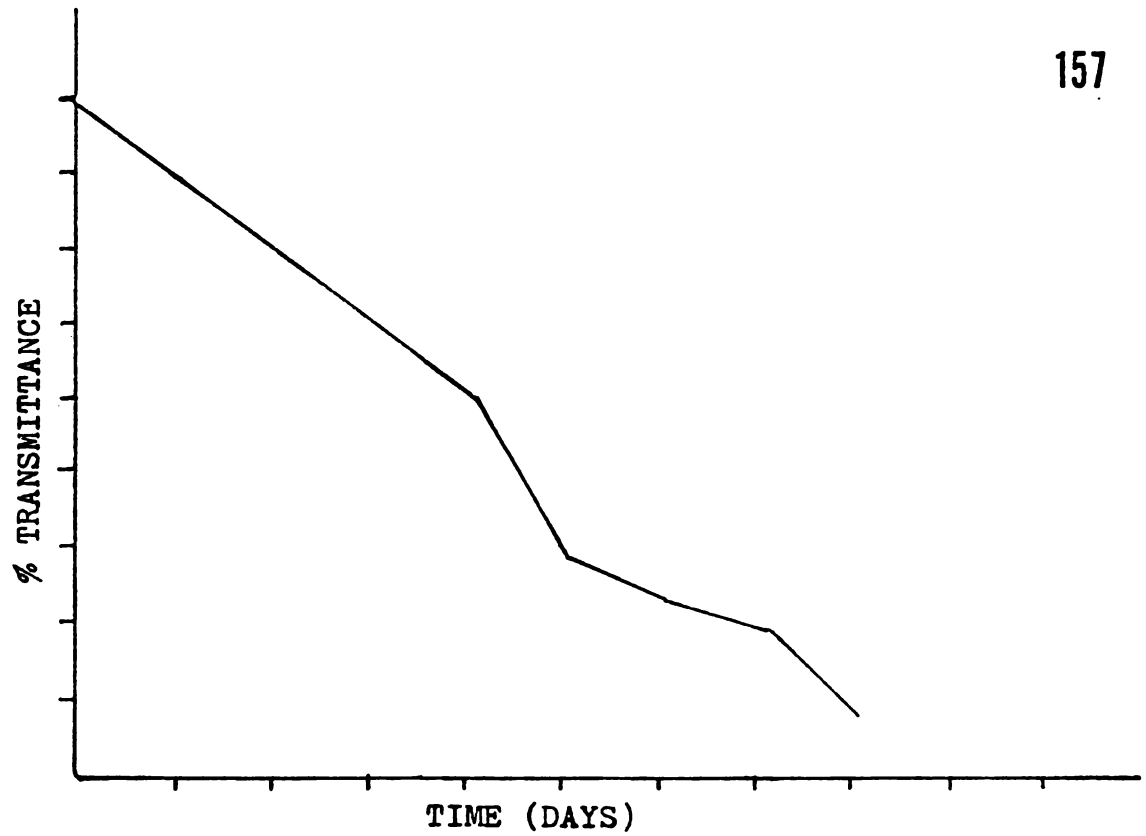


Plate XXXVII

Plate XXXVIII. Diagrammatic Representation of Life Cycle.

Figure 158. Life cycle: 1. Motile vegetative cell; 2. Vegetative cell with 2 pyrenoids; 3. Non-motile cell prior to mitosis; 4. Mitosis complete, cytokinesis taking place; 5. Cytokinesis complete; 6. 2 daughter cells inside parent lorica; 7. Second division; 8. 4 daughter cells inside parent lorica; 9. Released daughter cells; 10. Fusion of isogametes; 11. Two-headed stage in zygote formation; 12. Quadriflagellate planozygote; 13. Aplanozygote; 14. Germination of aplanozygote. (Diagram courtesy of Linda Pocratsky).

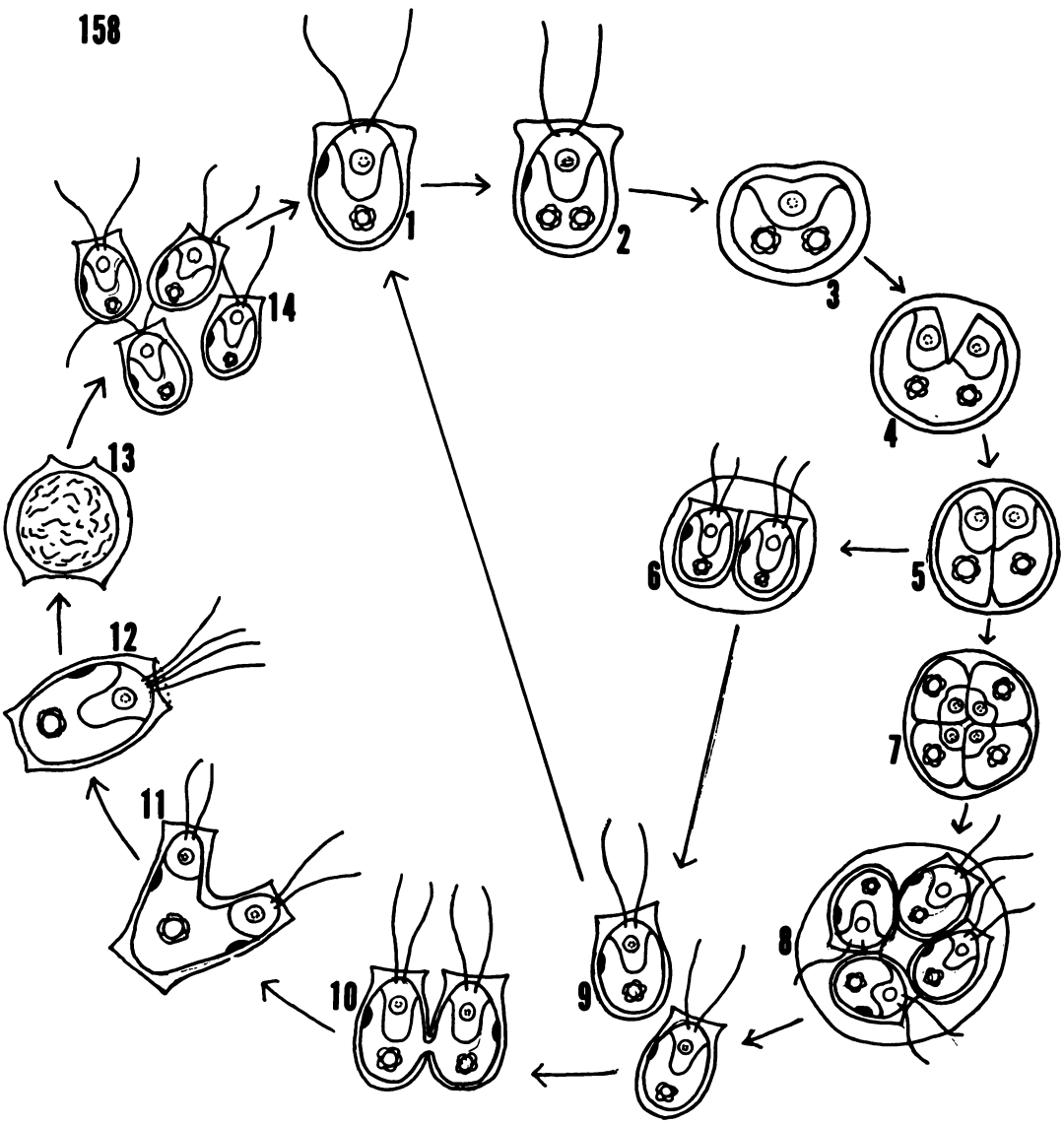


PLATE XXXVIII

Plate XXXIX. Cell Division: Two-Cell Stage.

Figure 159. Rounded cell shape and 2 pyrenoids (P) characterize impending asexual reproduction in this cell. LM Nomarski differential-interference optics. 7000x.

Figure 160. Non-motile cell with 2 pyrenoids and 1 nucleus prior to mitosis. LM oblique illumination. 6000x.

Figure 161. Binucleate cell during cytokinesis; chloroplast (C) has not divided and both nucleoli are apparent (arrows). LM oblique illumination. 6500x.

Figure 162. Two daughter cells, each with one nucleus and one pyrenoid. LM oblique illumination. 6500x.

Figure 163. Two fully formed daughter cells inside the parent lorica. LM Nomarski differential-interference optics. 6500x.

Figure 164. CPD preparation shows parent lorica collapsed over dividing cell. SEM. 6,000x.

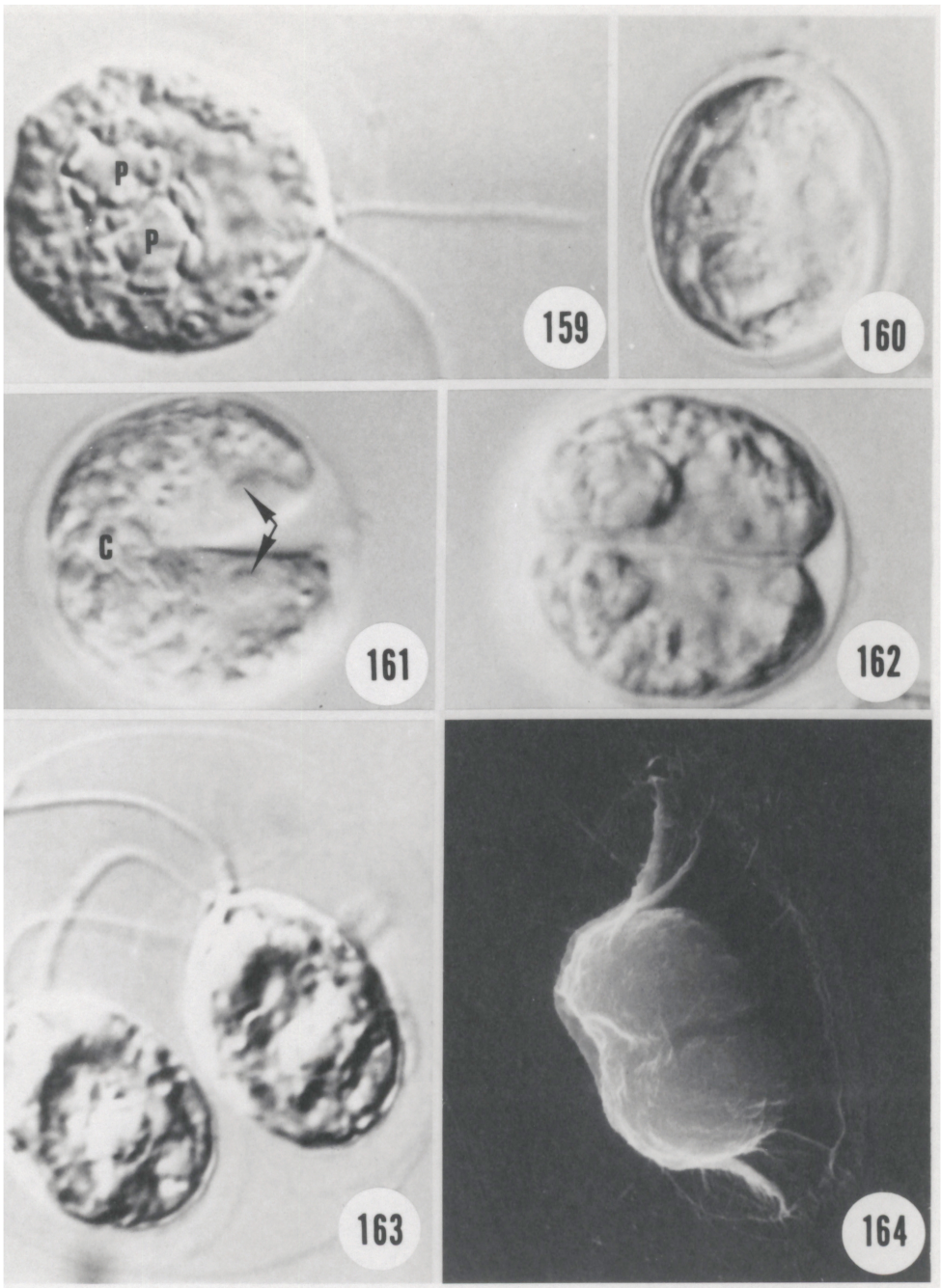


PLATE XXXIX

Plate XL. Cell Division.

Figure 165. Motile cell prior to cell division shows 2 connected pyrenoids. TEM thin-section. 30,000x.

Figure 166. Cell with 2 separated pyrenoids. TEM thin-section. 36,000x.

Figure 167. Prior to mitosis pyrenoids are visible in opposite lobes of the chloroplast. Swollen thyalkoids result from simultaneous glutaraldehyde-osmium tetroxide fixation. TEM thin-section. 38,000x.

Figure 168. Tangential section through a metaphase nucleus shows metaphase plate and one pole with 2 basal bodies (BB). Nuclear membrane is still instact. TEM thin-section. 32,000x.

Figure 169. Section through phycoplast between 2 closely appressed nuclei. MT (arrows) parallel the phycoplast. TEM thin-section. 35,000x.

Figure 170. Higher magnification of phycoplast region shows numerous microtubules (arrows), dictyosome profiles and RER. TEM thin-section. 51,000x.

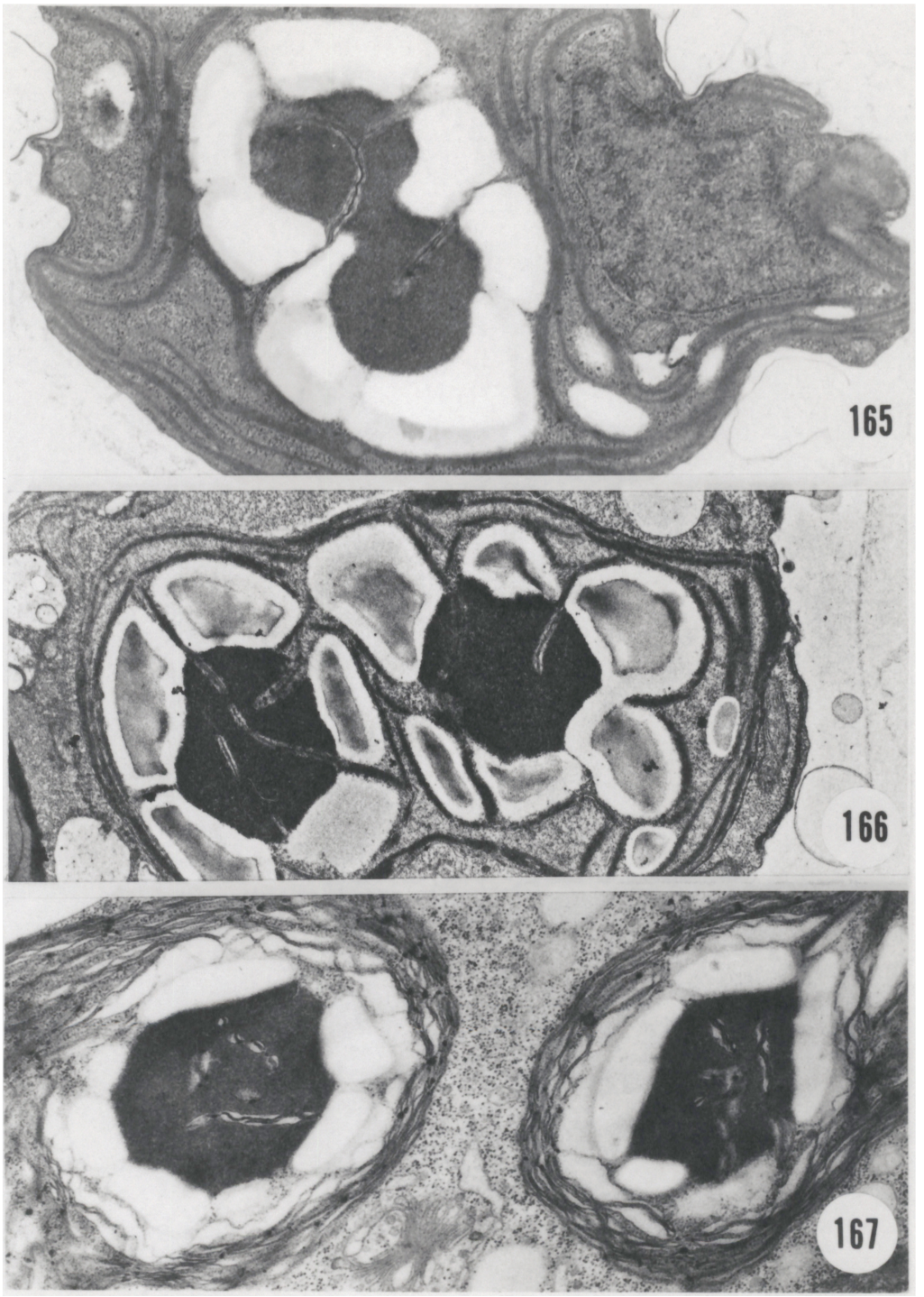


PLATE XL

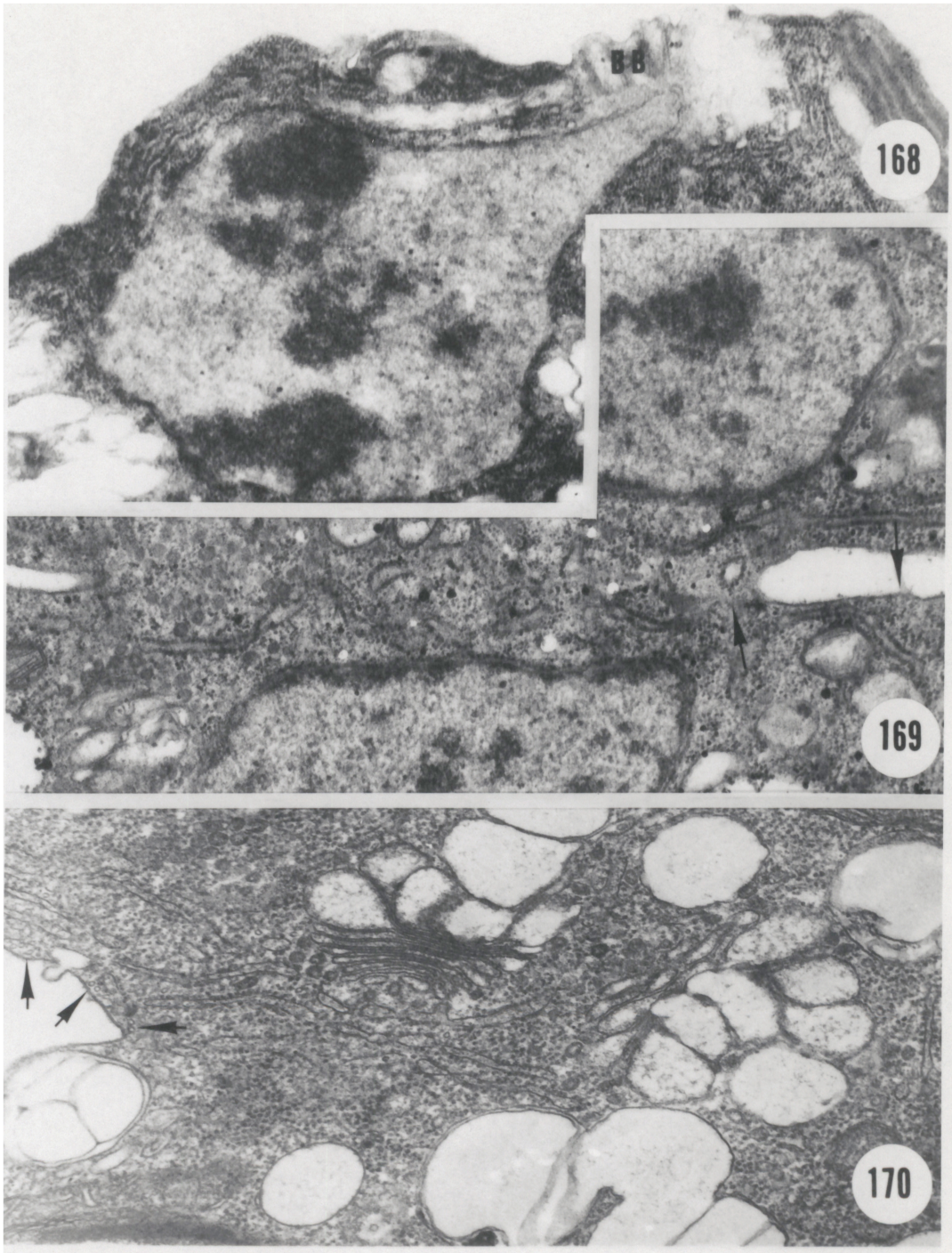


PLATE XL (Continued)

Plate XLI. Cytokinesis.

Figure 171. Nuclei are close to the phycoplast during cytokinesis; MT (arrows) parallel the division plane. TEM thin-section. 65,000x.

Figure 172. Late cytokinesis with PLPM in vesicles between the forming daughter cells. Bilayered parent lorica persists (arrows). TEM thin-section. 50,000x.

Figure 173-175. Serial sections through cell undergoing cytokinesis. Section number in parentheses.

Figure 173. Section through one nucleus shows large gap between formative daughter cells (1). TEM thin-section. 35,000x.

Figure 174. Cytoplasmic connections evident between 2 formative daughter cells (5). TEM thin-section. 35,000x.

Figure 175. Section shows few signs of cytokinesis and only one chloroplast (30). TEM thin-section. 35,000x.

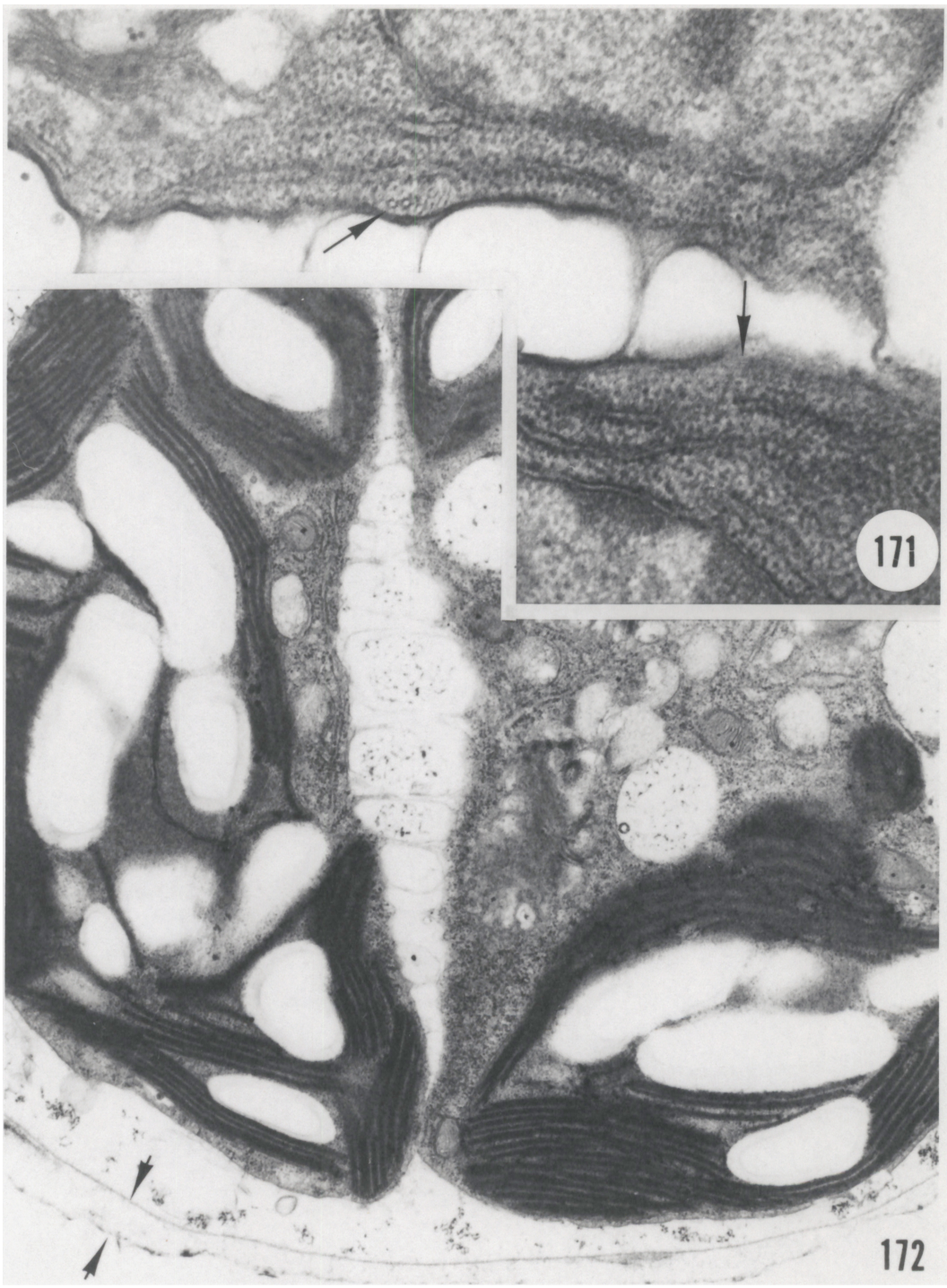


PLATE XLI

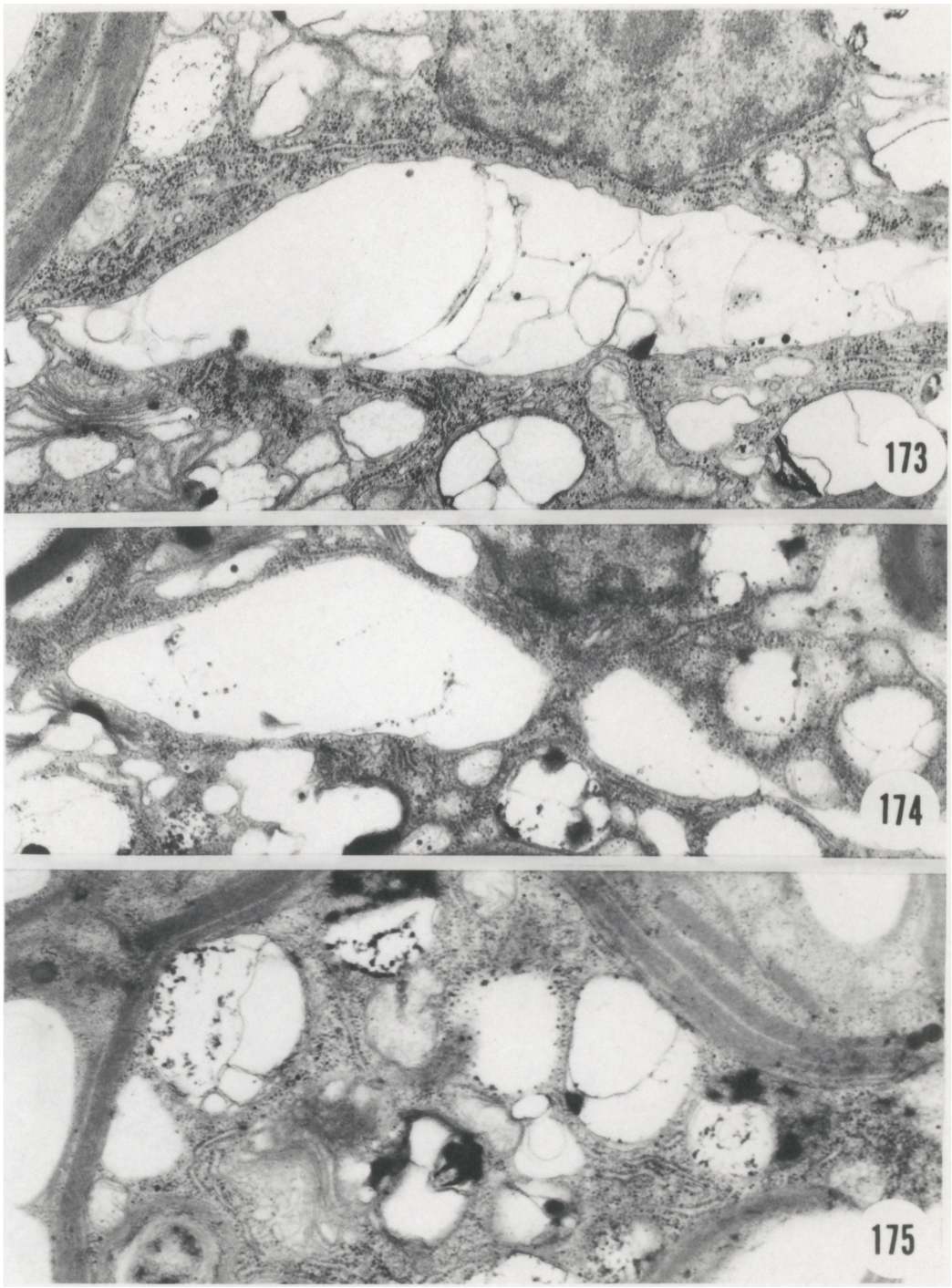


PLATE XLI (Continued)

Plate XLII. Cell Division: Four-Cell Stage.

Figure 176. Four formative daughter cells inside parent lorica (arrow). LM oblique illumination. 5500x.

Figure 177. CPC preparation shows 4 daughter cells with winged loricas (arrows) inside the parent lorica. SEM. 6000x.

Figure 178. Four fully formed daughter cells, each with a single pyrenoid (P) prior to release from parent lorica. LM oblique illumination. 6000x.

Figure 179. Section through 4 formative daughter cells. PLPM is visible in Golgi cisternae. Parent lorica is bilayered (arrows). 8000x.

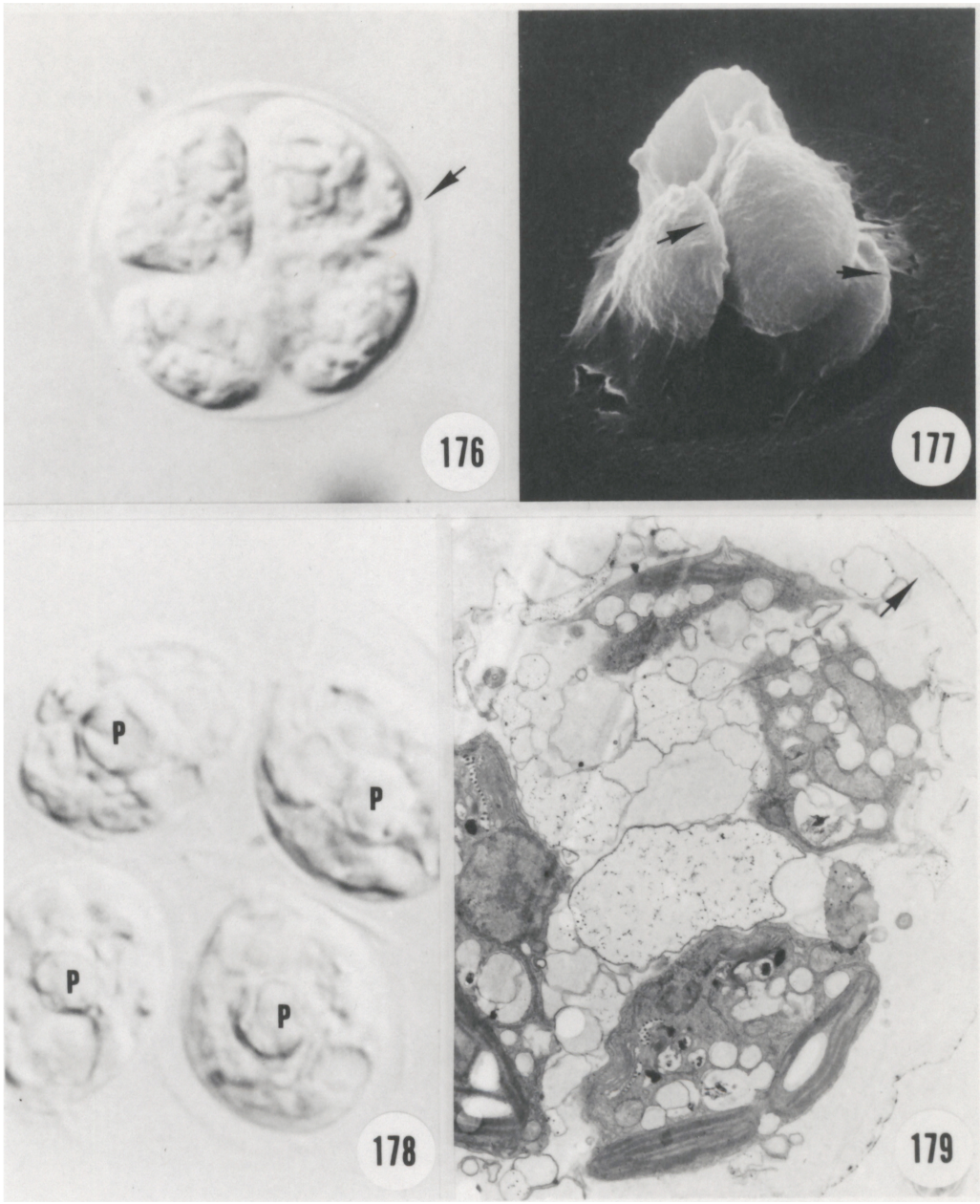


PLATE XLII

Plate XLIII. Sexual Reproduction.

Figure 180. Cytoplasmic connection between 2 isogametes. Loricas of both gametes persist. TEM whole-mount. 14,000x.

Figure 181. Intiation of fusion by means of a posterior cytoplasmic connection. LM oblique illumination, reverse image. 3000x.

Figure 182. Thick section (2u) shows zygote with single pyrenoid. This section was remounted and thin sections cut to obtain data shown in Figs. 183-184. 3000x.

Figure 183. Section shows bilayered lorica (arrows) with 2 wings. TEM thin section. 11,000x.

Figure 184. Section shows single pyrenoid and a single stigma (arrow). TEM thin-section. 11,000x.

Figure 185. CPD preparation of formative zygote shows 4 flagella and 2 lorica wings (arrows), one around anterior ends of the cell. SEM. 24,000x.

Figure 186. Micrograph shows "two-headed," quadriflagellate stage of zygote formation. LM Nomarski differential interference contrast optics. 4000x.

Figure 187. Lorica of formative zygote is clearly seen in this preparation. Phase-contrast. 4000x.

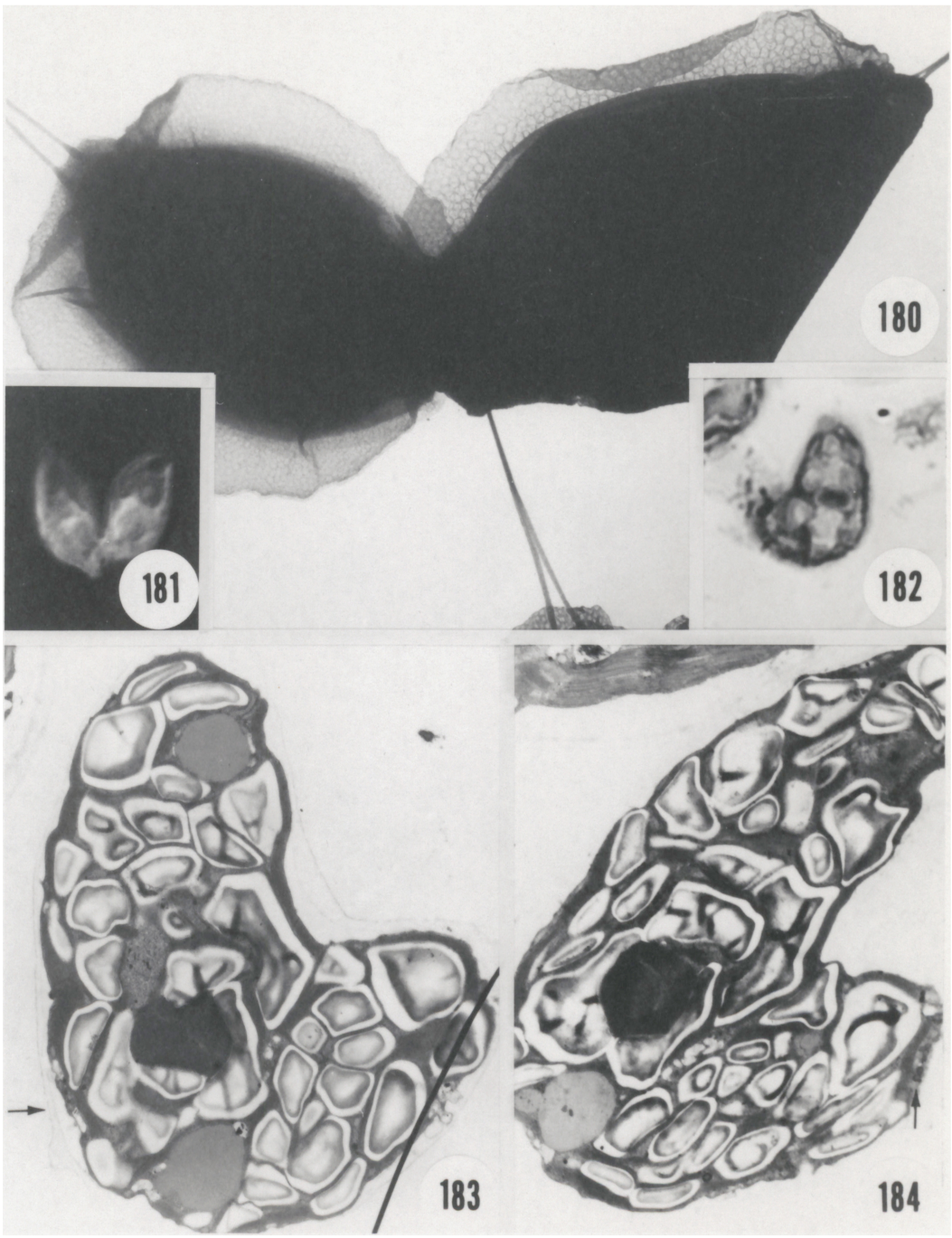


PLATE XLIII

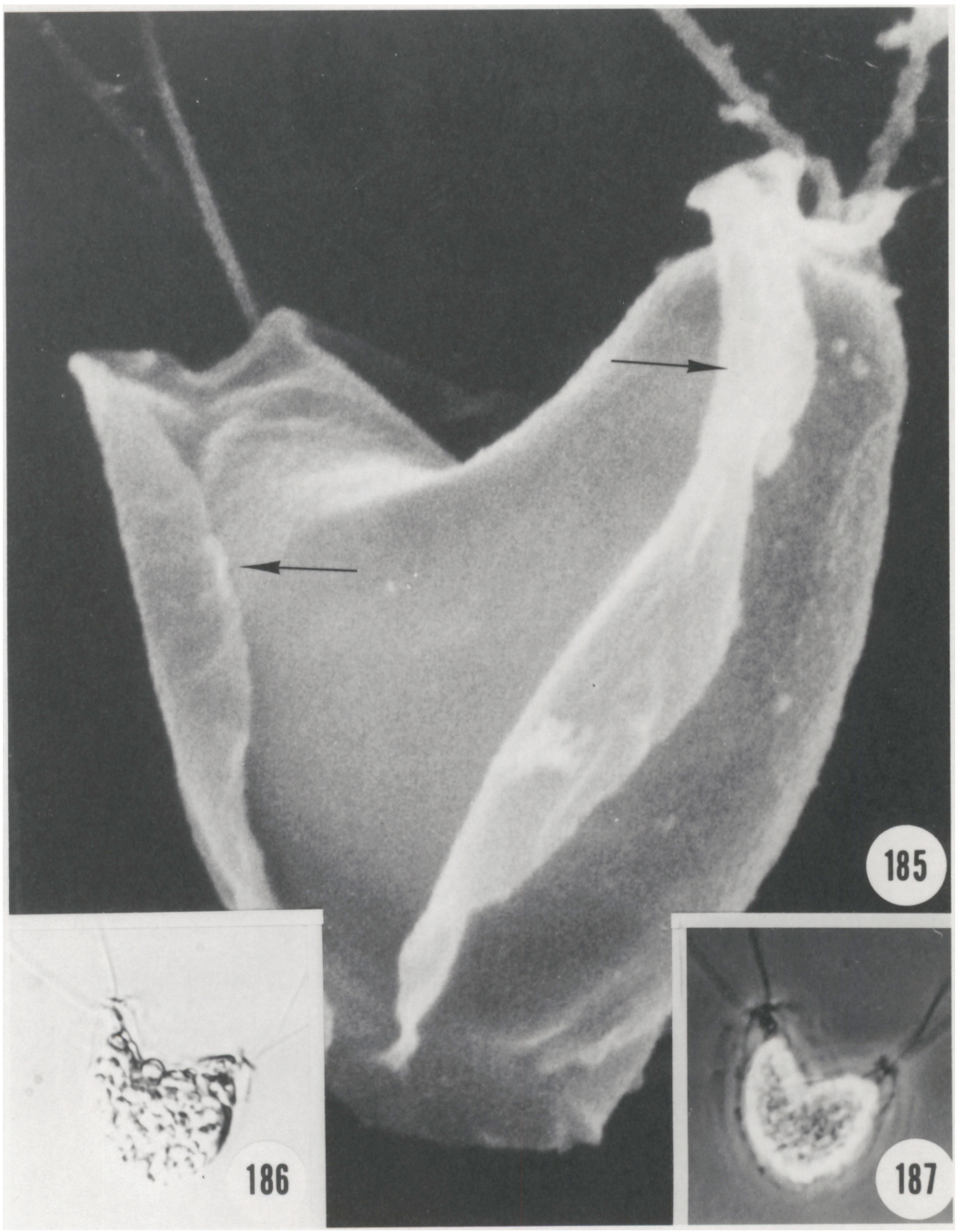


PLATE XLIII (Continued)

Plate XLIV. Aplanozygote

Figure 188. CPD preparation shows "single-headed" quadriflagellate planozygote, with 2 lorica wings and hexagonal surface pattern. SEM. 22,000x.

Figure 189. Fully formed spherical aplanozygote with large amounts of starch shows remnants of both lorica wings. LM oblique illumination. 4500x.

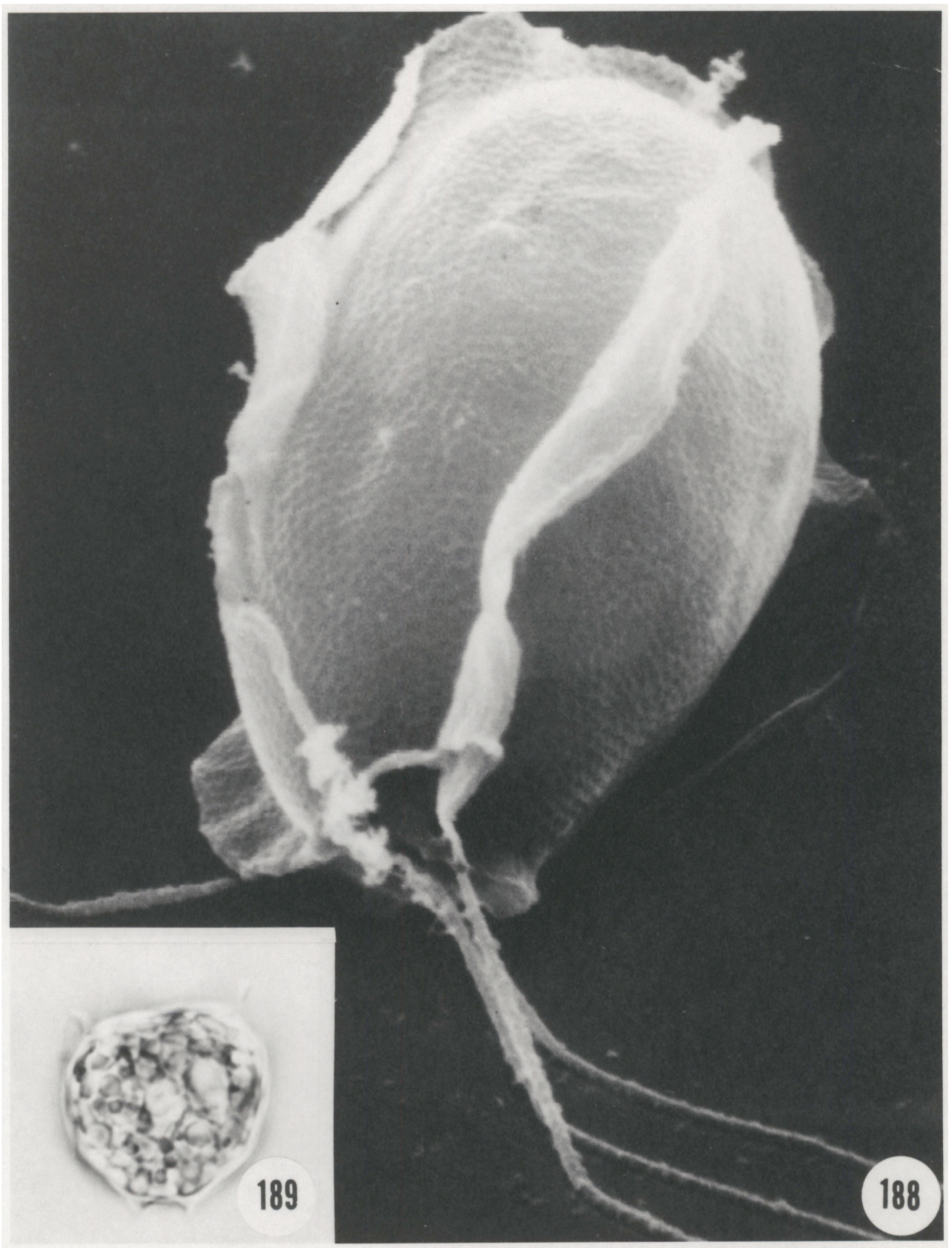


PLATE XLIV

VITA

David A. Gerard, the fourth of Floyd and Huldah Gerard's six children, was born September 15, 1947, in Latrobe, Pennsylvania. He attended elementary school in Greensburg, Pennsylvania and graduated from Greensburg-Salem High School in 1965. He received the Bachelor of Arts Degree with majors in Biology and Secondary Education in 1969 from William Jennings Bryan College, Dayton, Tennessee. He was listed in the 1969 edition of Who's Who in American Colleges and Universities. He taught biology and coached basketball and football at Spring City High School, Spring City, Tennessee for 2 years and subsequently spent 2 years in the Army as a biological science assistant stationed at Walter Reed Army Institute of Research, Washington, D. C., working as an electron microscopy technician in the Department of Experimental Pathology. He entered graduate school at The University of Tennessee, Knoxville, in 1973, and received the Master of Science Degree with a major in Science Education in 1974.

He entered the graduate school of The University of Tennessee, Knoxville, Department of Botany in 1975 where he held the positions of Graduate Assistant, Graduate Teaching Assistant and Research Associate. He completed the Doctor of Philosophy Degree in Botany in August 1980.

He is married to the former Ruth Ann Sheppard of Greenwich, New Jersey.